THE APPLICATION OF SPECTROSCOPIC TECHNIQUES TO PROBLEMS IN TRANSITION METAL COORDINATION CHEMISTRY.

A thesis submitted for the degree of

Doctor of Philosophy in the

University of Southampton.

by

R. E. COLLIS

Southampton,

August, 1969.

To my wife and parents

ACKNOWLEDGEMENTS

The Author wishes to thank his Supervisor, Professor I. R. Beattie, for providing him with the opportunity to present this thesis and for his continued help and encouragement; Dr. T. R. Gilson and Dr. D. E. Rogers for the use of programmes for vibrational analysis, his colleagues in the Department of Chemistry for many helpful discussions and Messrs. British Titan Products Ltd., for generous financial support.

CONTENTS

Chapter	Title	Page
	Abbreviations.	iii
	Abstract.	iv
I	Introduction.	1
II	The isolation and characterisation of acetylacetonato-titanium oxide chloride $[TiOCl(acac)]_2$.	13
III	The vibrational spectra of the 1:1 adducts of phosphine, methylphosphine, dimethylphosphine and trimethylphosphine with titanium tetrachloride.	41
IV	The vibrational spectra and stereochemistries of some adducts of the type L_2TiX_4.	90
V	The preparation of some 1:2 adducts of the trichlorides of metals in the first transition series with trimethylamine and trimethylphosphine.	124
VI	The vibrational spectra of some adducts of general formula $MCl_3,2NMe_3$ for metals of the first transition series.	137
VII	The vibrational spectra of some adducts of general formula $MCl_3,2PMe_3$ for metals of the first transition series.	152

Chapter	Title	Page
VIII	A comparison of the vibrational spectra obtained for the 2:1 complexes of trimethylamine and trimethylphosphine with the trichlorides of metals in the first transition series.	172
Appendices		
A	Vibrational analysis of $TiCl_4, PR_3$ in C_{2V} and C_{3V} symmetries.	195
B	Vibrational analysis of $TiCl_4, 2CH_3CN$ in C_{2V} symmetry.	209
C	Vibrational analysis of $TiCl_3, 2XMe_3$ in D_{3h} symmetry.	219
References		228

ABBREVIATIONS

P	=	polarised
DP	=	depolarised
v	=	very
s	=	strong
m	=	medium
w	=	weak
br.	=	broad
sh	=	shoulder
Hacac	=	acetylacetone
cps	=	cycles per second
md	=	millidynes
S.V.F.F.	=	simple valence force field
G.V.F.F.	=	general valence force field
ppm	=	parts per million
Me	=	methyl
Et	=	ethyl
L	=	ligand
Py	=	pyridine
ν	=	stretching mode
δ	=	deformational mode
ρ_r	=	rocking mode
$\emptyset$	=	phenyl
π	=	out of plane deformational mode

ABSTRACT

FACULTY OF SCIENCE

CHEMISTRY

Doctor of Philosophy

THE APPLICATION OF SPECTROSCOPIC TECHNIQUES TO PROBLEMS IN TRANSITION METAL COORDINATION CHEMISTRY

by Robert Edwin Collis

The techniques of x-ray diffraction, NMR. spectroscopy and Raman and infrared spectroscopy and their applications to problems in inorganic stereochemistry are briefly discussed.

The isolation and characterisation of the complex TiOCl(acac) (where Hacac = acetylacetone) is described. On the basis of molecular weight determinations in benzene it is formulated as a dimer. The infrared and Raman spectra have been measured and point to the existence of Ti$<^{O}_{O}>$Ti bridge bonds. In the light of the results of ^{1}H. NMR. spectral measurements, several oxygen bridged dimeric structures are proposed.

The vibrational spectra of the 1:1 adducts of phosphine, methylphosphine, dimethylphosphine and trimethylphosphine with titanium tetrachloride have been measured, and are discussed in terms of their

geometries. Cryoscopic molecular weight data, taken in conjunction with the spectroscopic data, showed the adduct $TiCl_4,PMe_3$ to be monomeric in benzene, and from a comparison with the results for $TiCl_4,NMe_3$, it is probable that it adopts a C_{3V} structure based on a trigonal bipyramidal distribution of the ligands with axial trimethylphosphine. In the case of the other species, the phosphine ligand is probably in an equatorial position. Matrix isolation Raman studies on $TiCl_4,PH_3$ in tetramethylsilane have been reported, and suggest that it too is monomeric. The partial assignments of the vibrational spectra have been supplemented by G.V.F.F. calculations.

The vibrational spectra have been measured for the 1:2 adducts of titanium tetrachloride with trimethylphosphine, pyridine and methylcyanide, and the 1:2 adducts of titanium tetrabromide with pyridine and methylcyanide. The spectra of the adduct $TiCl_4,2PMe_3$ have been interpreted in terms of a trans - D_{4h} monomeric octahedral structure. It was found that the spectra of the adducts $TiCl_4,2MeCN$ and $TiBr_4,2MeCN$, taken in conjunction with conductivity data for solutions of $TiCl_4$ and $TiBr_4$ in methylcyanide, and a G.V.F.F. calculation on C_{2V} $TiCl_4,2MeCN$, could be interpreted in terms of a probable cis - C_{2V} monomeric octahedral structure for both of these adducts. Unambiguous interpretation of the spectral results for $TiCl_4,2Py$ and $TiBr_4,2Py$ in terms of structure could not be carried out. Powder x-ray measurements showed them to be isomorphous with the adducts $SiCl_4,2Py$ and $SnCl_4,2Py$ which from single crystal x-ray studies are

known to adopt a trans octahedral structure.

The preparation, characterisation and vibrational spectra have been described for two series of complexes $MCl_3,2NMe_3$ and $MCl_3,2PMe_3$ (where M = Sc, Ti, V, Cr, Fe; and M = Sc, Ti, V, Cr, Fe, Co, Ni, respectively). Cryoscopic molecular weight data for $CrCl_3,2PMe_3$ indicate it to be monomeric in benzene. The vibrational spectra have in every case been interpreted in terms of a trans D_{3h} trigonal bipyramidal structure, supplemented by G.V.F.F. calculations on D_{3h} $TiCl_3,2NMe_3$ and $TiCl_3,2PMe_3$. Previous x-ray determinations on the adducts $TiCl_3,2NMe_3$, $VCl_3,2NMe_3$ and $CrCl_3,2NMe_3$ had shown them to adopt such a structure.

The spectra obtained are compared, and in the light of competition experiments carried out on the pairs of complexes $ScCl_3,2PMe_3$; $ScCl_3,2NMe_3$ and $FeCl_3,2NMe_3$; $FeCl_3,2PMe_3$, differences in the spectra between the series of phosphine and amine complexes for different members of the series are discussed in terms of the nature of the bonding involved, Class (b) acceptor character, force field parameters and steric effects.

C H A P T E R I.

Introduction

I.1 General

Any theory of chemical bonding must provide a satisfactory understanding of two fundamental areas of chemical knowledge. Firstly, it must provide a rational account of the formation of chemical bonds between elements and of the resulting bond energies; secondly it must account satisfactorily both for the shapes which molecules adopt and also the molecular dimensions which are observed. A formidable array of physical methods has been employed, with varying degrees of success, to gain a better understanding of the factors involved in these two areas. As far as spectroscopic techniques are concerned, interpretation of results in terms of molecular stereochemistry is generally found to be on a much sounder basis than conclusions concerned with the nature of the bonding involved.

For inorganic coordination compounds, the techniques of x-ray and neutron diffraction in structure determination are definitive. However, their use is limited to crystalline solids. Electron diffraction and microwave spectroscopy are normally confined to studies in the gas phase.

A great deal of effort in the recent past has been devoted to the study of transition metal coordination compounds, whose formal electronic configurations involve a central metal ion possessing a partially filled d-shell. The results of magnetic measurements and electronic absorption spectroscopy have been successfully rationalised to a large extent by the crystal field and ligand field

theories in terms of the local symmetry of the ligands surrounding the central metal ion. Advances in the understanding of the bonding involved in these complexes have similarly been made.

In addition to these techniques involving effects due to electrons in partially filled d-shells, there remain the techniques of vibrational spectroscopy and nuclear magnetic resonance spectroscopy. Indeed, for coordination compounds involving acceptors with either nd^0 or nd^{10} electronic configurations, these are the principal methods available for structure determination apart from x-ray diffraction and related techniques. Although, as stated above, results from x-ray diffraction experiments are definitive, they are normally confined to the solid state. Vibrational and NMR. spectroscopy are invaluable for yielding structural information for solutions and the liquid state.

I.2 NMR. Spectroscopy

In principle, chemical shifts can be resolved in spectra of solid compounds provided that the line widths, which are primarily governed by dipolar interactions in solids, are small compared with the chemical shifts involved. Thus, the ^{205}Tl spectrum of solid Tl_2Cl_3 consists of two peaks of relative intensities 1:3, consistent with the formulation as $(Tl^+)_3(TlCl_6^{3-})$, (1). In a study of the ^{31}P resonance spectrum of solid PCl_5, dipolar broadening effects were minimised by high speed rotation ($\rangle$ 800 rps) of the sample on an axis

at an angle of $54^{0}\ 44^{1}$ to the direction of the magnetic field. The spectrum observed was consistent with a formulation as PCl_4^+ PCl_6^- in a tetragonal lattice (2). However, the study of the NMR. spectra of solids is still rather limited.

The vast majority of stereochemical studies of inorganic molecules involving NMR. spectroscopy, however, have involved high resolution NMR. measurements on either vapours, liquids or solutions. This technique yields, in favourable cases, from an analysis of the spectra in terms of chemical shifts and spin spin coupling constants, a simple, unique assignment of stereochemistry. In contrast to its obvious value in structural organic chemical problems, examples of inorganic structures first demonstrated by NMR. are few. Typically, organic compounds are liquids or solids easily soluble in a large number of non polar solvents and they contain hydrogen atoms which have an ideal nucleus from the point of view of NMR., both in regards to detection, and also interpretation of results in terms of the electronic structure of the bonds involved. By contrast, inorganic compounds are largely solids of low solubility and few contain nuclei which have a nuclear spin = 1/2 (with a zero quadrupole moment). Thus, NMR. of inorganic chlorides is generally of little value since both ^{35}Cl and ^{37}Cl possess large quadrupole moments, a feature leading to excessive line broadening due to quadrupolar relaxation. Furthermore, examination of paramagnetic species is prohibited, since strong electron-nucleus relaxation

broadens the resonances to such an extent that only a single broad absorption signal is observed. However, if electron relaxation times and exchange times are favourable (3), one may observe for paramagnetic species, the unusually large chemical shifts known as contact shifts. The great advantages of NMR. as a technique for structural determinations are its speed and simplicity of interpretation. Even in cases where second order effects are operating, spectral analysis is relatively speedy to carry out. In this connection, recent advances in double resonance techniques (4), especially for heteronuclear spin coupling effects, have greatly facilitated spectral assignments, and allow the relative signs of coupling constants to be determined.

Although relatively few atomic nuclei are amenable to study by NMR., a great deal of significant structural work has been carried out. In this field the study of fluorides has been particularly successful. Thus, the ^{19}F NMR. spectrum of SF_4 can be interpreted in terms of a C_{2V} structure based on a trigonal bipyramid with the lone pair in an equatorial position (5). Moreover, the interpretation of the ^{19}F NMR. spectrum of antimony pentafluoride (6) in terms of a polymeric structure involving cis-fluorine bridging provided structural information which probably could not have been obtained as simply by any other physical technique. Of special relevance to the work described in this thesis is the work carried out by Dean and Evans on the ^{19}F NMR. of some tin(IV) fluoro-complexes (7a), and

by Muetterties (7b) on the stereochemistry of adducts of transition metal fluorides, and in particular TiF_4, SnF_4, SiF_4, GeF_4 and MoF_4. This work illustrates the ease with which the spectra of L_2MF_4 species may be interpreted in terms of stereochemistry, but it also draws attention to the effects of intermolecular exchange phenomena. As a result of this, the interpretation of spectra consisting of a single resonance in terms of all nuclei being magnetically equivalent is a very dangerous procedure in the absence of a temperature variation study and/or adequate supporting evidence. In this connection, intramolecular exchange phenomena may also sometimes be important, especially if the alternative structures have a very low energy barrier for interconversion between them, as for example trigonal bipyramidal and tetragonal pyramidal geometries. Indeed, many coordination compounds possessing trigonal bipyramidal geometry have NMR. spectra which show spectroscopic equivalence of the ligands (e.g. PF_5, VF_5, AsF_5 and the ^{13}C spectrum of $Fe(CO)_5$).

Applications of ^1H NMR. have been successful, particularly in the structural chemistry of hydrides, (where x-ray diffraction is of little value) and in organometallic chemistry. Direct bonding of hydrogen atoms to metals is characterised by abnormally large proton chemical shifts, and NMR. has yielded much information in the field of transition metal olefin complexes.

I.3 Vibrational Spectroscopy

As may be seen from the problems with ligand exchange and stereochemical non-rigidity encountered in NMR. studies, the time scale for this technique is relatively slow (i.e. $10^{-1} \rightarrow 10^{-9}$ secs.). A great advantage of vibrational spectroscopy is that it is a much "faster" technique, the time scale involved being of the order of 10^{-13} secs. Thus, few processes commonly occurring for molecules in their ground states are too fast for vibrational spectroscopy to follow.

Infrared and Raman spectroscopic techniques yield complementary information about molecules. However, until three years ago the application of Raman spectroscopy to problems of chemical interest was extremely limited, due to the extreme feebleness of the effect. With the use of lasers as sources of excitation, however, this technique is now probably more accessible and more convenient to use as a diagnostic tool in stereochemical studies than is infrared spectroscopy.

Applications of vibrational spectroscopy in the sodium chloride region, with the simple idea of group frequencies, to obtain information about functional groups, the approach found most useful in organic chemistry, have been very successful in the fields of organometallic and hydride chemistry. However, nearly all the metal ligand vibrations of interest to the structural inorganic chemist occur below this region, and require the extension of the accessible

infrared region down to about 200 cm.$^{-1}$. Assuming that certain metal-ligand vibrations are relatively "pure" modes, and using the concept of "stretching regions", the symmetry of a molecule can in favourable cases often be decided from the number of vibrations observable in the stretching region, using the results of simple group theory.

With large molecules, however, and where differences in symmetry are small, this approach is less dependable. The infrared region down to 30 cm.$^{-1}$ is now readily accessible through the use of instruments such as the Beckman I.R.11, and as stated above, Raman spectroscopy is now much more easily studied since the introduction of laser sources. Given these practical possibilities complete vibrational spectra of molecules over the whole infrared region may now easily be obtained. Using the concepts of stretching and bending regions, Raman and infrared activities, depolarisation ratios for solutions and coincidences in the Raman and infrared, the stereochemistries of fairly complex molecules may be assigned. However, the possibilities of Fermi resonance or, for solids, crystal field effects should always be borne in mind. Furthermore, modes which are, from group theoretical considerations, shown to be, say, Raman active may have very low intensities and escape detection, and neither should the possibilities for accidental coincidences be overlooked. Indeed, because of the very wide range of masses and bond force constants found for inorganic molecules, even the concept of

"stretching rgions" is of very limited applicability.

The advent of new computer techniques (8), (9) has meant that vibrational analyses of quite complicated molecules may be carried out. Force constants are transferred from simple symmetrical molecules whose structure and vibrational assignments are well known. Even using extensive approximations, results are generally obtained which are a great aid in assigning spectra. Stretching frequencies are usually readily calculated to within 10% of observed values, and the relative degrees of mixing of normal modes may be determined, as a test of the validity of the common assumption that certain stretching vibrations are relatively pure modes. This approach is limited by the number of simple molecules whose vibrational spectra have been unambiguously assigned, and for which a reliable set of force constants has been calculated. Molecules whose structures have been confirmed using vibrational spectroscopy in conjunction with vibrational analyses are AlH_3,$2NMe_3$ (10), MCl_4,NMe_3 (M = Si, Ge, Ti, Sn) (11) and CH_3PCl_4 (12). Results obtained with these molecules suggest that in certain cases stretching vibrations are relatively pure but none the less, the concept of "group frequencies" is not a helpful one for inorganic compounds. Results obtained in this thesis indicate, furthermore, that in cases of coordination complexes involving ligands complexing through the heavier group V and VI donor atoms (e.g. P and S) that mixing of skeletal and ligand modes is much more serious.

Useful though approximate vibrational analyses undoubtedly are, there remain cases where genuine ambiguity still arises in the assignment of certain modes, (for instance in the assignment of one of the stretching modes ($\nu_2 e_g$) compared with one of the deformations ($\nu_5 f_{2g}$) in octahedral MX_6 species (13)).

The well defined plane polarised nature of laser radiation has made studies of the single crystal Raman spectra of inorganic species a practical possibility. The Raman tensor which describes the polarisability of the molecule or crystal for each mode is subject to restrictions by the symmetry of the scattering system. This tensor may be used to predict Raman activities and directional intensity changes in the Raman scattering for each mode, leading, in favourable cases, to unambiguous assignments. Thus the ambiguity mentioned above for MX_6 has been resolved by single crystal measurements (13). For studies involving more complex molecules, single crystal results can resolve ambiguities arising from approximate normal coordinate calculations brought about by our lack of knowledge of force fields.

By a combination of far infrared, Raman and single crystal studies, supported by an approximate vibrational analysis, confident assignments may be made for quite complex structures. Considerable advances in the study and interpretation of the spectra of polymeric species such as NbF_5 (14), Au_2Cl_6, Nb_2Cl_{10}, Nb_2Br_{10} etc. (15) have been made, and assignments have been made even for three dimensional crystals such as rutile (16), anatase, cassiterite and molybdenum trioxide (13).

Undoubtedly the most significant advance has been the introduction of lasers as sources in Raman spectroscopy. Powdered solids may now be studied with ease, especially with the 180° collection system employed in the Cary 81 spectrometer, and with the use of such instruments as the Spex monochromator which employ detection systems of high sensitivity, vapours may be conveniently studied without the need for multipass cells. The production of stable helium/neon and argon ion lasers has opened the way to the study of a wide range of highly coloured species, especially transition metal coordination compounds. Despite these important advances however, results must still often be treated with caution. Problems due to correlation splitting, birefringence and crystal imperfections should always be borne in mind in single crystal studies (13), as should the possible occurrence of the resonance Raman effect (17) in the study of coloured compounds, and perturbations of observed intensities as a result of scattering by spin waves or magnons in magnetic materials (18). The relative importance of such effects is still uncertain, however.

I.4 Scope of the Present Work

Hitherto, studies of the stereochemistry of inorganic complexes by vibrational spectroscopy have been largely confined to species involving either filled d-shells or empty d-shells of rather high energy. It was felt that preliminary studies (8) should be made on

systems where the possibility of bonding involving empty d-orbitals and electrons in d-orbitals was not a complicating factor. A fairly large amount of data for these systems has now accumulated, especially for neutral adducts of the halides of group III(b), group IV(b) and group V(b) elements (19), (8), (20). In particular, the existence of 5-coordinate species appears to be quite common, and the actual arrangement of the ligand around the central acceptor atom appears to be the result of quite a fine balance between steric and electronic effects (7), (8).

Most of the work described in this thesis is devoted to studies involving adducts of titanium (IV) halides. Comparisons are made between the results for adducts of group IV(b) halides and the Ti(IV) systems where low lying empty d-orbitals are present. Studies of the vibrational spectra of some adducts of a range of transition metal trihalides of the first series (21) have also been carried out. Comparisons are made with compounds involving group III(b) acceptors and the effects of partially filled d-shells on metal ligand vibrations are examined. Tentative conclusions concerning the nature of the bonding in these complexes are put forward.

C H A P T E R II.

The isolation and characterisation of dimeric acetylacetonato-titanium oxide chloride $[TiOCl(acac)]_2$.

II.1 The Occurrence of Multiple Bonding

A fundamental difference between the behaviour of elements in the first row of the Periodic Table and those of succeeding rows is the relative ease with which the former participate in the formation of multiple bonds, involving pπ-pπ bonding. As a general rule, multiple bonding of this type is restricted to bonds between first row elements and the non-transition elements of group VI. This behaviour could be attributed to a combination of such factors as (i) small inner shell ($1s^2$) repulsions of the first row elements, leading to extensive pπ-pπ overlap, (22a), (ii) the smaller size of the first row elements leading to low coordination numbers, and (iii) the more efficient filling of orbitals in the polymer as compared with the monomer (22b). Thus, the polymerisation of BOCl and MeBO could be attributed to (iii). The unusual behaviour of the non transition elements of group VI is brought out by a comparison of the molecular species SO_2 as compared with the polymeric PO_2^-, with which it is isoelectronic. The behaviour of the group VI(b) elements suggests that electronegativity differences may be important. For example, where the other element involved is more electropositive than sulphur, the d-orbitals might be expected to be less accessible than in cases where sulphur is bonded to more electronegative atoms.

With regard to systems in which d-orbital participation may be reasonably postulated, one must consider the possibility of dπ-pπ

bonding. However, the factors favouring this and even the extent to which bonds may possess dπ-pπ character are much less clear than for the pπ-pπ case. Furthermore, there is the possibility that either nd or (n-1)d orbitals may be involved. For bonding involving transition metal ions, clearly the (n-1)d orbitals are sufficiently accessible for possible dπ-pπ bonding with ligands surrounding the central ion. The case for dπ-pπ bonding involving back donation of electrons, formally confined to the central metal, into suitable empty orbitals on the ligands rests largely on the observations of bond lengths, stabilities and ligand stretching force constants in transition metal carbonyl, cyanide and nitrosyl complexes. It is well known that these ligands are especially effective in stabilising very low formal oxidation states of transition metals, and the consequent large numbers of electrons in the transition metal d-orbitals could well be stabilised by back donation, and hence give rise to partial double bond character in the metal ligand bonds. In support of this, it has been noted that complexes of this type are much more stable than those involving ligands such as Cl^- and Br^-, and that the metal-ligand bond lengths of complexes of this kind are typically short. The case for π-bonding in phosphine and arsine complexes is much less clear cut, however. A comparison of the chemical behaviour of phosphine and arsine complexes with that of carbonyl, cyanide and nitrosyl complexes suggests that considerable

$d\pi$-$p\pi$ bonding might occur, but this has not been convincingly demonstrated as yet (23).

Experimental evidence for the occurrence of $nd\pi$-$np\pi$ bonding is similarly abundant, the most well known example being the planarity of trisilylamine. The ions SiO_4^{4-}, PO_4^{3-}, SO_4^{2-} and ClO_4^{-} might all involve a certain degree of $d\pi$-$p\pi$ bonding, and the stability of the MO_4^{n-} ions of P, As, S, Se and Cl with respect to polymerisation may be contrasted with the ease with which the oxyanions of V, Mo, W and Cr polymerise.

Since the publication of Pauling's paper (24) on the hybridisation of atomic orbitals, the ability of d-orbitals to participate in covalent bonding has been quite extensively discussed. Whereas Pauling discussed the problem on the basis of the angular part of atomic eigenfunctions, in a paper by Craig et al (25) the whole problem was reconsidered on the basis of interactions of the radial part of the eigenfunctions. From a calculation of Slater overlap integrals it was suggested that the conditions for good over - lap were very different for the two cases of $d\pi$-$p\pi$ bonding. For hybridisation involving 3d, 3s and 3p orbitals, ligands would have to be electronegative enough to lower the energy of the 3d orbitals, by reducing screening at the nucleus, so that efficient overlap might occur for them to make a significant contribution to the bonding. It was noted that it is just the most electronegative elements which tend to combine with second row elements in their highest valency

states, for example sulphur hexafluoride. For the case of hybridisation involving 3d, 4s and 4p orbitals, as for example in the case of elements in the first transition series, it was suggested that, in contrast, highly electronegative ligands were undesirable, as the decreased screening induced by them at the nucleus would result in 3d orbitals which were of too low an energy for significant contribution to the bonding. Moreover, it was shown that, for good overlap "acceptor" and ligand orbitals should be of comparable "sizes". It thus seems likely that the extent of d-orbital participation might depend on the extent to which the surrounding ligands perturb the d-orbitals of the central atom.

Further calculations (26) of optimum exponent values for 3s, 3p and 3d orbitals of sulphur in sulphur hexafluoride suggest that the promotion energy to the sp^3d^2 configuration for sulphur (estimated to be 25-31 ev.) can be compensated by molecule formation. The calculations show that the 3d orbitals contract to approximately one half the free atom size in the molecular field of sulphur hexafluoride. Further work (27) has been carried out on the valence state energies of excited configurations involving 3d, 4s and 4p orbitals in the later second row elements (Si, P, S and Cl) and their ions, from data obtained from spectral term energies. The results indicate that for later second row elements with high covalencies, the weight of configurations involving high energy orbitals is likely to be largely dependent on the degree of perturbation of the ligands, in agreement

with the earlier work (25). However, it is noteworthy that the results obtained indicate that the 4s orbitals are always slightly more stable than 4p and 3d orbitals. Thus the contribution of 4s orbitals to the valence state is expected to be at least as comparable or possibly larger than that of 3d orbitals. In addition, recent calculations by Gianturco (28) suggest that for the second row elements Al, Si, P, S and Cl, inclusion of configurations such as s^{n-1}, p^m, d^2 and s^n, p^{m-1}, d^2, results in much more compact outer d-orbitals, without necessarily invoking a strong ligand polarisation. It seems evident from the foregoing results that although the contribution of high energy orbitals to the bonding of second row elements is generally quite feasible from both symmetry and overlap considerations the specific participation of high energy d-orbitals in the bonding is much less clearly demonstrated.

II.2 The Occurrence of Multiple Bonding in Titanium Oxo Species

Metal oxo cations such as titanyl, TiO^{2+}, and zirconyl, ZrO^{2+}, had formerly been regarded as well characterised species. However, the study of compounds thought to contain such species, especially by the techniques of x-ray diffraction and infrared spectroscopy, have shown that nearly all of them are actually polymeric, containing single M-O bonds, which may or may not possess partial multiple bond character arising from d-orbital participation. This state of affairs is in marked contrast to the very common and well

authenticated existence of the oxo vanadium (IV) cation, vanadyl, VO_2^+, which dominates the aqueous chemistry of vanadium (IV), and instead parallels closely the behaviour of the elements of group IV(b). Thus, typically, silicon oxygen double bonds are unknown, presumably due to the participation of d-orbitals in partial double bonding in the polymeric species observed in practice, as in the siloxanes. As a further example, the polymeric nature of $GeO(acac)_2$ may be quoted (8).

The use of infrared spectroscopy as a diagnostic tool for M = O species has been much discussed. Studies on several mononuclear species containing M = O bonds have indicated (29) that the usual region of stretching vibrations of this grouping is 900-1100 cm^{-1}. For most of the "titanyl" compounds studied, however, broad bands are observed in the 900 $cm.^{-1}$ region, suggestive of vibrations of Ti-O-Ti- chains. This is the situation for all of the oxyhalides of the type $TiOX_2$ (X = F, Cl, Br or I) and also for the complexes $TiOF_2,H_2O$ (30) and $TiOCl_2,2Py$ (31). In a recent paper, Fowles (32) assigned bands at 976 and 978 $cm.^{-1}$ to Ti = O stretching vibrations in the complexes $TiOCl_2,2Me_3N$ and $TiOCl_2,2(\alpha\text{-picoline})$. It was noted that the former complex was isomorphous with the complex $VOCl_2,2Me_3N$ which exhibits a band at 990 $cm.^{-1}$ in its infrared spectrum and has been shown by x-ray studies to exist as a monomeric unit with discrete V = O bonds. Other complexes of $TiOCl_2$ studied, with such donors as methylcyanide and bipyridyl, showed no strong bands in this region,

but strong broad bands in the 900 - 780 $cm.^{-1}$ region, attributed to Ti-O-Ti polymeric chains.

Possibly the most well authenticated example of the existence of a titanium oxygen double bond is that of the $TiOCl_4^{2-}$ ion. For the compounds $(Me_4N)_2TiOCl_4$ and $(Et_4N)_2TiOCl_4$ $\nu_{Ti=O}$ is reported to be at 975 $cm.^{-1}$ (33), (34), and recent x-ray work (35) confirms that this anion is indeed monomeric.

In addition to the formation of polymeric Ti-O-Ti chains, in so called titanyl species, there is the possibility of the formation of oxygen bridged dimers, involving the unit $Ti\langle^{O}_{O}\rangle Ti$. Considerable confusion has arisen in the past over the nature of "Titanyl acetylacetonate". It was long thought (29), that it was monomeric in benzene and had a Ti = O stretching frequency at 1085 $cm.^{-1}$, comparable with $\nu_{M=O}$ at 990 $cm.^{-1}$ for $VO(acac)_2$, which has been shown from x-ray studies to be monomeric (36). Other work suggests (37) that $\nu_{Ti=O}$ for $TiO(acac)_2$ may lie at 1030 $cm.^{-1}$, although it would then be in the region of the CH_3 rocking vibrations of the acetylacetone. However, further work (38) suggested that the compound is a dimer in benzene when prepared by the hydrolysis of dibutoxytitanium-bis-acetylacetonate. There now (34) seems to be little doubt that it is a dimer, and probably contains $Ti\langle^{O}_{O}\rangle Ti$ bridging groups, whose infrared vibrations occur below 800 $cm.^{-1}$.

With regard to the use of infrared spectroscopy in the assignment of metal oxygen stretching vibrations, it has been pointed out

(34) that it is conceivable that M = O and M-O-M stretching vibrations need not always be distinguishable. S.V.F.F. calculations indicate that the stretching vibration of a linear M-O-M grouping will occur at the same frequency as that of an M = O grouping, if the M-O-M stretching force constant is assumed to be one half of the value of the M = O force constant. On decreasing the M-O-M angle from 180° , then ν_{M-O-M} decreases in frequency. From this it is evident firstly that bands at ∽ 1000 cm.$^{-1}$ need not necessarily be due to M = O, to the exclusion of M-O-M, and secondly, the exact vibrational frequency depends not only on the force constant, but also on the M-O-M angle assumed. It therefore seems reasonable to conclude that the use of vibrational frequencies of metal oxygen vibrations as indications of bond strength, and hence of multiple bond character, must be treated with some caution, especially if the detailed geometry of the molecule (from x-ray measurements) is not available.

II.3 The Isolation of TiOCl(acac).

During an extended study of the properties of $TiO(acac)_2$ (39) it was noted that minor changes in the infrared spectrum of the compound could frequently be observed in the 800 cm.$^{-1}$ region. Typically, a weak to medium band was observed at 810 - 820 cm.$^{-1}$, which was not always reproducible in succeeding preparations of the compound. In particular, the preparation of $TiO(acac)_2$ from $TiOCl_2$

and acetylacetone in the presence of acridine resulted in material having a strong, broad band at 811 cm.$^{-1}$, whilst in contrast the preparation from $TiOCl_2$ and sodium acetylacetonate showed no band at 811 cm.$^{-1}$. These results seemed to suggest the formation of small amounts of either another compound or perhaps a polymeric form of $TiO(acac)_2$ involving Ti-O-Ti chains, in addition to the suspected dimer.

In view of the rather uncertain nature of these results, it was decided to repeat the preparation of $TiO(acac)_2$ using Cox's procedure (40). This involved the reaction of an aqueous solution of titanium (III) chloride with a very large excess of acetylacetone dissolved in benzene, in the presence of excess aqueous sodium carbonate, to remove the hydrogen chloride formed. The $Ti(acac)_3$ formed was then allowed to oxidise in air to yield $TiO(acac)_2$. The procedure was modified however, in that a mole ratio of $TiCl_3$:Hacac of 1:3 was employed, in presence of the calculated amount of sodium carbonate, as opposed to the large excess normally employed, as it was suspected that the presence or absence of the 811 cm.$^{-1}$ band might be due in some way to inefficient removal of all hydrogen chloride formed during the reaction between $TiOCl_2$ and acetylacetone in the presence of acridine, as performed in the previous study (39). The blue product, obtained as a solution in benzene, and presumed to be $Ti(acac)_3$ as in previous preparations by this method, was oxidised in air, and yielded the expected crop of yellow crystals. The

infrared spectrum of the product (Table II.1.), showed, in addition to the usual bands reported for $TiO(acac)_2$ (39), a strong, sharp band at 810 $cm.^{-1}$.

In an attempt to separate any possible mixture present, the crude product was digested with a small quantity of benzene, and partly dissolved. The undissolved yellow solid was filtered off and dried giving the I.R. spectrum typical of $TiO(acac)_2$. (Table II.1.). The benzene solution was evaporated to dryness and yielded a crop of well formed colourless crystals which gave an infrared spectrum which was different from that of $TiO(acac)_2$ in that it possessed, in addition to the two strong acetylacetone vibrations common to all acetylacetonates in the 1020 $cm.^{-1}$ and 930 $cm.^{-1}$ regions, an additional strong band at 810 $cm.^{-1}$. Moreover, the medium band at 776 $cm.^{-1}$ observed for $TiO(acac)_2$ was entirely absent. These spectra are summarised in Figure II.1. for comparison.

The two samples obtained from this separation were analysed for carbon and hydrogen, the results being given on page 39. Clearly, both the analysis results and the I.R. data indicate that the yellow solid, which was less soluble in benzene is $TiO(acac)_2$. As far as the more soluble, colourless component of the mixture is concerned, the best fit to the analytical results was given by the formula TiOCl(acac). In an attempt to demonstrate the existence of chloride in the compound, a solution in methylcyanide was treated with a solution of silver nitrate in methylcyanide. A copious precipitate

of silver chloride was obtained. Using this method, a determination of chloride was then carried out, and the result agreed with the formulation as TiOCl(acac). In view of these results, a "rational" preparation of this complex was next attempted. Cox's method was again used, this time a mixture of $TiCl_3$ to acetylacetone of 1:2 was employed, in the presence of the calculated quantity of aqueous sodium carbonate. The resulting Ti(III) acetylacetonate was not isolated, but allowed to oxidise in situ, to yield an orange benzene solution. This on evaporation gave a yellow brown material. Extraction with methanol (to remove the brown tarry material), followed by recrystallisation yielded colourless crystals which from analysis and infrared results (Table II.2.) were shown to be TiOCl(acac), identical with the colourless, soluble fraction described above.

These results suggest that TiOCl(acac) is probably present in many of the preparations of $TiO(acac)_2$ carried out hitherto. Further, formation of the former is likely to be promoted in preparations of the latter both by inefficient removal of HCl, and the use of relatively low concentrations of acetylacetone. In this way, the presence of the extra band at 811 $cm.^{-1}$ in $TiO(acac)_2$ formed via $TiOCl_2$ and acetylacetone in the presence of acridine is explicable especially since this band is absent when the $TiO(acac)_2$ is formed from $TiOCl_2$ and sodium acetylacetonate.

II.4. The Structure of TiOCl(acac).

The complex of composition TiOCl(acac) isolated as described in the previous section forms monoclinic crystals and, like $TiO(acac)_2$, is quite stable with respect to hydrolysis, in contrast to most Ti(IV) halo complexes. It is soluble in a wide range of organic solvents such as benzene, dichloromethane and methylcyanide, but is much less soluble in more polar solvents like water, ethanol and acetone. Its molecular weight was determined, by cryoscopy, for solutions in benzene and dichloromethane, and it was found to be dimeric in both cases.

The infrared spectrum of the solid and Raman spectra of both the solid and its solution in benzene are quoted in Table II.2. It may be noted that considerable difficulty was encountered in obtaining Raman spectra, due to intense fluorescence of the samples. This could not be minimised by treatment with animal charcoal, but it was found that freshly prepared samples of the complex, one to two days old, did not fluoresce very strongly, and Raman spectra could be obtained with such samples. The fluorescence increased with time, and for samples older than about four days, the Raman scattering was completely masked by this fluorescence. Examination of the vibrational spectra reveals a lack of strong bands in the 1000 $cm.^{-1}$ region of the spectrum which can be attributed to a terminal Ti = O stretching vibration. As already stated, the band at 1025 $cm.^{-1}$ occurs for a variety of metal acetylacetonates, and

has been assigned to the acetylacetonate ring methyl rocking mode (41). This is in contrast to the behaviour of $TiOCl_4^{2-}$ where $\nu_{Ti=O}$ is at 975 cm.$^{-1}$ (34), and for $VO(acac)_2$, $\nu_{V=O}$ at 990 cm.$^{-1}$ (41). Comparison of the vibrational spectra of TiOCl(acac) and $TiO(acac)_2$ (Table II.3.) reveals the presence of an additional strong band in the infrared and Raman spectra of TiOCl(acac), at 340 cm.$^{-1}$, which is shown to be polarised for solutions in benzene (Table II.2.), and which is absent from the spectra of $TiO(acac)_2$. This may therefore be assigned to the titanium chlorine stretching mode, and in view of the coincidence of this mode in the Raman and infrared, if one assumes a dimeric formulation for the molecule, it seems a reasonable assumption to treat the titanium chlorine stretching vibrations as being largely uncoupled, otherwise in phase and out of phase coupling should lead to two non-coincident modes, one strongly infrared active and one strongly Raman active and polarised. In addition, the strong band at 810 cm.$^{-1}$ observed in the infrared for $TiOCl(acac)_2$ is absent for $TiO(acac)_2$, but may correspond to the band at 776 cm.$^{-1}$ observed for the latter. It may be noted that $GeO(acac)_2$ has a broad, strong band at 830 - 860 cm.$^{-1}$ in the infrared. This compound is known to be polymeric (8). It can reasonably be assumed (in view of the dimeric nature of TiOCl(acac) in benzene) that this species contains Ti  Ti bridging units in solution, and in the solid state.

The ^{1}H. NMR. spectrum of TiOCl(acac) at 100 mc./sec. as a

solution in dichloromethane-d_2 is given in Table II.4. The peaks observed occur in the same general regions as those observed for the ring hydrogens and ring methyl groups of $TiO(acac)_2$ and $TiCl_2(acac)_2$ (39). The two peaks of equal intensity observed in the 220 - 212 c/sec. region of the spectrum are three times as intense as the peak at 571 c/sec. Assuming that both acetylacetonate rings in the dimer are in equivalent environments, this latter peak must be assigned to proton (a) of the acetylacetonate rings, and the two more intense bands to the methyl protons (b) and (c) (Table II.4.). These results indicate that the ring methyl groups are in different environments, and have different chemical shifts.

Assuming trigonal bipyramidal coordination for the titanium atoms, the possible oxygen bridged dimeric structures which are consistent with the ^1H. NMR. spectrum are shown in Figure II.2. Assumption of trigonal bipyramidal rather than square pyramidal coordination is not unreasonable, as a related compound $TiCl_2(OC_6H_5)_2$ has been shown by x-ray measurements to adopt a dimeric oxygen bridged structure based on trigonal bipyramidal coordination for the titanium atoms (42).

The dimeric nature of this compound in solution, and probably in the solid state, is remarkable, as it would appear that the compound favours dimeric 5-coordination over monomeric 4-coordination. This result is in contrast to the behaviour of $TiO(acac)_2$, which has been shown to adopt a dimeric 6-coordinate structure in solution as

opposed to a monomeric 5-coordinate structure. Perhaps an important factor is the formation in each case of strong titanium oxygen bridge bonds. In spite of the complex nature of the vibrational spectra, it would be tempting to assign the 810 $cm.^{-1}$ band (infrared), and 750 $cm.^{-1}$ band (Raman; polarised) to asymmetric and symmetric stretching vibrations of the Ti 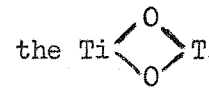 Ti ring grouping. However, it is worth noting that acetylacetonate bands sometimes occur in this region for certain metal acetylacetonates, which have been assigned to π(CH) (41).

II.5. Adduct Formation by TiOCl(acac).

It is well known that $VO(acac)_2$ readily forms stable adducts with ligands such as pyridine, with a consequent change in the frequency of the vanadium oxygen stretching vibration (43). It was hoped that, in view of the probable 5-coordination involved in $[TiOCl(acac)]_2$ that it would form adducts with ligands rather readily, either with breakage of the bridge bonds to form monomers of the type TiOCl(acac)L or TiOCl(acac)2L, or simple addition of two ligands per dimer without breakage of bridge bonds, to give structures involving 6-coordination for the titanium atoms. Moreover, in view of the change in $\nu_{V=O}$ for $VO(acac)_2$ on adduct formation, it was hoped that changes might be observed for the Ti 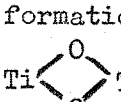 Ti stretching frequencies, which would then facilitate their assignment.

Dissolution of $[TiOCl(acac)]_2$ in pyridine, methylcyanide, trimethylamine and trimethylphosphine yielded yellow-orange solutions. Evaporation to dryness in vacuo, however, yielded the starting material in each case (from a study of the infrared spectra). Thus, it must be concluded that no stable adducts are formed at room temperature, and it is relevant to note that a similar state of affairs exists for $TiO(acac)_2$ (39). It is certainly evident that for both these compounds, it is not possible to break the titanium oxygen bridge bonds by adduct formation.

II.6. The Attempted Preparation of $TiCl(acac)_2$.

In view of the fact that $TiO(acac)_2$ can be prepared by the oxidation of $Ti(acac)_3$, presumably via the oxidation:

$$4Ti(acac)_3 + 2H_2O + O_2 \longrightarrow 4TiO(acac)_2 + 4Hacac,$$

an attempt was made to prepare the analogous intermediate for $TiOCl(acac)$. Assuming that both reactions proceed via a similar path, this would be expected to be $TiCl(acac)_2$.

The interest in isolating this compound stemmed from the possibility of employing it as a route to the compound $TiF(acac)_2$, which would be isoelectronic with $VO(acac)_2$ and might be expected to be monomeric. The preparation of what was claimed to be dimeric $TiCl(acac)_2$ (by refluxing $TiCl_3$ and Hacac under nitrogen) has been reported (44), but repetition of this during the course of the present work resulted in the formation of a brown tar, in contrast

to the red, air stable, solid reported. More recent work, however, has shown that the product of this reaction contains quadrivalent rather than tervalent titanium, and that it may contain an oxygen atom bridging the two halves of the molecule (40). In view of this result, a second approach was tried, involving the reaction of $TiCl_3$ and thallous acetylacetonate in methylcyanide solution.

$$TiCl_3 + 2Tl(acac) \rightarrow TiCl(acac)_2 + 2TlCl$$

A blue solution was obtained, together with a white precipitate of thallous chloride, on mixing together solutions of the reactants in methylcyanide under nitrogen. Evaporation of the blue solution in vacuo, however, yielded only a brown tarry residue.

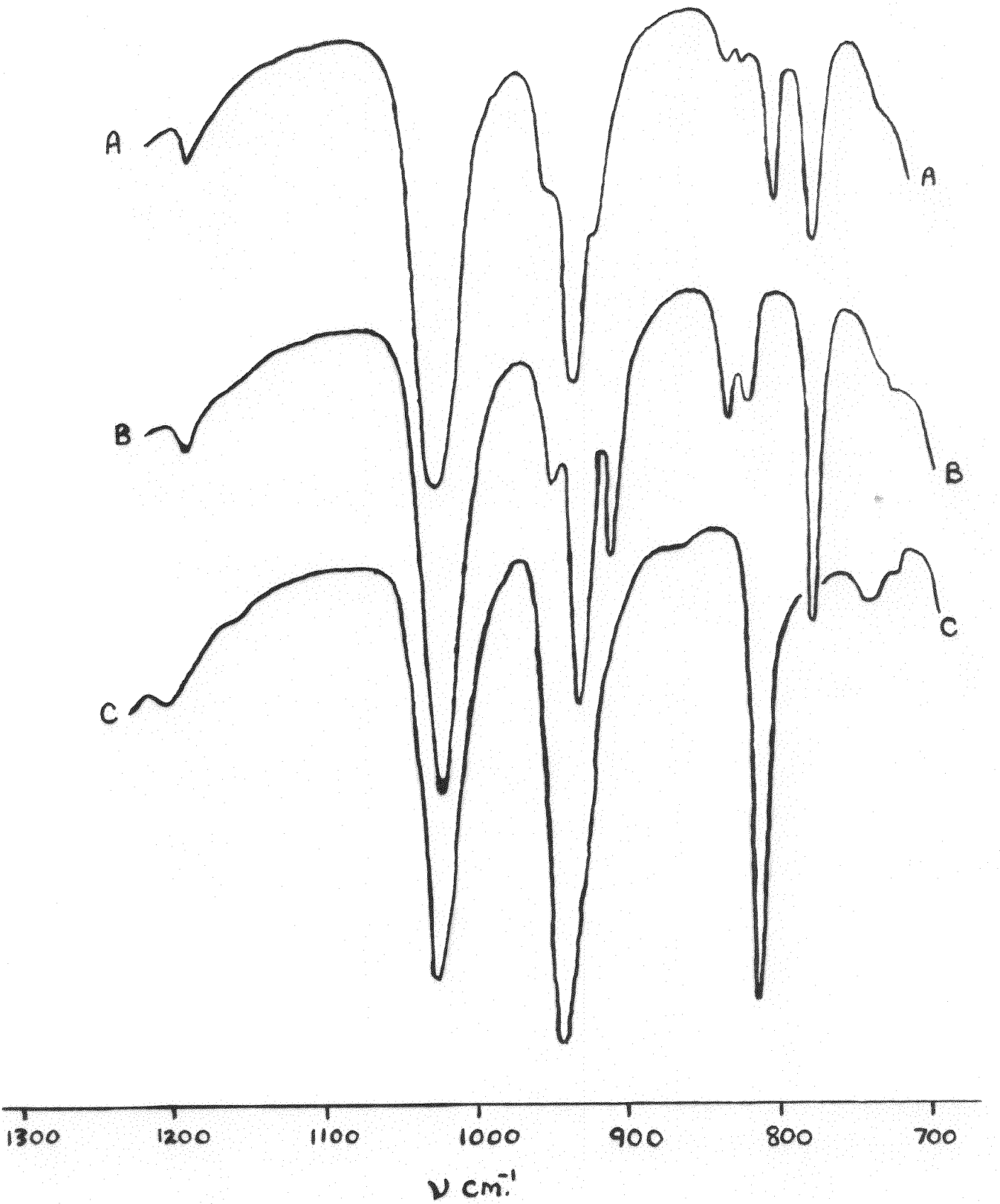

FIGURE II.1. THE SEPARATION OF THE $TiO(acac)_2$/$TiOCl(acac)$ MIXTURE: INFRARED SPECTRA OF (A) MIXTURE (B) $TiO(acac)_2$ (C) $TiOCl(acac)$.

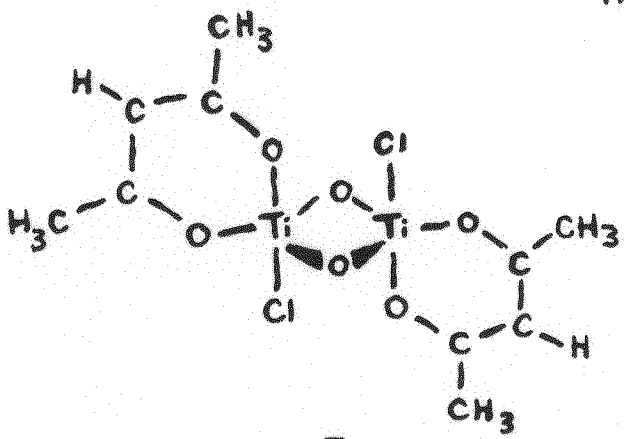

I

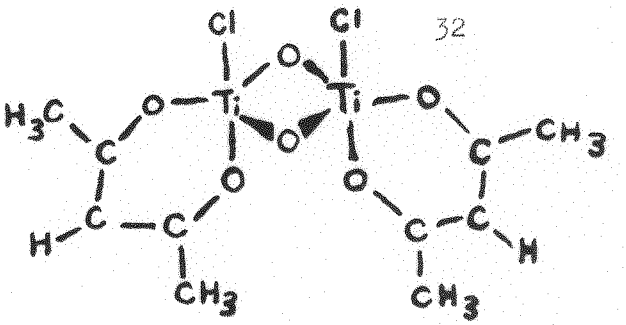

II

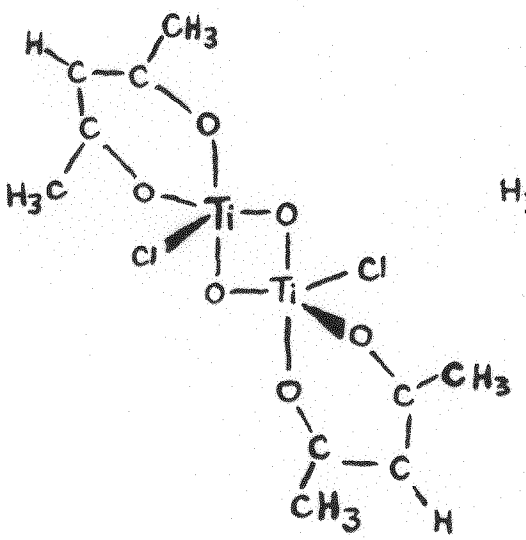

III

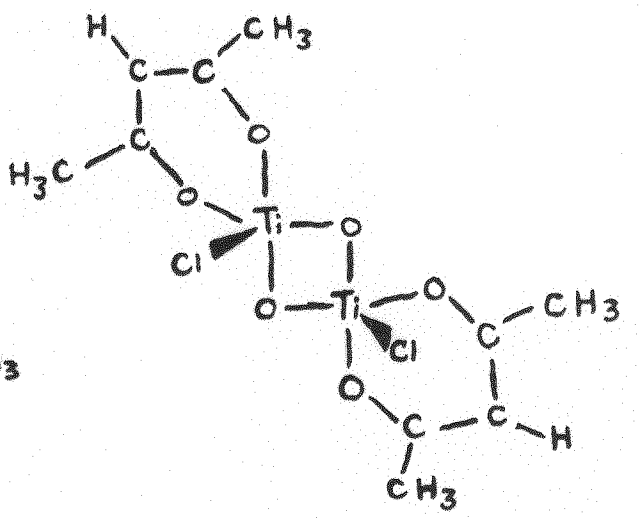

IV

FIGURE II.2. THE POSSIBLE OXYGEN BRIDGED DIMERIC STRUCTURES FOR TiOCl(acac)

T A B L E II. 1.

The Separation of the $TiO(acac)_2$/TiOCl(acac) Mixture.

The near infrared spectra of (A) the mixture; (B) $TiO(acac)_2$ ("insoluble component"); (C) TiOCl(acac) (soluble component) (ν $cm.^{-1}$)

A	B	C
1280 v.s.	1280 v.s.	1280 v.s.
1025 v.s.	1025 v.s.	1025 v.s.
947 m.sh.	947 m.sh.	-
930 v.s.	930 v.s.	940 v.s.
910 s.	910 s.	-
830 w.	830 w.	-
820 w.sh.	819 w.sh.	-
810 m.	-	810 v.s.
770 s.	772 s.	-
-	-	730 w.
688 m.	688 m.	685 m.
665 m.	665 m.	-
655 m.sh.	-	650 m.

TABLE II. 2.

Infrared and Raman Spectra of $[TiOCl(acac)]_2$.

(Infrared Spectra taken as Nujol Mulls).

Infrared ν cm.$^{-1}$	Raman $\Delta\nu$ cm.$^{-1}$	
	Solid	Soln. in Benzene
1280 v.s.	1200 w.	1200 v.w.
1025 v.s.	1028 w.	1025 v.w.
940 v.s.	940 m.	940 w.
810 v.s.	-	-
730 w.	-	750 m.br.(P).
685 m.	685 w.	690 w.(br.)
650 m.	647 w.	-
592 s.	575 w.	-
557 w.	540 m.	540 w.(br.)
464 s.	460 v.s.	460 s.(P).
424 m.	413 w.	416 w.
340 v.s.	338 v.s.	340 s.(P).
295 w.	285 w.	286 w.(br.)
269 m.	265 w.	260 v.w.
232 m.	230 m.(br.)	226 w.(br.)
196 s.	180 m.(br.)	
	133 s.	

TABLE II. 3.

Far Infrared and Solid State Raman Spectra of $TiO(acac)_2$.

(Infrared Spectrum as Nujol Mull)

Infrared (ν cm.$^{-1}$)	Raman ($\Delta\nu$ cm.$^{-1}$)
	1028 v.w.
	950 w.
	916 w.
773 s.	693 m.
688 m.	674 m.sh.
665 m.	657 w.
605 s.	-
570 w.	588 w.
555 w.	560 v.w.
506 s.	-
-	473 v.s.
438 s.	450 m.
-	395 w.
355 m.	358 w.
304 m.	-

TABLE II. 4.

100 mc/sec. ^{1}H. NMR. Spectrum of a 0.1 M Solution of TiOCl(acac) in Dichloromethane -d_2 at 25°C.

(Peak positions measured in cps. relative to tetramethylsilane as reference)

	Ring hydrogen (a)	Ring methyl hydrogens (b and c)
Peak positions	571.2	222.5; 212.7
Relative Intensities	1	3 ; 3

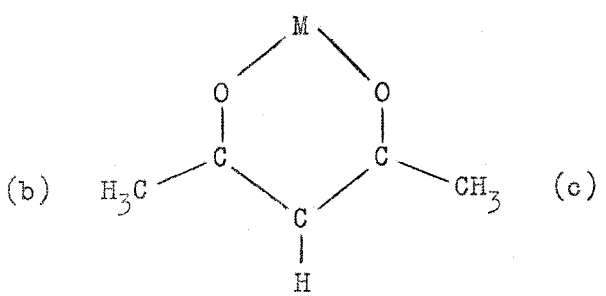

(a)

II.7. Experimental.

Preparation of solvents and reagents. Solvents and reagents used in the preparation of TiOCl(acac) and the mixture of this with $TiO(acac)_2$ were of normal laboratory reagent grade. Solvents for molecular weight determinations were dried over calcium hydride. Pyridine was dried over molecular sieve 4a, distilled and stored over molecular sieve 4a. Methylcyanide was dried over calcium hydride and stored in vacuum ampoules. Titanium trichloride was freed of hydrogen chloride by pumping for 24 hours, and was stored in vacuum ampoules. Acetylacetone for the $TiCl_3$ experiment was dried over molecular seive 4a, and stored in vacuum ampoules. Thallous acetylacetonate was prepared by a method described in the literature (45) and warmed to 60°C with pumping to remove moisture, and stored in vacuum ampoules.

Analyses. Carbon and hydrogen were determined by normal micro-analytical combustion methods. Chloride was determined gravimetrically as silver chloride by precipitation from methylcyanide solutions. The silver chloride was collected on a sinter, dried and weighed to constant weight, the silver chloride dissolved away by washing with ammonium hydroxide, and the sinter dried and weighed to constant weight. This procedure corrected for the possibility of errors arising from the precipitation of TiO_2 along with the silver chloride.

Spectra. Infrared spectra were recorded as Nujol Mulls on Perkin Elmer 337 (> 500 $cm.^{-1}$) and Beckman IR11 (500 $cm.^{-1}$) spectrometers, and Raman spectra on a Cary 81 spectrometer with helium/neon laser excitation. The ^{1}H. NMR. spectrum was recorded on a Varian Associates HA-100 spectrometer.

Preparation and separation of the $TiO(acac)_2$/TiOCl(acac) mixture. A solution of titanium tetrachloride (10 ml.) in concentrated hydrochloric acid (40 ml.) was reduced with metallic tin, filtered and diluted with water (40 ml.). The resulting solution was added dropwise under nitrogen, with vigorous stirring, to a mixture of acetylacetone (30 ml.) in benzene (100 ml.) and sodium carbonate (20 g.) in water (200 ml.). On completion of the reaction, as indicated by the subsidence of the evolution of carbon dioxide, the dark blue benzene layer was separated off, washed with boiled out water and dried over anhydrous magnesium sulphate. The dried benzene solution was then allowed to oxidise in the open air, resulting in a yellow-brown solution. On evaporation this yielded yellow crystals, which gave the I.R. spectrum (a) quoted in Table II.1.

The crude product was digested with benzene and filtered. The undissolved yellow solid gave the I.R. spectrum of $TiO(acac)_2$ (Table II.1. (b)) and the filtrate on evaporation to dryness and recrystallisation from dichloromethane yielded colourless crystals which gave the I.R. spectrum (c) quoted in Table II.1.

Analyses of components.

(1) Yellow solid, sparingly soluble in benzene:

Found: C, 44.37; H, 5.18%; $TiO(C_5H_7O_2)_2$ requires: C, 45.81; H, 5.34%.

(2) Colourless crystals soluble in benzene:

Found: C, 30.72; H, 3.65%; $TiOCl(C_5H_7O_2)$ requires C, 30.24; H, 3.65%.

Preparation of TiOCl(acac). The preparation described above was carried out, this time using acetylacetone (20 ml.) and sodium carbonate (14 g.). The addition of the titanium (III) solution was carried out in the open air, and the blue-purple product formed in the benzene layer allowed to oxidise *in situ*. The resulting yellow benzene solution was separated off, washed with water, dried over anhydrous magnesium sulphate, and evaporated to dryness yielding a yellow-brown solid. The complex was digested with methanol to remove most of the tarry brown material, and then recrystallised from dichloromethane as colourless crystals.

Analysis and molecular weight.

Found: C,30.35; H, 3.7; Cl, 17.58%; M, 346 (0.3 mM. in CH_2Cl_2); 416 (1.0 mM in C_6H_6). $TiOCl(C_5H_7O_2)$ requires C, 30.24; H, 3.65; Cl, 17.06%; M, 397.

Reaction of TiOCl(acac) with neutral ligands. Dissolution of TiOCl(acac) in pyridine gave a yellow solution which, on removal of the pyridine *in vacuo* yielded a white solid giving an infrared

spectrum identical to that of TiOCl(acac), with no additional bands due to pyridine.

Precisely similar results were found for dissolution of TiOCl(acac) in methylcyanide, trimethylamine and trimethylphosphine.

Reaction of $TiCl_3$ with acetylacetone. $TiCl_3$ (3 g.) was refluxed with acetylacetone (4 g.) under nitrogen for four hours. A dark brown tar was obtained.

Reaction of $TiCl_3$ with Tl(acac). $TiCl_3$ (1 g.) and Tl(acac) (2 g.) were mixed as solutions in methylcyanide under nitrogen. A white precipitate and a blue solution were obtained. The blue solution was filtered off and the methylcyanide removed by distillation in vacuo, leaving a dark brown tarry residue.

C H A P T E R III.

The vibrational spectra of the 1:1 adducts of phosphine, methylphosphine, dimethylphosphine and trimethylphosphine with titanium tetrachloride.

III.1. Introduction.

The existence of pentacoordinate compounds for the elements of groups III(b), IV(a), IV(b) and V(b) is now known to be quite widespread (46), (11). In particular, adducts of the type LMX_4 are known for silicon, germanium, tin and titanium (with L = trimethylamine) and there is an accumulation of evidence for formulating these as pentacoordinate monomers, (11), (47), (52), both in the solid state and in solution in non-polar solvents.

The assumption of trigonal bipyramidal coordination for these adducts leads to the possibility of two isomeric forms, (I), (II) possessing C_{2V} or C_{3V} symmetry respectively.

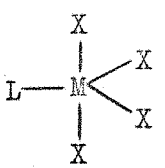

(I) C_{2V}

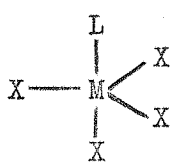

(II) C_{3V}

Prediction of the actual symmetry observed in any given case of LMX_4 coordination may involve several factors. From a consideration of the electronegativities of the coordinating atoms, Muetterties (48) has suggested that, other factors being equal for pentacoordinate light atoms of d^0configuration (e.g. P(V)), the most electronegative ligand atoms will occupy the axial positions. This is rationalised on the assumption that the bonding orbitals used by the central acceptor atom in pentacoordinate species can be described approximately in terms of sp^2 hybrids for the equatorial positions, and dp hybrids

for the axial positions (see Chapter VIII for a more detailed account). In the formation of σ bonds, the more electropositive ligand atoms might be expected to enjoy the greatest overlap with the sp^2 hybrids, whilst the more electronegative ligand atoms especially F and Cl, which might be supposed to form more ionic bonds, would form stronger bonds in the axial positions, involving dp hybrid orbitals of the central acceptor atom. In agreement with this, a C_{2V} formulation for OSF_4 is indicated from an analysis of its vibrational spectrum (49), (50), whilst for $FPCl_4$ a C_{3V} formulation is suggested (51). Similarly, $MePCl_4$ is most likely to possess C_{2V} symmetry (12). There is however, no basis to assume that this generalisation will hold for heavier atoms with low lying d-shells, and it is apparent moreover, that increase of the steric requirements of L might conceivably force a C_{3V} configuration. For example, the 1:1 trimethylamine adducts of the group IV tetrachlorides are all probably of C_{3V} symmetry, although here electronegativity differences are not large, and on this basis either C_{2V} or C_{3V} symmetry might be acceptable. Finally, although the extent of $d\pi$-$p\pi$ bonding in compounds of this sort is very much an unknown factor, on the assumption that Cl ligands will participate in this to a larger extent than R_3N, it has been suggested (8) from symmetry arguments, that C_{3V} symmetry appears to be favoured by considerations of π-bonding. However, it is likely that, in the compounds discussed here, π-bonding effects are not as important as electronegativity and steric

considerations, in determining stereochemistry.

In the case of $TiCl_4$, the adduct $TiCl_4,NMe_3$ has been formulated as a monomeric five coordinate species with axial Me_3N (52), (11). In view of the C_{2V} stereochemistry likely for $MePCl_4$ (12), it was thought that the adduct $TiCl_4,NH_3$, if it existed, might exhibit C_{2V} trigonal bipyramidal stereochemistry, and if so, comparison of the series $TiCl_4,L$ where $L = NH_3,MeNH_2,Me_2NH,Me_3N$ might bring out the relative importance of electronegativity and steric considerations in determining the stereochemistries of these adducts. Unfortunately, there is ample evidence of the instability of adducts of protonic amines with $TiCl_4$ relative to ammonolysis type reactions (53).

However, since the compounds $TiCl_4,PH_3$ and $TiCl_4,2PH_3$ had both been characterised (54), and did not appear to undergo decomposition reactions of this type, it was decided to attempt the preparation and characterisation of 1:1 complexes of titanium tetrachloride with the series of phosphine ligands, PH_3, $MePH_2$, Me_2PH and Me_3P. This series represented a regular increase in steric requirements, and moreover the electronegativity difference between P in R_3P and Cl is rather more clearcut than in the case of R_3N. It was hoped that, from an analysis of the vibrational spectra of these compounds, their probable geometries might be deduced, assuming them to be pentacoordinate monomers based on a trigonal bipyramidal model. Assuming that Muetterties' generalisations

for pentacoordinate light atoms (48) might possibly be applicable to $LTiCl_4$ species, it was hoped by this means to be able to assess the relative importance of electronegativity and steric effects in determining their geometry. It should be noted that π-bonding effects may be much more important for titanium (IV) than for the case of the group IV(b) tetrahalides, due to the much lower energy of the 3d metal orbitals.

Alkyl phosphine and sulphide complexes of group IV tetrahalides are quite common, and, in qualitative terms, generally appear to be at least of comparable stability with the analogous oxygen and nitrogen coordinated complexes. Although in the classification of acceptors, Si^{4+}, Ge^{4+}, Sn^{4+} and Ti^{4+} are normally considered to exhibit "class a" or "hard" acceptor properties*, the existence of stable phosphorus and sulphur complexes of the group IV tetrahalides is not necessarily surprising, since, firstly, the two common schemes of classification of donors and acceptors were drawn up on the basis of values of thermodynamic quantities for the formation of metal halides from metal ions and halide ions either in the gas phase or in aqueous solution, and secondly, the acceptor properties of MX_4 need not necessarily bear much similarity to those of M^{4+}.

*See Chapter VIII for a discussion of the classification schemes for donor-acceptor interactions.

Although a certain amount of work has appeared on the vibrational spectra of phosphine and alkyl phosphine adducts of the group III(b) halides (55), (56), and on some trimethylphosphine adducts of the group IV(b) tetrahalides (47), the work on adducts of the titanium tetrahalides is quite scarce. The preparation and vapour pressures of the weak complexes $TiCl_4,PH_3$ and $TiCl_4,2PH_3$ have been reported (54), whilst Chatt (57) has prepared adducts of titanium tetrachloride with PEt_3 (1:2); $P(C_6H_5)_3$ (1:2); $C_2H_4(PMe_2)_2$ (1:1) and $O\text{-}C_6H_4(PMe_2)_2$ (1:1). In a paper dealing with complex formation between $TiCl_4$ and some mono- and bi-dentate ligands involving P, As, S and Se donor atoms, Westland (58) describes both 1:1 and 1:2 complexes between $TiCl_4$ and triphenylphosphine. Infrared spectra (down to 250 $cm.^{-1}$) are reported for these complexes, and bands are assigned to Ti-P stretching vibrations, in a rather arbitrary way.

In view of this rather unsatisfactory state of affairs, the work described in this chapter was initiated by a re-examination of the vibrational spectra of $TiCl_4,Me_3N$. Information from the infrared was extended down to 33 $cm.^{-1}$, and the advent of lasers opened up the possibility of obtaining, for the first time, information on the Raman spectra of the solid adduct in addition to a more complete spectrum for the adduct in solution. The results obtained are compared with Beattie and Gilson's earlier and more limited data (11) and with the calculated spectra for both C_{2V} and C_{3V} models based on a trigonal bipyramid.

Using this as a point of departure, the 1:1 phosphine complexes of $TiCl_4$ with PH_3, $MePH_2$, Me_2PH and Me_3P were prepared and characterised. The vibrational spectra were then measured and interpretation in terms of molecular geometry attempted, in conjunction with the results of calculations of the vibrational spectra to be expected from both C_{2V} and C_{3V} models.

As stated earlier for LMX_4 (L taken as a point mass), the two possibilities for pentacoordinate monomers based on a trigonal bipyramidal geometry are shown as in (I) and (II).

For the C_{3V} case, the normal modes in cartesian coordinates split up (after removal of translational and rotational modes) as:

$$\Gamma_{mol} = 5A_1 + A_2 + 3E$$

The A_1 and E modes are both Raman and infrared active, whilst the A_2 mode is inactive in both and need not be considered. For the C_{3V} case there are therefore eight fundamental vibrational modes, and of these, three are expected to occur in the "Ti-Cl stretching region", namely $2A_1 + E$, since lowering the symmetry of tetrahedral $TiCl_4$ from Td to C_{3V} results in a splitting of the two "stretching" modes for the Td case as follows:

$$T_d \longrightarrow C_{3V}$$
$$a_1 \longrightarrow a_1$$
$$f_2 \longrightarrow a_1 + e$$

For the C_{2V} case the normal modes split up as:

$$\Gamma_{mol} = 5A_1 + A_2 + 3B_1 + 3B_2$$

All modes are both Raman and infrared active except the A_2 mode which is Raman active only.

For the C_{2V} case there are therefore twelve fundamentals, and of these four ($2a_1 + b_1 + b_2$) might be expected to occur in the Ti-Cl stretching region, since we have:

$$T_d \longrightarrow C_{2V}$$
$$a_1 \longrightarrow a_1$$
$$f_2 \longrightarrow a_1 + b_1 + b_2$$

In addition to the three (C_{3V}) or four (C_{2V}) skeletal Ti-Cl stretching fundamentals occurring in this region we must consider the possibility of the occurrence of the Ti-P vibration in this region, and in addition the occurrence of both the deformational and PC_3 rocking modes of the ligands Me_3N and Me_3P. If these ligand modes are readily identifiable, then in principle it should be possible to differentiate between C_{2V} and C_{3V} LMX_4, provided that the position of νTi-P does not complicate matters, simply on the basis of the number of "Ti-Cl stretching modes" observed in the spectra. The reliability of this simple approach is examined in the light of the observed results and of the results of the calculations for LMX_4 in C_{2V} and C_{3V} symmetries.

III.2. The Adducts $TiCl_4$,NMe_3 and $TiCl_4PMe_3$.

(i) $TiCl_4$,NMe_3. The adduct was prepared as described in the literature (52). It is known to be monomeric in solution in benzene

(52), (11), and has been formulated in terms of a C_{3V} structure on the basis of its vibrational spectra.

The vibrational spectra obtained during the course of this work for this adduct are collected in Table III.1. whilst the corresponding data for the adduct with deuteriated trimethylamine $(CD_3)_3N$ are given in Table III. 2. The data in Table III. 1., agree closely with the measurements of Beattie and Gilson (11), although the infrared measurements given here represent an extension of the region examined down to 33 $cm.^{-1}$. More extensive Raman data for solutions in benzene plus the spectrum of the solid powdered adduct are also given.

Bands occurring in the stretching region (500 - 300 $cm.^{-1}$) call for little comment, the assignment given in Table III. 1. agreeing with that of Beattie and Gilson (11) on the basis of a C_{3V} model. Comparison of Tables III. 1. and III. 2. reveal that on deuteriation the 500 $cm.^{-1}$ band (polarised) shifts by approximately 60 $cm.^{-1}$ and the 435 $cm.^{-1}$ band on deuteriation, appears to be masked by the bands occurring in the region 450 - 340 $cm.^{-1}$, in the infrared. It is likely that the band at 390 $cm.^{-1}$ in the Raman spectra (Table II. 2.) corresponds to this band, representing a shift of approximately 50 $cm.^{-1}$. In view of these shifts, their assignment as the symmetric and antisymmetric ligand deformations respectively, seems to be a realistic one, especially since, as has been observed before (11), bands in these two regions are found for a wide variety of trimethylamine complexes. The band at 456 $cm.^{-1}$, shifting to 420 $cm.^{-1}$ on

deuteriation and absent in the Raman effect, is confirmed as the e type vibration of the planar $TiCl_3$ grouping. The two remaining bands in this region, both strong and polarised in the Raman and practically unaffected by deuteriation can be assigned as the two a_1 Ti-Cl stretching vibrations. The changes in frequency and relative intensity for these two bands on comparing solid and solution data are disturbing, but it is worth noting that Beattie and Gilson observed a precisely similar frequency shift for the 368 - 388 $cm.^{-1}$ band in the infrared. Assuming that these changes are due to some perturbation in the solid state, from the solution data, it is tempting to assign the a_1 equatorial stretching mode to the band at 348 $cm.^{-1}$ (strong and narrow) and the a_1 axial stretching mode to the broader band at 380 $cm.^{-1}$. However, it should be borne in mind that the results of the vibrational analysis performed for this molecule by Gilson (8) indicate that considerable mixing of these two modes is to be expected. They have therefore been bracketed together in the partial assignment of Table II. 1.

For the region of the spectrum below 300 $cm.^{-1}$, the deuteriation shift of approximately 20 $cm.^{-1}$ for the weak polarised band at 210 $cm.^{-1}$ suggests that it is the a_1 titanium-nitrogen stretching vibration. The position, intensity, polarisation data and deuteriation shift agree well with single crystal Raman data on the related compound $GeCl_4,NMe_3$ where the a_1 Ge-N vibration has been assigned at 232 $cm.^{-1}$. The value of 210 $cm.^{-1}$ for the Ti-N

stretching frequency agrees well with that calculated by Gilson (8) for a value of the titanium-nitrogen bond stretching force constant = 0.8 → 1.5 md . $Å^{-1}$. For this range of values the frequency of the a_1 Ti-N stretching mode was calculated to be in the range 191 → 228 $cm.^{-1}$.

(ii) $\underline{TiCl_4}$,$\underline{PMe_3}$. Since the assignment of the vibrational spectrum of the adduct $TiCl_3$,NMe_3 can be most satisfactorily carried out on the basis of the C_{3V} model, the adduct $TiCl_4$,PMe_3 was next examined.

It has recently been shown that the 1:2 adduct of silicon tetrachloride with trimethylphosphine is the only species formed during tensiometric titration of the reagents at room temperature (47), and is the only species detectable (by vibrational spectroscopy) in solution in benzene. By contrast, titanium tetrachloride and tertiary phosphines form both 1:1 and 1:2 complexes (57), (58). Accordingly, both 1:1 and 1:2 adducts of titanium tetrachloride with trimethylphosphine have been isolated and studied in this work. The 1:2 adduct is described in Chapter IV.

The 1:1 adduct was prepared by mixing benzene solutions of Me_3P and $TiCl_4$. ($TiCl_4$ in excess). It was obtained as dark red lustrous crystals, which were very soluble in common organic solvents. A cryoscopic molecular weight determination showed that the adduct is monomeric in benzene solution.

The vibrational spectra obtained for this adduct are summarised in Table III. 3. Comparison of the infrared data with that of $TiCl_4,NMe_3$ reveals a high degree of similarity between the two. The bands due to the Me_3N deformations are of course absent, the corresponding modes for Me_3P coming much lower, generally in the ranges 350 - 315 $cm.^{-1}$ for the symmetric deformation and 270 - 255 $cm.^{-1}$ for the antisymmetric deformation. In the infrared, four bands are seen in the Ti-Cl stretching region, a fact which might at first sight appear to favour the C_{2V} formulation. However, the strongly similar Raman spectra of $TiCl_4,PMe_3$ and $TiCl_4,NMe_3$ (Table III. 3. and Figure III. 1.) suggest that the complexes might well have the same shapes. If this is so, then only three of the four bands in the stretching region of the infrared of $TiCl_4,PMe_3$ can be "Ti-Cl stretching modes". Since the fourth is unlikely to be the symmetric ligand deformation, when Raman activities are considered, the most likely possibility is that it is the a_1 titanium phosphorus stretching mode.

Turning to the Raman spectra, it should be noted here, that the spectrum obtained using the 60 milliwatt He/Ne laser as source was quite weak, due to the very dark red colour of the adduct. Decomposition of the adduct in the laser beam was observed, giving rise to a very strong sharp band at 320 $cm.^{-1}$, the intensity of which increased with time. This band could possibly arise either by decomposition into $TiCl_6^{2-}$ (ν_1 observed in the Raman at 320 $cm.^{-1}$,

strong and sharp (59)) or into $TiCl_4,2PMe_3$ which also has a strong sharp band at 320 cm.$^{-1}$ in the Raman effect (see Chapter IV). The bands quoted in Table III. 3. are those which decreased with time. Examination of the Raman spectrum of a solution of the complex in benzene revealed only the band at 355 cm.$^{-1}$ (polarised), and no band at 320 cm.$^{-1}$.

The obvious similarity of the spectra of $TiCl_4,Me_3N$ and $TiCl_4,Me_3P$ (especially the Raman spectra - see Figure III. 1.) leave little doubt that this latter adduct also adopts a trigonal bipyramidal structure with C_{3V} symmetry. In Tables III. 4. and III. 5. are given the frequencies calculated for the C_{2V} and C_{3V} models respectively. Details of the vibrational analysis are given in Appendix A. The results quoted are for a value of the titanium-phosphorus bond stretching force constant (f_{Ti-P}) = 1.8 m.d. Å^{-1}, this value giving the "best fit" of calculated to observed frequencies. A comparison of Tables III. 3. III. 4. and III. 5., reveal that the results for the C_{3V} calculation do not agree more closely with the observed spectra than do the results obtained for the C_{2V} case. The main contributors to each calculated frequency are listed (only potential energy contributions > 25% listed; contributions > 75% listed as "pure" modes). However, the results of Tables III. 4. and III. 5., suggest considerable mixing of the a_1 titanium-chlorine stretching modes with both the a_1 titanium-phosphorus stretching mode and the symmetric Me_3P deformation. The

calculation for $TiCl_4,NMe_3$ suggested that little mixing occurred between skeletal and ligand vibrations in this case (8), and that separation into skeletal and ligand modes was a reasonable approximation. The results given here suggest that coupling between skeletal and ligand modes is likely to be much more serious in the case of Me_3P complexes, and that assignment of bands in terms of individual normal vibrational modes is less realistic.

Despite the ambiguous results obtained for the C_{2V} and C_{3V} calculations for this molecule, the extreme similarity of the vibrational spectra observed for $TiCl_4,NMe_3$ and $TiCl_4,PMe_3$ together with the molecular weight data, suggest that a trigonal bipyramidal structure with C_{3V} symmetry is most likely for both of these adducts.

III.3. The Adduct $TiCl_4,PH_3$.

The adduct was prepared by mixing titanium tetrachloride with an excess of phosphine at -127°C. Removal of excess reactants left a yellow amorphous powder, easily sublimable to orange yellow crystals. The vapour pressure above the solid was measured and found to be 6 mm. at 0°C and 30 mm. at 25°C. This agrees well with the value quoted in the earlier literature (54). The high dissociation pressure of this adduct meant that no infrared mull or solution spectra could be obtained. In either case only bands due to free $TiCl_4$ were obtained. Raman spectra were taken on samples at equilibrium in ampoules filled on a vacuum line. Infrared data were obtainable only from samples

sublimed onto a caesium iodide plate cooled to liquid nitrogen temperatures, and these were of rather poor quality.

The Raman and infrared data for both $TiCl_4,PH_3$ and $TiCl_4,PD_3$ are summarised in Tables III. 6. and III. 7. Comparison of the data in Table III. 6. with that in Table III. 3. and comparison of the corresponding Raman spectra in Figures III. 1. and III. 2. will show immediately that the solid state Raman spectrum of $TiCl_4,PH_3$ is very different from that of $TiCl_4,PMe_3$. In particular there are many more strong bands in the region 500 - 280 $cm.^{-1}$ for the PH_3 case. This immediately suggests a C_{2V} formulation for this adduct. In support of this suggestion we may note that the Raman spectrum of $MePCl_4$ is in many ways extremely similar (12). For example, in $MePCl_4$ the a_1 PCl_2 equatorial stretch of the assumed C_{2V} species is assigned at 441 $cm.^{-1}$ (strong and polarised in the Raman effect), while the corresponding a_1 axial PCl_2 stretch is assigned at 288 $cm.^{-1}$ (medium and polarised in the Raman effect). By contrast, for $FPCl_4$ (60) the a_1 PCl_3 equatorial stretch of the C_{3V} species is assigned at 422 $cm.^{-1}$ (very strong and polarised in the Raman effect) while the corresponding a_1 axial PCl stretch is assigned at 384 $cm.^{-1}$ (medium weak, and polarised in the Raman effect). It is evident that the Raman spectra of $TiCl_4,NMe_3$, $TiCl_4$, PMe_3 and $FPCl_4$ are similar (probably C_{3V}) and that those of $TiCl_4$, PH_3 and $MePCl_4$ are similar (probably C_{2V}).

Calculated spectra for both $TiCl_4,PH_3$ and $TiCl_4PD_3$ (values in

parentheses) are quoted in Tables III. 8. and III. 9. for C_{2V} and C_{3V} models respectively. In support of the correlation of bands suggested by the comparison of the Raman spectra of $MePCl_4$ and $TiCl_4,PH_3$ outlined above, the calculations based on the C_{2V} model suggest that the bands at 286 cm.$^{-1}$ and 426 cm.$^{-1}$ be assigned to the a_1 $TiCl_2$ axial and equatorial stretches, although the list of principal contributions to each mode included in these Tables suggest that mixing of these two modes will occur, and that they will also be mixed appreciably with the a_1 P-Ti stretching mode. The data in Table III. 7. for $TiCl_4,PD_3$ suggest that the shoulder at 450 cm.$^{-1}$ (shifting under the 426 cm.$^{-1}$ band on deuteriation) should be assigned principally as the a_1 P-Ti stretch. No other shifts of this magnitude are observed in either the infrared or the Raman effect, so that the assignment of this band to the a_1 P-Ti stretch can be made with some confidence.

The band around 385 cm.$^{-1}$ in the Raman effect might at first be assigned as ν_1 of any free $TiCl_4$ due to dissociation. However, the band is asymmetric, and examination of the liquid nitrogen temperature Raman spectrum (Figure III. 3.) shows that this band, though weaker in intensity relative to the 426 cm.$^{-1}$ band, is still present. Since no appreciable dissociation of the adduct into free $TiCl_4$ is to be expected at this temperature, it must be concluded that this residual band represents a genuine band due to the adduct - possibly the b_1 TiCl equatorial stretch.

It is extremely unfortunate that the unstable nature of this compound rendered the measurement of solution spectra, and the determination of its molecular weight impossible. In lieu of molecular weight studies, a matrix isolation study on this adduct was carried out. Figure III. 3. shows the Raman spectra obtained for (a) pure $TiCl_4,PH_3$; (b) 10 mol. % $TiCl_4,PH_3$ in tetramethylsilane as substrate; and (c) 4 mol. % $TiCl_4,PH_3$ in tetramethylsilane, all run at liquid nitrogen temperatures. The similarity of the matrix Raman spectra (once the tetramethylsilane bands have been accounted for) with the spectrum of the pure adduct suggest that the adduct is, like $TiCl_4,PMe_3$, monomeric. The change in relative intensity of the 420 $cm.^{-1}$ and 385 $cm.^{-1}$ bands is somewhat disturbing. However, since there is likely to be some free $TiCl_4$ and free PH_3 in the dilute matrix, the increase in intensity on dilution of the 385 $cm.^{-1}$ band is most likely to be due to ν_1 of free $TiCl_4$.

In conclusion it can be said that from the observed and calculated results discussed above, that the adduct $TiCl_4,PH_3$ probably adopts a trigonal bipyramidal C_{2V} structure. The great difference in the Raman spectra of $TiCl_4,PMe_3$ and $TiCl_4,PH_3$, the similarity to the spectrum of $MePCl_4$ and the presence of five bands in the Ti-Cl stretching region all point to a C_{2V} formulation. The calculated spectra given for a value of f Ti-P = 1.8 md . $Å^{-1}$ are those which gave the best fit, and a comparison shows that the observed spectral results are best described by the results from the C_{2V} model. The

calculated results suggest a considerable degree of coupling between the a_1 Ti-Cl stretching modes and the a_1 Ti-Cl and a_1 Ti-P stretching modes. No ligand modes are found in the titanium chlorine stretching region, these being well separated from any modes occurring below 500cm.$^{-1}$. However, even without this complicating factor the calculations suggest that the assignment of bands to individual normal modes of vibration in the stretching region can only be regarded as an approximation.

III.4. The Adducts $TiCl_4$,PH_2Me and $TiCl_4$,$PHMe_2$

These adducts were prepared by direct reaction of the donor and acceptor. $TiCl_4$,PH_2Me was prepared by mixing an approximately 1:1 mole ratio of reactants, whilst $TiCl_4$,$PHMe_2$ was prepared by reacting Me_2PH with an excess of $TiCl_4$ in benzene solution.

Unlike the adduct $TiCl_4$,PH_3 the two adducts described here are much more stable with respect to dissociation, vapour pressures above the solid adduct were found to be approximately:

$TiCl_4$,PH_2Me	12 mm.
$TiCl_4$,$PHMe_2$	5 mm.

at 25°C. However, both these adducts, at room temperature, were found to decompose slowly to a brown yellow solid, presumably by a "phosphinolysis" reaction analogous to the ammonolysis reactions undergone in the $TiCl_4/MeNH_2$ and $TiCl_4/Me_2NH$ systems (53). However, the rate of decomposition in the phosphine adducts is much slower than

in the amine adducts; $TiCl_4,PH_3$ is indefinitely stable; $TiCl_4,PH_2Me$ decomposes slowly over the course of 1-2 months (as judged by the Raman spectrum of the solid adduct contained in a vacuum ampoule) whilst $TiCl_4,PHMe_2$ decomposes in a week. Examination of the Raman spectra of decomposed samples of these last two adducts revealed a band at 320 $cm.^{-1}$, suggesting again the presence of $TiCl_6^{2-}$ in the mixture. Since the rate of decomposition increases with the basic strength of the phosphine involved in the adduct, the following decomposition scheme is suggested as probable:

$$TiCl_4,PHMe_2 \longrightarrow TiCl_4 + PHMe_2$$

$$TiCl_4,PHMe_2 + PHMe_2 \longrightarrow TiCl_3,PMe_2 + Me_2P^+H_2Cl^-$$

$$2Me_2P^+H_2Cl^- + TiCl_4 \longrightarrow [Me_2PH_2]_2^+ [TiCl_6]^{2-}$$

To support this, a sample of $[Me_3PH]_2^+ [TiCl_6]^{2-}$ was prepared. Examination of its Raman spectrum revealed the following bands, all attributable to the $TiCl_6^{2-}$ ion (59):

ν ($cm.^{-1}$)	intensity	assignment (59)
320	v.s.	ν_1
233	v.w.br	ν_2
175	s.	ν_5

For the purpose of recording the Raman and infrared spectra of these two adducts, freshly prepared samples were always used.

The relevant vibrational spectra are recorded in Tables III. 10. and III. 11. It is immediately obvious, from an examination of Figure III. 2., that the Raman spectra of $TiCl_4,PH_3$; $TiCl_4,PH_2Me$

and $TiCl_4,PHMe_2$ are all closely similar and suggest that they all have the same shape, probably the C_{2V} trigonal bipyramidal structure. The similarity is again brought out in their infrared spectra, but it should be noted here that any band at around 490 $cm.^{-1}$ (suggested to be the b_2 axial Ti-Cl stretch by the C_{2V} calculation for $TiCl_4,PH_3$) would be masked in the case of the infrared data given here, by ν_3 of $TiCl_4$ consequent on the slight dissocation of both of these adducts in the mull and in benzene solutions.

In view of the unstable nature of $TiCl_4,PH_2Me$ and $TiCl_4,PHMe_2$, Raman spectra were also run at liquid nitrogen temperatures, because of the possibility that local heating of the sample at room temperature by the laser beam could cause decomposition. However, the low temperature spectra were identical with those recorded for samples at room temperature. In view of this it is unlikely that any of the bands observed in the Raman spectra are due to decomposition.

In conclusion, it should be stated that the solution Raman measurements for $TiCl_4,PHMe_3$ were of very poor quality and may be in error. There was some evidence for decomposition having occurred during the course of the measurement, since a small quantity of a brown solid had precipitated from the solution, and was covering the walls of the capillary Raman cell in which the solution was contained.

No molecular weight data were obtainable for these adducts, due to their instability with respect to dissociation. Nonetheless, the

great similarity between their vibrational spectra, and the corresponding data for $TiCl_4$,PH_3 strongly suggests that they are monomeric, and like the latter probably adopt a C_{2V} configuration.

III.5. Conclusion.

It is evident, from a comparison of their Raman spectra, that the 1:1 $TiCl_4$ adducts with PH_3, $MePH_2$ and Me_2PH all have the same stereochemistry. Matrix isolation studies on the $TiCl_4/PH_3$ system suggest that the complex is molecular, and it is therefore likely that all of these complexes possess a pentacoordinate trigonal bipyramidal geometry with C_{2V} symmetry.

The complexes with Me_3N and Me_3P are shown to be molecular in solution and from their vibrational spectra are expected to possess a trigonal bipyramidal structure with C_{3V} symmetry. The steric requirements of Me_3N and Me_3P are assumed to determine the structure and these ligands therefore adopt axial positions.

Since the steric requirements of Me_2PH must also be fairly large, it is quite surprising to find that the results obtained suggest that the adduct $TiCl_4$,$PHMe_2$ prefers a C_{2V} structure, with an equatorial phosphine ligand. It is evident that when steric requirements are not large, the C_{2V} structure (favoured by consideration of the electronegativities of the ligand atoms) is favoured. Even for $MePH_2$ and Me_2PH, which would seem to be quite bulky ligands, the stereochemistry adopted is that favoured by electronegativity considerations.

Steric requirements evidently do not dominate until Me_3N or Me_3P are considered.

Since the vibrational spectra for $TiCl_4,NMe_3$ and $TiCl_4,PMe_3$ suggest that these two compounds are isostructural, but neither is isostructural with $TiCl_4,PHMe_2$, powder x-ray photographs of these three adducts were taken, in order to see if they were isomorphous. The results, quoted in Table III. 12. show that none of them are isomorphous. This does not of course preclude any of them from being isostructural. The case for dividing the adducts studied into two structural types must therefore rest on the data provided by vibrational spectroscopy, until x-ray studies of single crystals of these adducts have been undertaken.

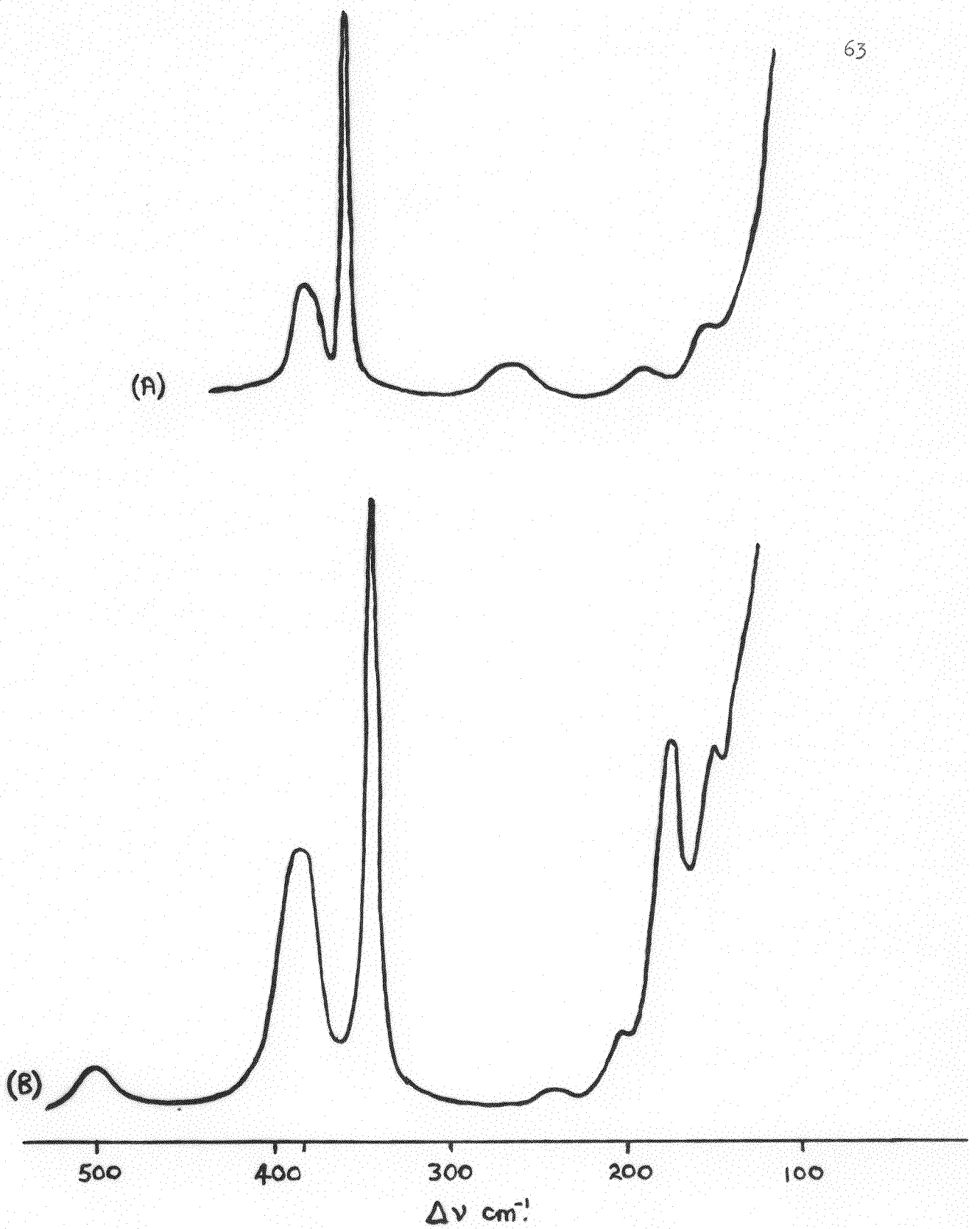

FIGURE III.1. He/Ne LASER RAMAN SPECTRA OF (A) $TiCl_4.Me_3P$ POWDER AND (B) $TiCl_4.Me_3N$ POWDER

FIGURE III.2 He/Ne LASER RAMAN SPECTRA OF

(A) $TiCl_4 \cdot PH_3$

(B) $TiCl_4 . MePH_2$

(C) $TiCl_4 . Me_2PH$

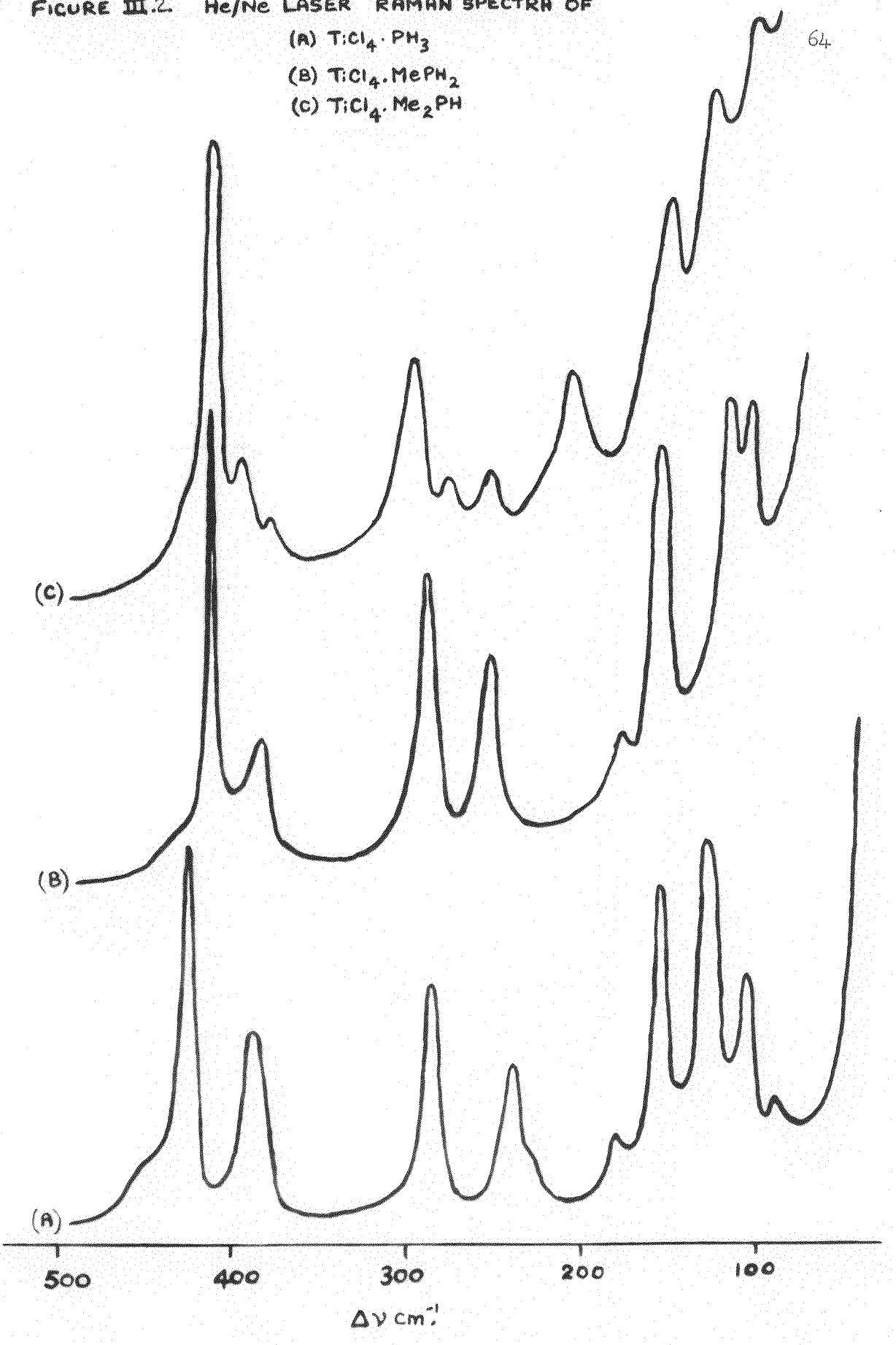

FIGURE III.3. He/Ne LASER RAMAN SPECTRA OF

(A) PURE $TiCl_4 \cdot PH_3$.
(B) MATRIX 10% $TiCl_4 \cdot PH_3$ IN 90% TETRAMETHYLSILANE.
(C) MATRIX 4% $TiCl_4 \cdot PH_3$ IN 96% TETRAMETHYLSILANE.
AT LIQUID NITROGEN TEMPERATURES.

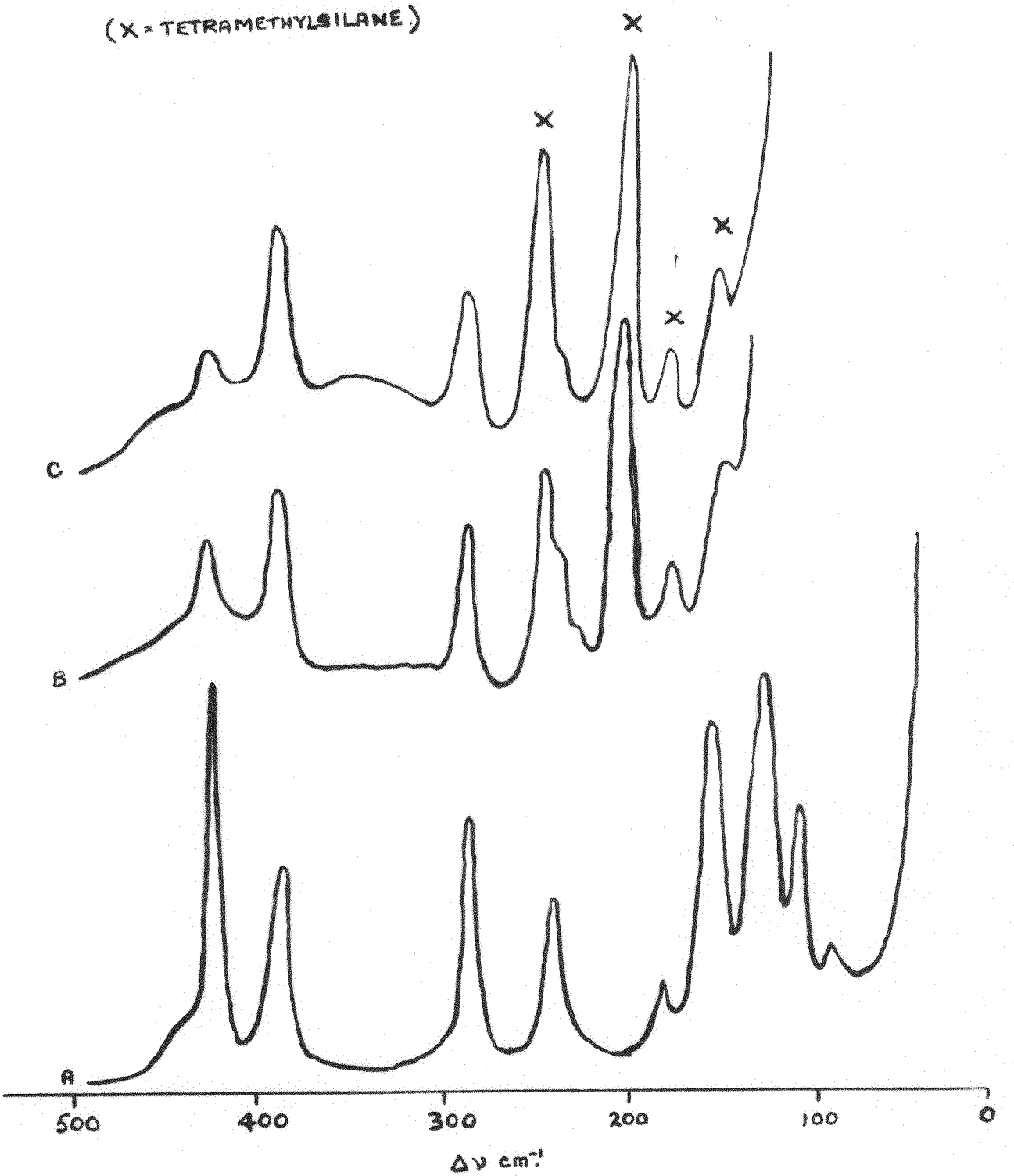

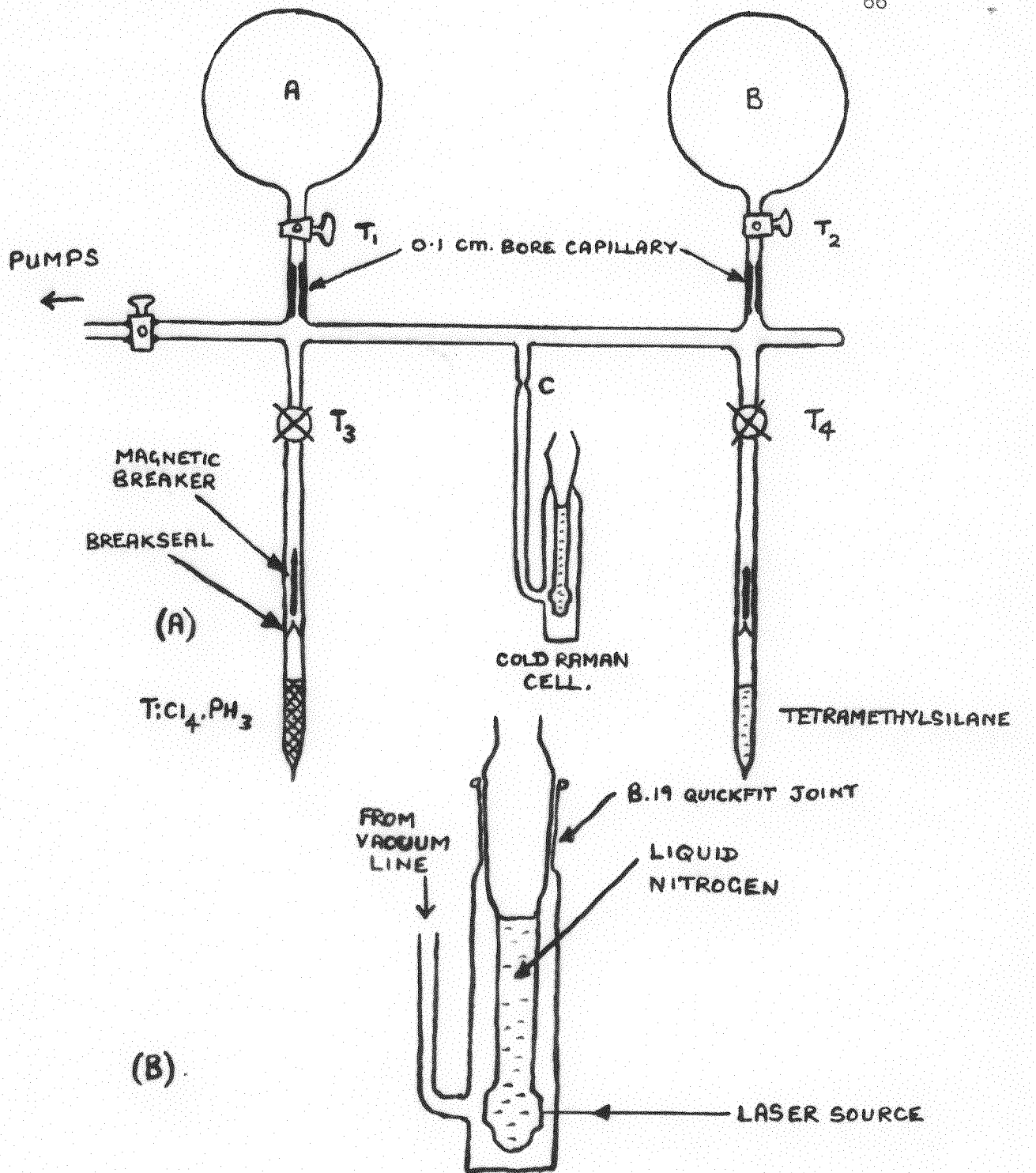

FIGURE III.4. (A) VACUUM LINE FOR MATRIX ISOLATION EXPERIMENT.
(B) DETAIL OF LOW TEMPERATURE RAMAN CELL.

TABLE III. 1.

Observed vibrational frequencies for $TiCl_4.NMe_3$.

(Frequencies in $cm.^{-1}$)

RAMAN		INFRARED		ASSIGNMENT
Solid	Benzene Soln.	Mull	Benzene Soln.	
80 s.		75 m.		
156 m.	147 m.(P.)	159 s.	149 m.	
176 s.	173 s.(D.P.)	174 m.	170 m.	
210 w.	200 w.sh.(P.)	210 w.	210 w.	$a_1 \nu Ti\text{-}N$
240 w.br.	240 v.w.br.(D.P.)			
348 s.	345 v.s.(P.)	346 m.	345 m.	$a_1 \nu TiCl_3$ eq.
368 v.s.	388 s.br.(P.)	370 s.	396 s.	$a_1 \nu TiCl$ ax.
462 v.w.br.	462 v.w.br.(D.P.)	435 sh. 456 s.	436 sh. 457 s.	$e\delta NC_3$ $e\nu TiCl_3$
500 w.	503 w.(P.)	504 w.	499 w.	$a_1 \delta NC_3$

TABLE III. 2.

Observed vibrational frequencies for $TiCl_4$, $N(CD_3)_3$.

(Frequencies in $cm.^{-1}$)

RAMAN		INFRARED	
Solid	Benzene Soln.	Mull	Benzene Soln.
77 s.		77 w.	
152 s.			
170 s.	171 s.(D.P.)	170 s.	170 s.
188 w.	188 w.	184 w.	
234 w.	234 w.(D.P.)		
346 m.	348 s.(P.)	344 w.sh.	344 w.sh.
366 s.	388 s.br.(P.)	370 s.	390 s.br.
390 w.		420 s.	420 s.
435 m.br.	436 m.br.(P.)	445 m.	446 m.

TABLE III. 3.

Observed vibrational frequencies for $TiCl_4$, Me_3P.

(Frequencies in $cm.^{-1}$)

RAMAN		INFRARED*	
Frequency	Intensity	Frequency	Intensity
154	v.w.br.	155	w.
190	v.w.br.	175	w.
259	v.w.br.		
355	s.P.	355	m.
379	w.br.	379	s.
		413	s.
		448	m.sh.

*Benzene Solution

TABLE III. 4.

Vibrational frequencies ($cm.^{-1}$) calculated for $TiCl_4$,PMe_3 on a C_{2V} trigonal bipyramidal model.

(f_{Ti-P} = 1.8 md. $Å^{-1}$)

OBSERVED	CALCULATED		P.E. CONTRIBUTIONS
	Frequency	Symmetry	
	75	b_1	$\delta PTiCl_{2eq}$ I.P. $\delta PTiCl_{2ax}$ O.P.
	81	b_2	$\delta PTiCl_{2ax}$ I.P.
	97	a_1	$\delta TiCl_{eq}$ $\delta TiCl_{ax}$
	115	b_1	$\delta PTiCl_{2ax}$ O.P. $\rho_r PC_3$
	127	b_2	$\delta PTiCl_{2eq}$ O.P.
	131	a_2	$\delta TiCl_{ax,eq}$
	140	a_1	$\delta TiCl_{eq}$
154	159	b_2	$\rho_r PC_3$
	169	b_1	$\rho_r PC_3$ $\delta PTiCl_{2eq}$ I.P.
190			
	228	a_1	δPC_3

T A B L E III. 4. (cont.)

OBSERVED	CALCULATED		P.E. CONTRIBUTIONS
	Frequency	Symmetry	
259	292	b_1	δPC_3
	292	b_2	δPC_3
355	322	a_1	$\nu TiCl_{ax}$
379	369	a_1	$\nu TiCl_{eq}$
413			
448	448	a_1	νTiP + $\nu TiCl_{eq}$
	457	b_1	$\nu TiCl_{eq}$
	496	b_2	$\nu TiCl_{ax}$

T A B L E III. 5.

Vibrational frequencies ($cm.^{-1}$) calculated for $TiCl_4$,PMe_3 on a C_{3V} trigonal bipyramidal model.

(f_{Ti-P} = 1.8 md. $Å^{-1}$)

OBSERVED	CALCULATED		P.E. CONTRIBUTIONS
	Frequency	Symmetry	
	67	e	δTiP
	110	e	$\delta TiCl_{ax}$
	122	a_1	$\delta TiCl_{eq}$ O.P.
154	136	e	$\delta TiCl_{eq}$ I.P. + $\rho_r PC_3$
	169	e	$\delta TiCl_{eq}$ I.P. + $\rho_r PC_3$
190	207	a_1	δPC_3
259	291	e	δPC_3
355	330	a_1	$\nu TiCl_{eq}$
379	373	a_1	$\nu TiCl_{ax}$ + δPC_3
413			
	457	e	$\nu TiCl_{eq}$
448			
	495	a_1	νTiP + $\nu TiCl_{ax}$

TABLE III. 6.

Observed vibrational frequencies for $TiCl_4$, PH_3.

(Frequencies in $cm.^{-1}$)

RAMAN		INFRARED*		
Frequency	Intensity	Frequency	Intensity	
89	w.			
105	s.			
126	s.			
153	w.			
181	w.			
238	s.			
286	s.	290	s.	
385	s.	380	s.	
426	v.s.	426	s.br.	complex
450	m.sh.			
		481	s.	

* Infrared spectrum recorded at liquid nitrogen temperatures.

T A B L E III. 7.

Observed vibrational frequencies for $TiCl_4$, PD_3.

(Frequencies in $cm.^{-1}$)

RAMAN		INFRARED*		
Frequency	Intensity	Frequency	Intensity	
87	w.			
103	s.			
124	s.			
152	w.			
178	w.			
233	s.			
282	s.	287	s.	
382	s.	380	s.	
429	v.s.	427	s.br.	complex
		479	s.	

* Infrared spectrum recorded at liquid nitrogen temperatures.

T A B L E III. 8.

Vibrational frequencies ($cm.^{-1}$) calculated for $TiCl_4$, PH_3 and $TiCl_4$, PD_3 (values in brackets) on a C_{2V} trigonal bipyramidal model.

($f_{Ti-P} = 1.8$ md. $Å^{-1}$)

OBSERVED	CALCULATED		P.E. CONTRIBUTIONS
	Frequency	Symmetry	
89 (87)	88 (87)	b_1	($\delta PTiCl_{2eq}$ I.P. ($\delta PTiCl_{2ax}$ O.P.
105 (103)	97 (97)	a_1	($\delta Ti\text{-}Cl_{ax}$ ($\delta Ti\text{-}Cl_{eq}$
126 (124)	113 (109)	b_2	$\delta PTiCl_{2ax}$ I.P.
153 (152)	131 (131)	a_2	$\delta Ti\text{-}Cl_{ax,eq}$
	137 (136)	b_2	$\delta PTiCl_{2eq}$ O.P.
181 (178)	152 (149)	b_1	($\delta PTiCl_{2eq}$ I.P. ($\delta PTiCl_{2ax}$ O.P.
238 (233)	169 (168)	a_1	($\delta Ti\text{-}Cl_{ax}$ ($\delta Ti\text{-}Cl_{eq}$
286 (282)	307 (303)	a_1	(νTiP
385 (382)	350 (346)	a_1	($\nu Ti\text{-}Cl_{ax}$ ($\nu Ti\text{-}Cl_{eq}$
426 (429)	433 (428)	a_1	($\nu Ti\text{-}P$ ($\nu Ti\text{-}Cl_{eq}$
450 (-)	452 (444)	b_1	$\nu Ti\text{-}Cl_{eq}$
	491 (474)	b_2	$\nu Ti\text{-}Cl_{ax}$

TABLE III. 9.

Vibrational frequencies ($cm.^{-1}$) calculated for $TiCl_4$, PH_3 and $TiCl_4$, PD_3 (values in brackets) on a C_{3V} trigonal bipyramidal model.

(f_{Ti-P} = 1.8 md. $Å^{-1}$)

OBSERVED	CALCULATED		P.E. CONTRIBUTIONS
	Frequency	Symmetry	
89 (87)	86 (84)	e	($\delta Ti-P$ ($\delta Ti-Cl_{ax}$
105 (103)			
126 (124)	116 (115)	e	$\delta Ti-Cl_{ax}$
153 (152)	138 (137)	a_1	$\delta Ti-Cl_{eq}$ O.P.
181 (178)	158 (157)	e	$\delta Ti-Cl_{eq}$ I.P.
238 (233)			
286 (282)	302 (295)	a_1	($\nu Ti-Cl_{ax}$ ($\nu Ti-P$
385 (382)	351 (349)	a_1	$\nu Ti-Cl_{eq}$
426 (429)			
450 (-)	453 (445)	e	$\nu Ti-Cl_{eq}$
	491 (486)	a_1	($\nu Ti-P$ ($\nu Ti-Cl_{ax}$

TABLE III. 10.

Observed vibrational frequencies for $TiCl_4$, $PMeH_2$.

(Frequencies in $cm.^{-1}$)

RAMAN	INFRARED	
Solid	Mull	Benzene Soln.
112 s.		
125 s.		
156 v.s.		
179 w.	190 v.w.br.	
256 s.	232 v.w.br.	
291 s.	282 m.br.	282 m.br.
383 m.	387 v.s.sh.	387 s.sh.
415 v.s.	418 v.s.br.	410 s.br.
430 m.sh.	433 v.s.sh.	430 s.sh.
	456 s.	450 s.sh.
	496 m.	500 v.s.

T A B L E III. 11.

Observed vibrational frequencies for $TiCl_4$,$PHMe_2$.

(Frequencies in $cm.^{-1}$)

RAMAN		INFRARED	
Solid	Benzene Soln.	Mull	Benzene Soln.
102 w.			
123 m.			
149 m.			
210 s.			
256 w.			
299 s.	315 s.	284 m.br.	284 m.
378 w.	349 s.	380 v.s.sh.	388 s.br.
414 v.s.	387 s.	410 v.s.	415 s.
430 w.sh.	413 v.w.br.	440 sh.	430 s.br.
		501 m.	504 m.

T A B L E III. 12.

d-spacings for $TiCl_4$,$PHMe_2$, $TiCl_4$,PMe_3 and $TiCl_4$,NMe_3

$TiCl_4$,$PHMe_2$		$TiCl_4$,PMe_3		$TiCl_4$,NMe_3	
Rel. Intensity	d	Rel. Intensity	d	Rel. Intensity	d
v.s.	6.098	w.	5.987	m.	6.812
m.	4.739	w.	5.30	s.	4.663
m.	3.930	v.s.	4.975	v.s.	3.930
m.	3.287	s.	4.663	s.	3.184
m.	2.903	v.s.	3.558	m.	3.115
w.	2.504	w.	2.632	w.	2.715
s.	1.845	w.	2.546	w.	2.504
w.	1.547	w.	2.283	m.	1.857
		m.	1.945	s.	1.793
		s.	1.911	m.	1.700
		s.	1.866	w.	1.643
		s.	1.775		
		s.	1.610		
		w.	1.572		
		w.	1.529		
		w.	1.392		
		w.	1.351		
		m.	1.312		
		m.	1.159		
		m.	1.132		
		s.	1.720		
		w.	0.9797		

III.6. Experimental.

(i) General. The purification and drying of the reactants and the preparation of adducts was carried out in all glass vacuum systems, the detailed description of which has been given elsewhere (61). The preparation of the crude phosphines was carried out in standard quickfit apparatus under white spot nitrogen. Mull and solution samples were all prepared in a nitrogen filled glove box. The nitrogen, which was continuously recirculated by means of a diaphragm pump, was passed over B.T.H. copper oxide catalyst at 60°C and subsequently through molecular seive 4a to remove oxygen and water vapour, respectively. The copper oxide and molecular seive columns were periodically regenerated (after approximately one month) and at these times the whole system was subsequently flushed out with fresh nitrogen. Using this system, the water vapour level in the drybox was kept in the range (20 - 50 ppm.).

Titanium tetrachloride was freed from chlorine by treatment with copper powder, and from hydrogen chloride by subsequent distillation *in vacuo* onto acridine. After four subsequent distillations *in vacuo* to remove traces of acridine, the purified material was stored in vacuum ampoules, fitted with breakseals (61). Benzene and trimethylsilane were both dried with calcium hydride and trimethylamine was purified and dried with pyridine and silicon tetrachloride (62).

(ii) Preparation of the phosphines. (a) Phosphine was prepared by the reduction of phosphorus trichloride with lithium aluminium hydride (63) in diglyme, which has first been dried by standing over calcium hydride. The phosphine generated was dried by successive trap to trap distillations from an n-pentanol slush bath (-127°C) to liquid nitrogen, and storage over fresh barium oxide. The phosphine was finally stored in gas bulbs fitted with breakseal sidearms at one atmosphere pressure. As a check on its purity, the infrared spectrum of the final product was measured, and found to be in agreement with that cited in the literature (64).

(b) Deuterophosphine was prepared by the action of deuterium oxide on calcium phosphine. Purification was effected as for phosphine, and the infrared spectrum recorded as a check on its purity (64). It was found that the use of commercial calcium phosphide resulted in a mixture of PH_3 and PD_3 in the approximated ratio of 1:2 (as judged from the relative intensities of the corresponding infrared bands, assigned to ν_3). A freshly prepared sample of calcium phosphide, prepared by the alumino thermic method (65), yielded a product which was at least 90% PD_3, (estimated from the relative areas of ν_3 for PH_3 and PD_3 in the infrared).

(c) Methylphosphine was prepared by the reduction of methyl-phosphorus dichloride with lithium aluminium hydride (66), and was purified and stored in a manner similar to phosphine. Again the product was characterised by measurement of its infrared spectrum (67).

(d) Dimethylphosphine was prepared by the following rather lengthy sequence:

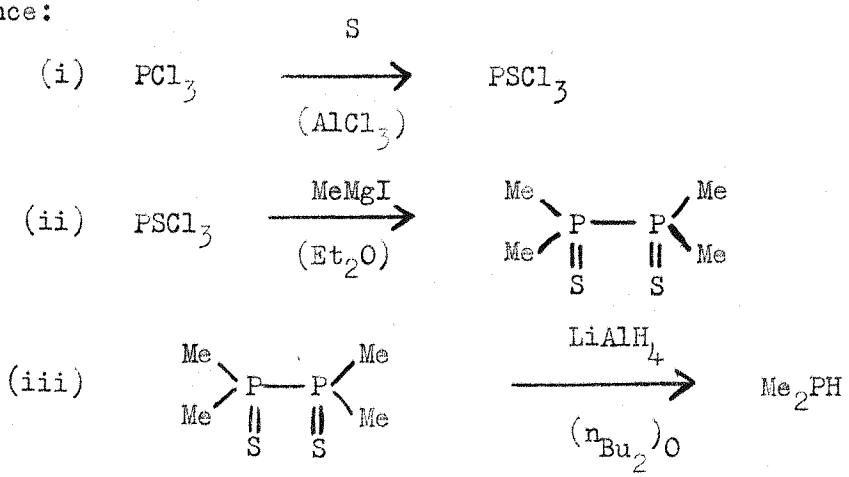

The preparation is therefore described in some detail.

(i) The preparation of thiophosphoryl trichloride (65). Phosphorus trichloride (200 g.) and flowers of sulphur (48 g.) were mixed in a flask and heated to boiling. Aluminium trichloride (6 g.) was then added, whereupon a violent reaction occurred, the sulphur dissolving to yield an orange liquid. After 10 minutes the reaction ceased, and the cooled liquid was shaken with a large volume of water. Decolourisation of the $PSCl_3$ resulted which was then separated from the aqueous layer and dried with anhydrous calcium chloride. Fractionation of the product gave 120 g. (48%) of colourless $PSCl_3$, boiling between 122-123°C. The freshly fractionated product was used immediately for the next stage.

(ii) The preparation of tetramethylbiphosphine disulphide, $(Me)_2P(S)\text{-}P(S)(Me)_2$. (68) A solution of methylmagnesium

iodide was prepared from methyliodide (223 g.) dissolved in sodium dry diethylether (520 ml.). This solution was added under whitespot nitrogen over the course of one hour to some dry magnesium turnings (38 g.) with vigorous stirring. After refluxing the resulting ethereal solution of the Grignard reagent for one hour, and subsequently cooling it to 0°C, a solution of thiophosphoryl trichloride (67 g.) in dry ether (42 ml.) was added under whitespot nitrogen over two hours, with vigorous stirring. A thick white precipitate separated out during the course of the reaction.

When all the $PSCl_3$ had been added, the stirring was stopped and the reaction mixture was poured onto ice (250 g.) contained in a 2 litre beaker. 10% sulphuric acid (450 ml.) was then added over the course of 15 minutes, with gentle stirring. The white solid was filtered off, washed with water (2 litres) and recrystallised from ethanol (1 litre). Finally it was dried over phosphorus pentoxide, the resulting yield being 20 g. (54%). The ^1H. NMR. spectrum of the solid as a solution in dichloromethane -d_2 was recorded at 100 mc/sec., and found to be identical with that quoted in the literature (69).

(iii) The preparation of dimethylphosphine. (70) A solution of lithium aluminium hydride (7.6 g.) in n-butyl ether (80 ml.) (dried over calcium hydride) was added dropwise, with vigorous stirring to a suspension of tetramethylbiphosphine disulphide (19 g.) in n-butyl ether (95 ml.) under whitespot nitrogen. The mixture was heated for one hour at 60°C. Any vapours carried off with the

nitrogen stream were condensed in a trap cooled in an acetone/CO_2 bath. The mixture was then cooled in ice, and water (50 ml.), which had previously been outgassed on a vacuum line, was next added dropwise to decompose the $LiAlH_4/Me_2PH$ complex formed. The mixture was then fractionated, and the dimethylphosphine (B.P. 25°C) was collected via a water cooled double surface condenser in a trap cooled in an acetone/CO_2 bath. When no more phosphine distilled over, the cold trap was removed and transferred to a vacuum line, where the dimethylphosphine was dried by distillation onto fresh barium oxide and subsequently onto calcium hydride. The product was finally distilled into breakseal vacuum ampoules for use. The vapour phase infrared spectrum was measured, and found to agree with that quoted in the literature (71). The yield of dimethylphosphine obtained was 9 g. (66%).

(e) Trimethylphosphine was prepared by the method of Mann and Wells (72). Since considerable difficulty was encountered in obtaining a high yield of trimethylphosphine, the procedure finally adopted, which consistently gave yields of approximately 40%, will therefore be described in some detail.

A solution of methylmagnesium iodide was first prepared from a solution of methyliodide (250 ml.) in diethylether (1,200 ml.), which had been dried over sodium and deoxygenated by refluxing and bubbling whitespot nitrogen through it. This solution was added over the course of three hours to magnesium turnings (97 g.) with vigorous stirring.

The resulting Grignard solution was then refluxed for one hour, and left to stand overnight at room temperature.

The Grignard solution was cooled to -30°C and phosphorus trichloride (56 ml.) in diethylether (140 ml.) (sodium dried and deoxygenated), was added in an atmosphere of whitespot nitrogen, dropwise over the course of twelve hours, with vigorous stirring. The mixture was then kept at 0°C overnight. To extract the product, the reaction mixture was distilled into a vigorously stirred solution of silver iodide (96 g.) dissolved in saturated potassium iodide solution, cooled in ice and salt. When the mixture in the reaction flask reached 200°C, the distillation stopped. The ethereal phosphine distillate was stirred with the silver iodide solution for a further two hours, after which the silver iodide phosphine complex was filtered off, washed with saturated potassium iodide solution, and dried over phosphorus pentoxide. The complex is a white, air stable solid. The trimethylphosphine was regenerated from the silver iodide complex, by heating the complex on a vacuum line with a small naked flame. The trimethylphosphine evolved was condensed in a trap cooled in an acetone/CO_2 bath, and was dried first over fresh barium oxide and subsequently over calcium hydride. Finally, the trimethylphosphine was distilled into breakseal vacuum ampoules ready for use. The vapour phase infrared spectrum of the product was measured, and found to agree closely with that cited in the literature (73).

Final yield of trimethylphosphine: 17.5 g. (40%).

(iii) Preparation of the adducts. $TiCl_4,PH_3$ was obtained as a yellow solid by condensation of excess phosphine onto solid $TiCl_4$ in a reaction flask cooled to -127°C. After eight hours, the excess phosphine was pumped off, the product being kept at -127°C to minimise dissociation, and the solid complex was then sublimed *in vacuo* to yield yellow-orange crystals.

[Found: Cl, 62.96% . H_3Cl_4PTi requires: Cl, 63.40%].

$TiCl_4,PD_3$ was prepared as orange sublimable crystals in an analogous manner.

[Found: Cl, 62.14%. D_3Cl_4PTi requires: Cl, 62.56%].

$TiCl_4,PH_2Me$ was prepared by mixing an approximately 1:1 mole ratio of $TiCl_2$ and methylphosphine at -127°C. After eight hours the excess reactants were pumped off, and the solid adduct sublimed *in vacuo* to yield orange crystals.

[Found: Cl, 58.86%. CH_5Cl_4PTi requires: Cl, 59.67%].

$TiCl_4,PHMe_2$ was prepared by adding dimethylphosphine to a large excess of $TiCl_4$ dissolved in benzene. Reaction occurred at once giving an orange-red solid and a red solution. The excess volatiles were then pumped off leaving an orange-red powder which did not sublime *in vacuo*, but decomposed to a dark brown mass.

[Found: Cl, 56.48%. $C_2H_7Cl_4PTi$ requires: Cl, 56.67%].

$TiCl_4,PMe_3$ was prepared by adding trimethylphosphine to an excess of $TiCl_4$ dissolved in benzene, and was obtained as a dark red crystalline solid.

/Found: Cl, 52.93%; M, 279 (0.3 mM. in C_6H_6);
286 (0.1 mM in C_6H_6); $C_3H_9Cl_4P.Ti$ requires:
Cl, 53.40%; M, 266_7.

$TiCl_4,NMe_3$ was prepared as described in the literature (9). Chloride analyses were obtained by potentiometric titration with silver nitrate after hydrolysis and oxidation of the ligand with dilute nitric acid.

$/Me_3PH/_2$ $/TiCl_6/$ was prepared by addition under nitrogen of trimethylphosphine to a solution of $TiCl_4$ in concentrated hydrochloric acid. The resulting solution was added dropwise to excess thionyl chloride with vigorous stirring. When evolution of gases had ceased, the yellow solid was filtered off and pumped to dryness in vacuo.
/Found: Cl, 49.52%; $C_6H_{20}Cl_6P_2Ti$ requires: Cl, 51.34%_7

(iv) The molecular weight determination on $TiCl_4,PMe_3$ was carried out in a cryoscope, the detailed construction of which has been described elsewhere (20). A thermistor was employed to measure the temperature of the solution, and this was calibrated using the freezing point of pure benzene, the freezing point of a solution of naphthalene in benzene of known concentration, and the freezing point of distilled water.

A solution of known concentration of $TiCl_4,PMe_3$ was made up in dry benzene in the nitrogen glove box, placed in the cell, and the freezing curve of the solution plotted, using an ice/water bath as the

cooling medium. The experiment was repeated using a second solution of different concentration, the freezing curve of the solution again being plotted. The two results were consistent, and the molecular weight was calculated using the calibration of the thermistor.

(v) The matrix isolation experiments were carried out using the vacuum line shown in Figure III. 4a. The breakseal ampoules of $TiCl_4$, PH_3 and tetramethylsilane were isolated from the rest of the line by neoprene diaphragm taps T_3 and T_4. For each run, samples of $TiCl_4$, PH_3 and tetramethylsilane vapours were separately admitted into the gas storage bulbs, A and B, both of which were of 500 ml. volume. The pressure of the vapour in each bulb was adjusted to give the desired mol % composition in the matrix, assuming Avogadro's hypothesis. The vapour pressure were measured on a simple mercury manometer of 11 mm. internal diameter (not shown in Figure III. 4a.). The contents of both bulbs were allowed to condense slowly and simultaneously through the capillary outlet tubes onto the target area of the cold Raman cell, by opening taps T_1 and T_2. The cold Raman cell employed is shown in detail in Figure III. 4b., and consists of a cold finger with two flat target areas which fits inside the outer evacuated jacket by means of a Q and Q B. 19 joint lubricated with silicone grease. The cold finger was filled with liquid nitrogen, and the side arm sealed off at the constriction C, once the sample had been sublimed onto the cold finger. Two samples, one on each target area were prepared on each run, before sealing

off. It was found that, although the cold finger was only of approximately 10 mls. capacity, it held liquid nitrogen for at least ten minutes before refilling was needed, with a good vacuum in the outer jacket. Optical contact between the outer jacket and the hemispherical lens of the Cary 81 by means of glycerol. The cold Raman spectra were also run in this cell, by essentially the same technique.

Cold infrared spectra were run by sublimation of the sample onto a caesium iodide plate cooled in liquid nitrogen in a vacuum cell fitted with caesium iodide windows. The detailed design of this cell has been described elsewhere (8). Infrared mull spectra were run between polythene plates, and solutions in cells made from polythene tubing. Solid Raman samples were contained in vacuum ampoules, whilst Raman solution samples were contained in 1 mm. pyrex capillary tubes filled on a vacuum line.

Infrared spectra were run on Beckman IR11 and Perkin-Elmer 225 spectrometers, and Raman spectra on a Cary 81 spectrometer with He/Ne laser excitation.

Powder x-ray photographs were obtained using Cu K_α radiation. Samples were contained in 0.5 mm. Lindemann tubes. The samples were prepared in the nitrogen drybox, except the sample of $TiCl_4$,PMe_2H, which was prepared <u>in situ</u> in the Lindemann tube from $TiCl_4$ and Me_2PH on a vacuum line.

C H A P T E R IV.

The vibrational spectra and stereochemistries of some adducts of the type L_2TiX_4.

IV. 1. Introduction

For adducts of the group IV tetrahalides with monodentate ligands, in which the donor:acceptor ratio is 2:1, the most probable model on which their stereochemistries may be based, is that of an octahedral distribution about the central metal atom, with the possibility of *cis*-*trans* isomerism. Considering a general adduct L_2MX_4, (where L = a monodentate ligand atom, and X = a halogen atom), the following possibilities occur:

(I) C_{2V} (*cis*) (II) D_{4h} (*trans*)

Several factors may be involved in determining whether (I) or (II) is favoured in practice.

It may at first sight appear that a *trans* adduct is favoured if only X - X repulsions are considered and all bond angles are 90°. However, if the *cis* adduct is distorted so that the MX_4 residue becomes more like the original tetrahedral halide molecule, then, considering X - X repulsions only, a *cis* adduct becomes probable (74). Small ligands can be envisaged as fitting into the free MX_4 tetrahedron, causing distortion, and effectively giving rise to a *cis* adduct. If, however, L is a large ligand atom or sterically hindered ligand molecule, then X - L repulsions may dominate, and a *trans* configuration may be adopted. It should, however, be noted that from ^{19}F. NMR.

studies, the ion $SnF_4I_2^{2-}$ has recently been shown to adopt a cis configuration (7a). The general picture which has emerged so far from studies of the L_2MX_4 species of the group IV(b) elements with ligand molecules is that small ligand molecules tend to give cis adducts (e.g. MeCN (7b)), whilst bulky ligand molecules tend to give trans adducts (e.g. Me_3N, Me_3P and pyridine).

The examination of the stereochemistry of L_2MX_4 species at equilibrium in solution is conveniently carried out by an examination of their infrared and Raman spectra. Simple group theoretical considerations allow us to predict the number of infrared and Raman active fundmental vibrational modes to be expected for each symmetry type. Assuming L to be a point mass, the results of the simple theory will now be given.

(i) C_{2V} L_2MX_4. Lowering of the symmetry of the MX_4 octahedron from Td to C_{2V} involves a splitting of the fundmental modes as follows:

$$T_d \longrightarrow C_{2V}$$
$$a_1 \longrightarrow a_1$$
$$f_2 \longrightarrow a_1 \quad b_1 + b_2$$

The representation of the molecule after removal of rotational and translational degrees of freedom is

$$\Gamma_{mol} = 6a_1 + 2a_2 + 3b_1 + 4b_2$$

with all modes infrared and Raman active, except the a_2 mode, which is Raman active alone. There are thus fifteen fundmental modes, of

which four ($2a_1 + b_1 + b_2$) might be expected to occur in the "M - Cl stretching region" of the spectrum, in both the Raman and infrared.

(ii) $\underline{D_{4h}L_2MX_4}$. Here, after removal of rotational and translational modes, we have

$$\Gamma_{mol} = 2a_{1g} + 2a_{2u} + b_{1g} + b_{2g} + b_{2u} + e_g + 3e_u$$

Since the molecule has a centre of symmetry under D_{4h} symmetry, then the mutual exclusion rule is operative, and all <u>gerade</u> modes are Raman active only, and all <u>ungerade</u> modes are infrared active only. The exception is the b_{2u} mode, which is inactive in both. Since we have:

$$T_d \longrightarrow D_{4h}$$
$$a_1 \longrightarrow a_{1g}$$
$$f_2 \longrightarrow b_{1g} + e_u$$

of the eleven fundmentals we might expect three to occur in the "M - Cl stretching region", one in the infrared and two in the Raman.

On this simple treatment, it might at first sight appear to be a simple matter to differentiate between the two cases, from a consideration of their vibrational spectra. However, in practice, several complicating factors may frequently be encountered. Most monodentate ligands L whose adducts with MX_4 have been studied in this way, (such as pyridine, trimethylamine and methylcyanide) are polyatomic molecules which cannot be treated satisfactorily as a point mass. Ligands such as these have vibrational modes which are foundin the vicinity of the "M - Cl stretching modes", and these,unless readily identifiable, may make assignments uncertain. Moreover, if rotation of these ligands is hindered, the symmetry of the adduct will be lowered,

and the degeneracy of the M - Cl e_u stretching modes for the trans case will be lifted. This effect has been encountered in the case of $SiCl_4$,2Py. This adduct has been shown by x-ray analysis to be trans, but on the basis of its vibrational spectra was originally assigned a cis stereochemistry (75). Calculations for a D_{2h} model (rotation of trans-pyridine ligands hindered) indicate that the D_{4h} degenerate Si -Cl stretching e_u pair are split, and that the resultant b_{2u} and b_{3u} modes in D_{2h} symmetry couple seriously (approximately 50%) with the pyridine in plane and out of plane ring deformations (76). The previous erroneous assignment in terms of the C_{2V} cis configuration can be understood in the light of this work. However, it is also made clear by these calculations that it is impossible in this case to distinguish between the C_{2V} (cis) and D_{2h} (trans) configurations on the basis of the vibrational spectra.

Yet another complicating factor in this connection is the possible proximity of the antisymmetric metal-ligand vibration, although deuteriation studies can be of some help in identifying this mode. Finally, unless solution data are available, the possibilities of crystal field and correlation splittings must also be borne in mind in interpreting spectra of this type.

It has been found that deduction of sterochemistry from vibrational data alone is, except in certain special cases, not possible. Independent evidence obtained from x-ray investigations is generally necessary before the vibrational spectra may be assigned

with any certainty. Even the complimentary information provided by a comparison of Raman and infrared data is not always helpful, since often Raman active bands in cis - L_2MX_4 adducts are found to be very weak or absent from the Raman spectra (76). For example, $SnCl_4$,2MeCN has now been shown to be cis from a single crystal x-ray study, but the vibrational spectra cannot be assigned with any certainty on this basis (77). Similarly, the 1:2 adducts of $SiCl_4$ (76), $GeCl_4$ (78), $SnCl_4$ and $SnBr_4$ (79) with pyridine have now been shown to be trans from single crystal x-ray studies, and the adduct $SeCl_4$,2Py has been shown to be isomorphous with $SnCl_4$,2Py from powder x-ray data (79). However, the structure of these adducts could not be deduced from the vibrational data, except in the case of $GeCl_4$,2Py (80) and $SnCl_4$,2Py (81). Nonetheless, vibrational spectroscopy can be of considerable use in selecting compounds for further study by x-ray diffraction.

The adducts studied during the course of this work represent an extension of these studies into group IV(a). Results are reported for L_2MX_4 species $TiCl_4$ and $TiBr_4$ with the ligands trimethylphosphine pyridine and methylcyanide. Comparisons could then be made between the analogous complexes of $TiCl_4$ and $TiBr_4$ with those of the group IV(b) elements already studied. From considerations of size, we might expect TiX_4 and SnX_4 to show similar behaviour in their L_2MX_4 adducts with a given ligand. However, a fundmental difference between Ti(IV) and Sn(IV) is the presence of low lying d-orbitals in the former, so that $d\pi$ - $p\pi$ bonding effects may become important for L_2TiX_4 adducts

in determining stereochemistries.

IV. 2. The Adduct $TiCl_4$,$2PMe_3$.

Previous work on 1:2 adducts of titanium tetrahalides with monodentate phosphine ligands is quite scarce. Chatt and Hayter (57) have prepared and characterised the complexes $TiCl_4$,$2PEt_3$ and $TiCl_4$,$2P\phi_3$, whilst Westland (58) has recorded the infrared spectrum of the latter adduct in the caesium iodide region of the spectrum. Bands at 445 $cm.^{-1}$ and 434 $cm.^{-1}$, both strong in the infrared, were assigned to Ti - P stretching modes, and the adduct was therefore assigned a cis-stereochemistry. In view of the large steric requirements of triphenylphosphine, the complicated nature of this ligand, and the results obtained for such adducts as $SiCl_4$,2Py (76), this assignment was considered to be unlikely. The ring deformations of the phenyl groups of this ligand are likely to occur in the region studied and from the calculations reported on $SiCl_4$,2Py (76) might confidently be expected to couple strongly with the metal-ligand vibrations, making assignment of the stereochemistry on this basis an impossible task.

Trimethylphosphine, however, is a simpler ligand, whose deformations occur in quite well known regions of the spectrum (82). It was felt that the vibrational data obtainable from $TiCl_4$,$2PMe_3$ would be easier to interpret. The complex was prepared by adding an excess of trimethylphosphine to titanium tetrachloride, both in solution in

benzene, in an all glass vacuum system. The reaction is strongly exothermic, yielding dark red crystals of the complex which are soluble in benzene to form a deep red solution. The complex is unstable with respect both to oxygen and atmospheric moisture.

The vibrational spectra obtained for this adduct are summarised in Table IV. 1., and immediately suggest a trans - D_{4h} stereochemistry. As outlined in Section IV. 1., assuming trans D_{4h} symmetry for L_2MX_4 we expect one strong e_u infrared active Ti - Cl stretching mode, and one strong a_{1g} Raman active Ti - Cl stretching mode. When L = PMe_3, if free rotation of the trimethylphosphine ligands occurs then the trans configuration of the adduct will still possess D_{4h} symmetry, assuming that the TiX_4 grouping is planar. Puckering of the TiX_4 grouping will lower the symmetry to D_{2d}, but the spectral results obtained will be the same, since we have:

$$D_{4h} \longrightarrow D_{2d}$$
$$a_{1g} \longrightarrow a_1$$
$$e_u \longrightarrow e$$

If the rotation of the ligands is hindered, however, all elements of symmetry are lost, and all vibrations become both Raman and infrared active. Inspection of the data in Table IV. 1., reveals one strong infrared active mode at 362 $cm.^{-1}$ (382 $cm.^{-1}$ in benzene solution) assignable to the D_{4h} e_u Ti - Cl stretching mode. The absence of splitting of this band suggests that the assumption of free rotation for the trimethylphosphine ligands is a valid one. The Raman data

reveal one strong band at 324 cm.$^{-1}$, polarised, which is assignable to the a_{1g} Ti - Cl stretching mode on the D_{4h} model. At first sight the mutual exclusion expected on a D_{4h} model appears not to be observed. However, the weak 360 - 380 cm.$^{-1}$ band observable in the Raman effect is shown to be polarised in solution, and may therefore represent a coincidence of the e_u νTi - Cl mode (infrared active) and the a_{1g} PC_3 deformation (Raman active). The symmetric and antisymmetric PC_3 deformations of the two PMe_3 ligands are expected to couple, giving rise to <u>four</u> deformational modes for the adduct as a whole according to the following scheme:

(1) sym δPC_3 + sym $\delta PC_3'$ overall a_{1g} (Raman).

(2) sym δPC_3 - sym $\delta PC_3'$ overall a_{2u} (infrared).

(3) antisym δPC_3 + antsym $\delta PC_3'$ overall e_g (Raman).

(4) antisym δPC_3 - antisym $\delta PC_3'$ overall e_u (infrared).

A G.V.F.F. calculation on $SnCl_4$,$2PMe_3$ suggests (47) that the a_{1g} and a_{2u} pair of deformations will occur at very similar frequencies, as will the e_g and e_u pair. The depolarised band observed at 264 cm.$^{-1}$ is therefore assignable to the e_g ligand deformation, and the corresponding band at 260 cm.$^{-1}$ in the infrared to the e_u deformation.

Comparison of the data observed for $TiCl_4$,$2PMe_3$ with that reported for $SnCl_4$,$2PMe_3$ (47) reveals a strong similarity, and suggests that both adopt a <u>trans</u> D_{4h} structure. This is reinforced by a comparison with the calculated spectrum reported for $SnCl_4$,$2PMe_3$ on the basis of a <u>trans</u> D_{4h} structure (47).

IV. 3. The Adducts $TiCl_4$,2Py and $TiBr_4$,2Py.

The adducts were prepared by mixing benzene solutions of $TiCl_4$ and $TiBr_4$, respectively, with an excess of a benzene solution of pyridine in an all glass vacuum system. The complexes were obtained as yellow and brown precipitates respectively, both insoluble in benzene and pyridine.

Very little work has been carried out on the vibrational spectra of these adducts. Beattie et al. (71) reported the infrared spectrum (down to 250 $cm.^{-1}$), and suggested that bands at 368 $cm.^{-1}$ and 280 $cm.^{-1}$ might be due to titanium chlorine stretching vibrations. They also pointed out that the band at 436 $cm.^{-1}$, originally assigned by Rao (73) to a Ti - Cl stretching mode was more likely to be due to coordinated pyridine. In support of this, recent calculations on $SiCl_4$,2Py (76) suggest that the coordinated pyridine ring deformations can be expected to occur in this region.

In the present study, a re-examination of the infrared spectrum of $TiCl_4$,2Py has been undertaken, and Raman data are reported for this complex for the first time. The vibrational data are summarised in Table IV. 2. The band observed by Beattie et al. (71) at 368 $cm.^{-1}$ in the infrared has been resolved into two components at 380 $cm.^{-1}$ and 390 $cm.^{-1}$ in the present study, and on the basis of the infrared data alone, either cis or trans formulations appear to be equally likely. The Raman spectrum shows one strong band only in the Ti - Cl stretching region, and, by comparison with the Raman data

for $TiCl_4$,$2PMe_3$, suggests a <u>trans</u> D_{4h} formulation for the adduct. However, as has been pointed out in connection with $SiCl_4$,2Py (76), the presence of only one strong Raman active band in the metal-halogen stretching region is not necessarily diagnostic of a <u>trans</u> stereochemistry for L_2MX_4 adducts. It has been shown that for the 1:1 adducts of $SiCl_4$ with 1,10 phenanthroline and 2,2'-bipyridyl, the Raman spectrum shows only one strong band in the Si - Cl stretching region. Making the assumption that these bidentate ligands are acting as chelates in a six-coordinate $SiCl_4$ complex, then the three other Raman active bands to be expected in this region are too weak to observe under the experimental conditions used.

In view of these results, samples of the 1:1 adducts $TiCl_4$,1,10 phen and $TiCl_4$,1,2 dimethoxybenzene were prepared, again by mixing benzene solutions of $TiCl_4$ with 1,10 phenanthroline and 1,2 dimethoxybenzene, with the $TiCl_4$ present in excess. Their Raman spectra were measured, and the results are summarised in Table IV. 3.

Quite clearly the bands at 318 $cm.^{-1}$ and 390 $cm.^{-1}$ both strong and polarised for the 1,2 dimethoxybenzene adduct and the bands at 303 $cm.^{-1}$ and 381 $cm.^{-1}$ for the 1,10 phenanthroline adduct can be associated with the two a_1 Ti - Cl stretching modes to be expected for the C_{2V} <u>cis</u> structure which we can reasonably assume is adopted for these adducts. Since these results indicate that two strong bands <u>can</u> be observed in the Raman for <u>cis</u> L_2MX_4 for the case of $TiCl_4$, the Raman results for $TiCl_4$,2Py may then with greater

justification be considered to be suggestive of a trans formulation. However, the evidence is still inconclusive. The infrared spectrum of $TiBr_4$,2PY is reported in Table IV. 4., and it is immediately obvious that it is extremely suggestive of a cis formulation, there being three strong bands in the Ti - Br stretching region. One of these might reasonably be expected to correspond to the strong 285 $cm.^{-1}$ band in the infrared spectrum of $TiCl_4$,2Py and might be associated with the Ti - N stretching vibration in each of these adducts. Unfortunately, no Raman data was obtainable for $TiBr_4$,2Py (to help resolve the problem) due to its dark brown colour. Moreover, due to the insoluble nature of both of these adducts no solution data were obtainable.

In order to resolve the ambiguity arising from these results, powder x-ray photographs were taken for samples of $TiCl_4$,2Py and $TiBr_4$,2Py. Reference to the d-spacings listed in Table IV. 5., will show immediately that both compounds are isomorphous with $SnCl_4$,2Py which is known to adopt a trans-structure from single crystal x-ray diffraction studies (83). Both $TiCl_4$,2Py and $TiBr_4$,2Py must necessarily therefore adopt a trans configuration too. The spectra of Tables IV. 2 and 4., may now be interpreted in terms of a trans-structure. The splitting of the 380 - 390 $cm.^{-1}$ band arises most probably from a lifting of the degeneracy of the e_u (D_{4h}) (formal) Ti - Cl stretching mode due to a lowering of the symmetry of the molecule to D_{2h} consequent on the rotation of the coordinated

pyridine molecules being hindered. Reference to the results for $SiCl_4$,2Py (76) and $SnCl_4$,2Py (83) reveal that the order of splitting of this mode for the tetrachlorides is

Si > Ti > Sn

Reference also to the calculations reported for these two molecules reveals that the degree of coupling of ligand and skeletal modes in molecules of this type is of such an order as to render the assignments of bands to individual normal modes of vibration a meaningless exercise. However, calculations carried out on $SnCl_4$,2Py (83) suggest that the strong band at 285 $cm.^{-1}$ in the infrared for $TiCl_4$,2Py is to be associated, at least in part, with the antisymmetric Ti - N vibration and that the strong band at 324 $cm.^{-1}$ in the Raman effect is principally the a_{1g} Ti - Cl stretching mode.

IV. 4. The Adduct $TiCl_4$,2MeCN.

The adduct was prepared as described in the literature (84), by mixing a benzene solution of $TiCl_4$ with a large excess of methylcyanide in an all glass vacuum system. It was obtained as a yellow sublimable amorphous solid, sparingly soluble in benzene and methylcyanide.

The infrared spectrum of this compound had previously been measured down to 260 $cm.^{-1}$ (85), and on the basis of the spectrum observed was assigned a cis formulation. The vibrational spectra measured during the course of this work for $TiCl_4$,2MeCN are summarised in Table IV. 6. The infrared data reported there above 260 $cm.^{-1}$

agree with the data previously reported (85), except that the strong broad band reported at 386 cm.$^{-1}$ has been resolved into three bands at 388 cm.$^{-1}$, 407 cm.$^{-1}$ and 424 cm.$^{-1}$ in this study. The Raman spectra obtained were complex. The Raman spectrum of a solution of the adduct in methylcyanide revealed that the strong bands at 398 cm.$^{-1}$ and 320 cm.$^{-1}$ are polarised. However, the Raman spectrum of a solution in benzene was found to be quite different. The 320 cm.$^{-1}$ band was considerably reduced in intensity and the 396 cm.$^{-1}$ band was absent. New bands were observed at 356 cm.$^{-1}$ (polarised) and 410 cm.$^{-1}$ (polarised). On pumping this solution to dryness <u>in vacuo</u> a yellow solid was obtained whose Raman spectrum (Table IV. 9.) was found to differ considerably from that of the solid 1:2 adduct. The 390 cm.$^{-1}$, 320 cm.$^{-1}$ and 370 cm.$^{-1}$ bands observed in the spectrum of the 1:2 adduct were considerably weaker, and the spectrum was now dominated by a very strong sharp band at 421 cm.$^{-1}$. Analysis of this solid suggested that its composition approximated to that of a 1:1 adduct. These results suggest that dissolution of the 1:2 adduct in benzene results in partial dissociation of the adduct into the 1:1 adduct. Evidence for a similar dissociation of $SnCl_4$,2MeCN in benzene has also been reported (86). It was found that sublimation of the 1:2 adduct <u>in vacuo</u> resulted in similar changes in the Raman spectrum.

In using alkyl cyanides as ligands in systems of this type, there is always a possibility of the formation of ionic species in addition to neutral adducts. An examination of the Raman spectrum of the

solid 1:2 adduct revealed that the bands:

320 s (P)

240 w

178 m.s.

were very similar in position and intensity to the bands assigned to ν_1, ν_2 and ν_5 in the Raman spectrum of $TiCl_6^{2-}$ (see Chapter III). This suggested the possibility that ionisation might have occurred in addition, or in preference to, simple adduct formation, and that species such as $(TiCl_2,4MeCN)(TiCl_6)$ had been formed. This latter species would be indistinguishable from the 1:2 adduct on the basis of chemical analysis. In the light of these considerations, a study of the conductance of solutions of $TiCl_4$ in methylcyanide was undertaken. The results (Table IV. 7 and Figure IV. 1.) suggest that solutions of $TiCl_4$ in methylcyanide are essentially non-conducting, a result which is in accord with measurements recently carried out on the conductance of $SbCl_5$ and $TeCl_4$ in solution in methylcyanide (87).

Since the formation of ionic species can therefore be ignored in interpreting the vibrational spectra, the Raman data presented in Table IV. 6., can be most satisfactorily interpreted in terms of a cis formulation for this adduct. From the results of the studies on benzene solutions of $TiCl_4$,2MeCN, it is suggested that the weak band observed at 412 $cm.^{-1}$ is due to a trace of the 1:1 adduct. The strong polarised bands at 391 $cm.^{-1}$ and 320 $cm.^{-1}$ can be assigned to the a_1 $TiCl_2$ axial and equatorial symmetric stretching modes. Reference to

the Raman spectra observed for $TiCl_4$,1,10 phen. and $TiCl_4$,1,2 dimethoxybenzene, Table IV. 3., assumed to be cis, supports this assignment. The infrared bands at 424 $cm.^{-1}$ strong, (430 $cm.^{-1}$ medium in the Raman) and 388 $cm.^{-1}$ strong, (probably the 370 $cm.^{-1}$ medium band in the Raman) may be tentatively assigned to the b_1 and b_2 $TiCl_2$ antisymmetric stretching modes. In support of this, deuteriation of the methylcyanide resulted in negligible shifts for these bands in the Raman. In the infrared, a very broad asymmetric band centred at 400 $cm.^{-1}$ was observed. The largest deuteriation shifts were observed for the weak bands at 240 $cm.^{-1}$ and 212 $cm.^{-1}$ in the Raman. Unfortunately, due to the relative insolubility of the adduct in methylcyanide, no polarisation data could be obtained for these two bands. However, the deuteriation shifts suggest that they are associated with the a_1 TiN_2 symmetric stretching mode and also with the C - N - Ti deformational modes. To support these conclusions a G.V.F.F. calculation on $TiCl_4$,2MeCN in C_{2V} symmetry was carried out, treating the CH_3 groups in full. Details of the calculation are given in Appendix B. The calculated frequencies shown in Table IV. 8., are those obtained for $f_{Ti-N} = 1.0$ md. $Å^{-1}$. Assignment of the 394 $cm.^{-1}$ band (strong, polarised) as the a_1 $TiCl_2$ equatorial stretching mode and the 320 $cm.^{-1}$ band as the a_1 $TiCl_2$ axial stretching mode is confirmed, as is also the assignment of the 435 $cm.^{-1}$ and the 370 - 380 $cm.^{-1}$ bands to the b_1 and b_2 antisymmetric $TiCl_2$ stretches respectively. The calculated deuteriation shifts agree well with

those observed for these bands. In addition, the calculations indicate that the a_1 TiN_2 symmetric stretch is to be expected around 220 cm.$^{-1}$. However, several other bands, associated partly with deformations of the ligands, are to be expected in this region, as the calculations indicate, and so the assignment of any band in this region to the a_1 symmetric TiN_2 stretching mode can only be tentative. It should be noted that no methyl rocking modes are to be expected in the region below 400 cm.$^{-1}$ from the results of the calculations.

From the foregoing it is apparent that the vibrational data measured for $TiCl_4$,2MeCN though complex, suggest a cis formulation as most likely. Recently, a single crystal x-ray diffraction study has shown that the corresponding $SnCl_4$ 1:2 adduct with methylcyanide adopts a cis formulation (77). In view of this, powder x-ray measurements were made on samples of these two adducts. The resulting d-spacings, given in Table IV. 12., suggest, however, that the two adducts are not isomorphous, unlike the 1:2 pyridine adducts. Nonetheless, comparison of the vibrational spectra of $TiCl_4$,2MeCN with those observed for $SnCl_4$,2MeCN suggests a high degree of similarity (77).

IV. 5. The Adduct $TiBr_4$,2MeCN.

This adduct was prepared in an analogous manner to the 1:2 $TiCl_4$ methylcyanide adduct in an all glass vacuum system. It was obtained as a red-brown sublimable solid, which was very soluble in methylcyanide.

The vibrational spectra observed for this adduct are shown in Table IV. 10. It is immediately obvious that a degree of similarity exists between these results and those obtained for $TiCl_4$,2MeCN. Furthermore, a study of the conductance of $TiBr_4$ in methylcyanide revealed that no appreciable ionisation occurred upon dissolution. Due to the greater solubility of $TiBr_4$,2MeCN in methylcyanide and to the increased separation between the methylcyanide band at 382 $cm.^{-1}$ and the Ti - Br stretching modes, more complete solution data were obtainable for this adduct than for the analogous $TiCl_4$ adduct. Although the spectra are quite complex, a cis formulation again seems probable. The strong polarised bands at 224 $cm.^{-1}$ and 334 $cm.^{-1}$ can be assigned by comparison with the $TiCl_4$,2MeCN results as the a_1 $TiBr_2$ axial and equatorial symmetric stretching modes respectively. In addition, the partially resolved bands at 308 $cm.^{-1}$ and 331 $cm.^{-1}$ in the infrared mull spectrum which are well resolved in methylcyanide solution, may be assigned to the b_1 and b_2 antisymmetric $TiBr_2$ vibrations respectively. This would require a near coincidence of the a_1 and b_2 $TiBr_2$ stretching vibrations observed in the solution Raman and infrared spectra.

The shift of approximately 14 $cm.^{-1}$ for the band observed in the Raman of the solid adduct on passing from solid to methylcyanide solution is somewhat disturbing, but a similar shift was also observed in the case of the adduct $TiCl_4$,NMe_3 for the a_1 TiCl axial stretching mode in both the Raman and the infrared, on passing from the solid to the solution state.

Since the vibrational spectra again suggest a cis formulation a powder x-ray study was undertaken for this adduct. The resultant d-spacings, (Table IV. 12.), however, suggest that the adduct is not isomorphous with either $SnCl_4$,2MeCN or $TiCl_4$,2MeCN. The assignment of cis stereochemistry for this adduct must therefore again rest on the spectra data presented, and its general similarity to the data obtained for $TiCl_4$,2MeCN and $SnCl_4$,2MeCN.

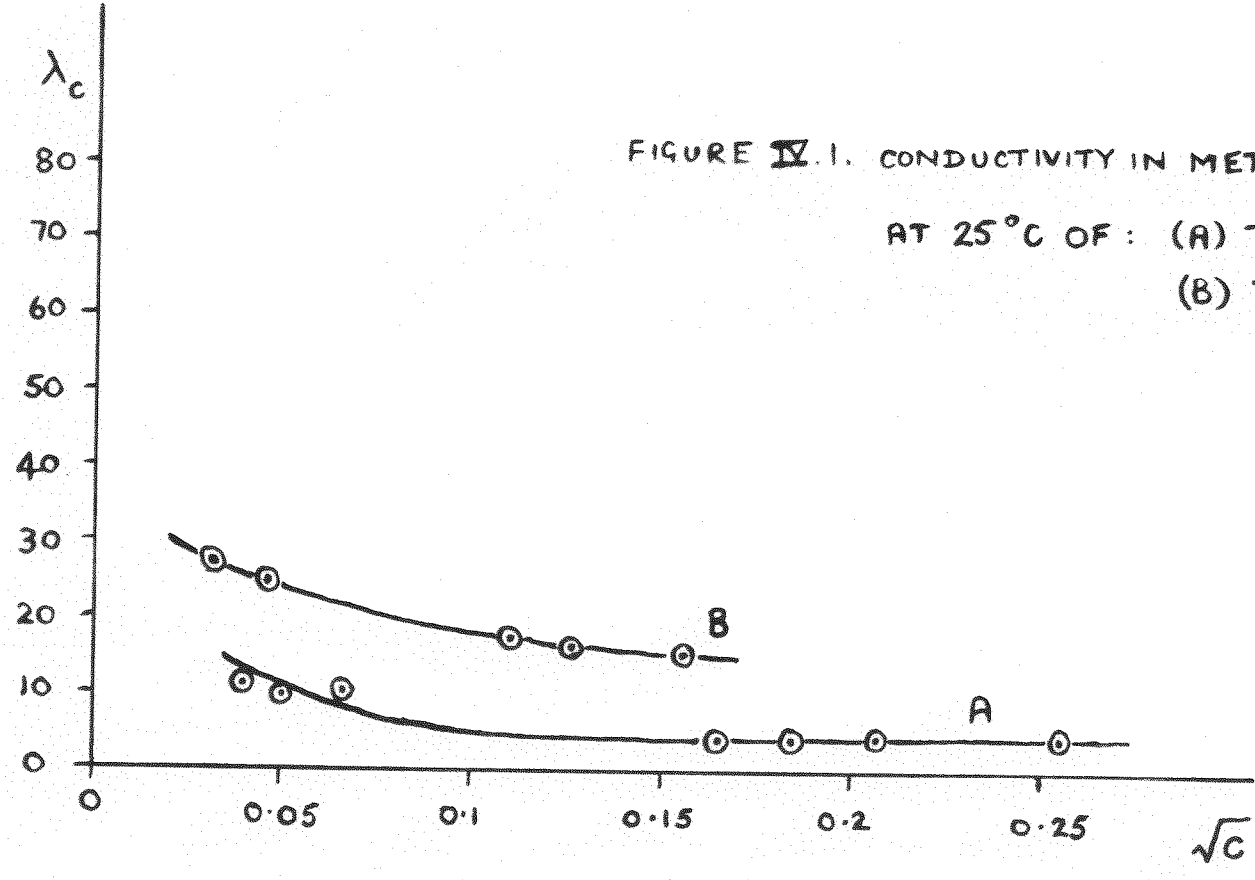

FIGURE IV.1. CONDUCTIVITY IN METHYL CYANIDE AT 25°C OF: (A) $TiCl_4$ (B) $TiBr_4$

T A B L E IV. 1.

Observed vibrational frequencies ($cm.^{-1}$) for $TiCl_4, 2PMe_3$.

RAMAN		INFRARED	
Solid	Benzene Soln.	Mull	Benzene Soln.
158 w.		159 w.	156 w.
188 w.	190 w.P.		
261 w.	264 w. D.P.	257 s.	260 m.
323 v.s.	324 v.s.P.	322 w.sh.	324 w.sh.
364 w.	380 w.P.	362 v.s.	382 v.s.

T A B L E IV. 2.

Observed vibrational frequencies ($cm.^{-1}$) for $TiCl_4, 2Py$.

RAMAN (Solid)	INFRARED (Mull)
	158 w.
170 w.	169 w.
182 w.sh.	
194 s.	192 v.w.
232 w.	
252 w.	
	285 s.
324 v.s.	
388 v.w.	380 v.s.
	390 v.s.sh.
434 v.w.	443 s.

TABLE IV. 3.

Raman spectra of 1,10 phen; $TiCl_4$.1,10 phen; 1,2 Dimethoxybenzene and $TiCl_4$,1,2 Dimethoxybenzene.

Free 1,10 phen (Solid)	$TiCl_4$ 1,10 phen (Solid)	Free Dimethoxy-benzene (Liquid)	$TiCl_4$ 1,2 Dimethoxy-benzene Solid	Benzene Soln.
			68 m.	
	136 w.		80 w.	
	146 m.		110 m.	
	173 m.		128 v.w.	
	180 w.		138 v.w.	
	198 w.sh.	212 m.	158 m.	
248 s.br.	232 m.br.	242 m.	168 w.sh.	210 w.
	303 s.		308 v.s.	318 s.P.
	356 w.br.	382 m.v.br.	340 v.w.br.	
	381 s.		396 v.s.	390 s.P.
412 s.	404 w.		416 s.	
	426 v.w.		428 m.sh.	
	436 v.w.	480 w.br.	478 w.	478 w.

SOUTHAMPTON UNIVERSITY LIBRARY

T A B L E IV. 4.

Observed vibrational frequencies ($cm.^{-1}$) for $TiBr_4$,2Py.

INFRARED (Mull)

140 w.

186 w.

274 s.

294 s.

308 s.

T A B L E IV. 5.

d-spacings for $TiCl_4$,2Py, $TiBr_4$,2Py and $SnCl_4$,2Py.

$SnCl_4$,2Py	$TiCl_4$,2Py	$TiBr_4$,2Py
5.16 v.s.	4.98 v.s.	5.16 v.s.
4.82 s.	4.67 v.s.	4.98 v.s.
3.74 s.	3.56 s.	3.74 m.
2.82 w.	2.68 w.	2.82 w.
2.47 s.	2.43 s.	2.47 s.
2.39 w.	2.29 w.	2.29 s.
1.97 m.	1.97 s.	1.97 s.
1.62 v.w.	1.85 v.w.	1.62 m.
1.54 m.	1.52 m.	1.54 s.
1.49 w.	1.48 w.	1.49 m.
1.41 w.	1.42 w.	1.43 m.
1.19 v.w.br.	1.19 w.br.	1.2 w.
1.11 v.w.br.	1.10 w.br.	1.11 w.

TABLE IV. 6.

Observed vibrational frequencies ($cm.^{-1}$) for $TiCl_4$,2MeCN, and $TiCl_4$,$2CD_3CN$ (values in brackets).

RAMAN			INFRARED
Solid	MeCN Soln.	ØH Soln.	Mull
110 s.			120 w.
140 (138) s.			(165) w.
160 (158) w.			(179) w.
178 (179) m.s.			196 (191) w.
212 (204) w.			(210) w.
240 (236) w.			(233) w.
320 (320) s.	320 s.(P)	322 m.(P)	322 (318) m.
370 (372) m.		356 m.(P)	388 v.s.
391 (386) v.s.	398 s.(P)		
412 (400) v.w.*		410 s.(P)*	407 (400)† v.s.
430 (430) m.			424 v.s.

* probably due to 1:1 adduct - see Table IV. 9.

† strong, very broad and asymmetric.

methylcyanide band at 382 $cm.^{-1}$ not listed.

TABLE IV. 7.

Conductivity data for solutions of $TiCl_4$ in methylcyanide at 25°C.

Specific conductance λ_c (ohm^{-1} $cm.^{-1}$)	$\sqrt{c}$
5.123	0.2570
5.205	0.2091
5.441	0.1856
5.744	0.1649
13.24	0.0642
12.29	0.0493
15.95	0.0406

TABLE IV. 8.

Calculated frequencies ($cm.^{-1}$) for C_{2V} $TiCl_4$,2MeCN and $TiCl_4$,$2CD_3CN$ (values in brackets) for f_{Ti-N} = 1.0 md. $Å^{-1}$.

Frequency	Symmetry	Potential energy contributions
55 (51)	a_1	(δCNTi (δN_2TiCl_2 I.P.
67 (64)	a_2	(δCNTi (δTiN_2OP
84 (79)	b_1	(δCNTi (δTiN_2 O.P.
84 (82)	b_2	δN_2TiCl_2 I.P.
127 (126)	a_1	$\delta TiCl_2$ax
150 (149)	a_2	$\delta TiCl_2$ eq. O.P.
151 (147)	b_2	$\delta TiCl_2$ ax.
181 (179)	a_1	(δN_2TiCl_2 eq. I.P. ($\delta TiCl_2$ ax.
181 (181)	b_1	$\delta TiCl_2$ eq. O.P.
208 (200)	b_2	νTiN_2
223 (215)	a_1	νTiN_2
227 (216)	a_2	(δCNTi (δCCN (δTiN_2 O.P.

T A B L E IV. 8. (cont.)

Frequency	Symmetry	Potential energy contributions
236 (231)	b_2	δN_2TiCl_2
250 (244)	a_1	$\nu TiCl_2$ ax. $\delta CNTi$ δL_2TiCl_2 eq. I.P. νTiN_2
252 (242)	b_1	δCCN δTiN_2 O.P.
302 (301)	a_1	$\nu TiCl_2$ ax.
389 (388)	b_2	$\nu TiCl_2$ eq.
394 (393)	a_1	$\nu TiCl_2$ eq.
435 (434)	b_1	$\nu TiCl_2$ ax.

TABLE IV. 9.

Raman spectrum ($\Delta\nu$ cm.$^{-1}$) of solid obtained from a solution of $TiCl_4$,2MeCN in benzene after pumping to dryness.

114 s.

128 w.

150 s.

178 m.w.

212 v.w.br.

237 w.br.

294 w.br.

322 w.

374 v.w.

388 m.

421 v.v.s.

TABLE IV. 10.

Observed vibrational frequencies ($cm.^{-1}$) for $TiBr_4, 2MeCN$.

RAMAN		INFRARED	
Solid	MeCN Soln.*	Mull	MeCN Soln.*
110 w.			
168 m.	166 w.	160	170
			198
225 s.	224 s.P.	228	225
		284	
		308 s.	308 s.
319 s.	334 s.P.	331 s.	324 s.
327 sh.	(		
	(		
345 m.s.	(obscured by		398 w.
	(MeCN band		
	(at 382 $cm.^{-1}$	410 w.	412 w.
		465 w.br.	468 v.w.br.

*methylcyanide band at 382 $cm.^{-1}$ not listed.

TABLE IV. 11.

Conductivity data for solutions of $TiBr_4$ in methylcyanide at 25°C.

Specific conductance λ_c (ohm^{-1} $cm.^{-1}$)	$\sqrt{c}$
17.01	0.1587
17.59	0.1265
18.34	0.1122
35.91	0.0446
26.99	0.0326

TABLE IV. 12.

d-spacings for $SnCl_4$,2MeCN, $TiCl_4$,2MeCN, $TiBr_4$,2MeCN.

$SnCl_4$,2MeCN	$TiCl_4$,2MeCN	$TiBr_4$,2MeCN
4.98 s.	6.81 m.	5.54 s.
4.49 s.	5.16 s.	4.27 s.
4.27 s.	4.4 s.	2.68 w.
3.94 w.	3.19 w.	2.41 w.
3.06 s.	2.64 m.	2.29 w.
2.68 m.	2.25 m.	2.02 s.
3.39 w.	1.85 w.	1.9 m.
2.13 w.	1.75 w.	1.83 w.
1.79 m.	1.54 w.	1.72 m.
1.43 w.	1.39 w.	1.63 m.
1.36 w.	1.32 w.	1.45 w.
		1.37 w.
		1.33 w.

IV. 6. Experimental.

(i) General. The purification and drying of the reactants and the preparation of the adducts was carried out in all glass vacuum systems. Powder x-ray, mull and infrared solution samples were made up in a dry box, whilst Raman solutions were made up and transferred to 0.1 mm. pyrex capillary cells in an all glass vacuum system. Solid Raman samples were contained in vacuum ampoules.

Titanium tetrachloride was purified as described in Chapter III, whilst titanium tetrabromide was purified by repeated sublimation in an all glass vacuum system, with continuous pumping. Both tetrahalides were finally stored in break-seal vacuum ampoules. Benzene, pyridine, methylcyanide and 1,2 dimethoxybenzene were dried with calcium hydride and stored in break-seal vacuum ampoules. Methylcyanide-d_3 was dried over molecular seive 4a and 1,10 phenanthroline by repeated sublimation in an all glass vacuum system with continuous pumping. Trimethylphosphine was prepared, purified and dried as described in Chapter III.

(ii) Preparation of the adducts. All the adducts were prepared by mixing benzene solutions of $TiCl_4$ or $TiBr_4$ with benzene solutions of the appropriate ligand, the complexes with trimethylphosphine, pyridine and methylcyanide using an excess of ligand, and the complexes with 1,10 phenanthroline and 1,2 dimethoxybenzene using an excess of the tetrahalide. The precipitated adducts were filtered off and washed with benzene to remove excess reactants. The chloride

analyses of all the adducts were carried out by hydrolysis in water, followed by potentiometric titration of the chloride with silver nitrate. The analysis results are summarised below:

Adduct	Experimental %Cl.	Theoretical %Cl.
$TiCl_4,2(P(CH_3)_3)$	41.39	41.53
$TiCl_4,2(NC_5H_5)$	40.24	40.81
$TiBr_4,2(NC_5H_5)$	60.46	60.94
$TiCl_4,2(CH_3CN)$	51.43	52.20
yellow solid from benzene solution of $TiCl_4,2(CH_3CN)$	57.91	61.48 (for 1:1 adduct)
$TiCl_4,2(CD_3CN)$	51.15	51.64
$TiBr_4,2(CH_3CN)$	70.82	71.27
$TiCl_4,(C_{12}H_8N_2)$	37.94	38.38
$TiCl_4,(C_{10}H_{16}O_2)$	38.87	39.67

(iii) The conductivity measurements. These were made in an all glass vacuum system. A solution of the tetrahalide was made up in the vacuum system, the volume of methylcyanide being measured in the barrel of a grade A burette which had been glass blown onto the system, with the tap removed and the end rounded off. The end correction had been previously determined. The tetrahalide contained in a fragile tipped ampoule, which had previously been weighed, was then broken open, the tetrahalide distilled out into the methylcyanide and the ampoule removed in its containing vacuum tube by collapsing a constriction. This latter was then opened and the empty ampoule plus

broken glass was washed out with distilled water and weighed by collection on a weighed sinter, the weight of tetrahalide then being found by the difference in the two weights. The conductivity of the solution was determined with a lightly platinized platinum electrode system (cell constant 0.085 $cm.^{-1}$) and a Pye conductivity bridge. The cell was thermostatted at 25°C. The specific conductance of the pure methylcyanide was 6.5×10^{-7} ohm^{-1} $cm.^{-1}$. Measurements were then made on solutions of increasing concentration by subsequently distilling off known amounts of the methylcyanide into the burette. Finally the bulk of the solution was removed by sealing off in a break-seal ampoule. In the experiment with $TiCl_4$, this solution was then transferred to a capillary Raman cell, its Raman spectrum measured, and found to be identical with the MeCN solution Raman spectrum reported in Table IV. 6. The remainder of the solution was then diluted with a fresh quantity of methylcyanide to provide readings for more dilute solutions. The results are plotted in Figure IV. 1., and listed in Tables IV. 7 and 11.

(iv) The spectra were measured as in Chapter III. Infrared solutions were recorded in polythene cells, and mulls between polythene plates. Raman solution samples were contained in pyrex capillary tubes of 1.0 mm outside diameter. The powder x-ray photographs were measured using Cu K_α radiation, and the samples were contained in 0.5 mm Lindemann tubes.

C H A P T E R V.

The preparation of some 1:2 adducts of the trichlorides of metals in the first transition series with trimethylamine and trimethylphosphine.

V. 1. Introduction.

Several species of general formula $MCl_3,2L$ where L = NMe_3 or PMe_3 have been prepared and characterised for the trichlorides of metals occurring in the first transition series, and there is an accumulation of physical data for these which may be interpreted in terms of a monomeric pentacoordinate structure with D_{3h} symmetry.

The isolation of the adduct $TiCl_3,2NMe_3$ was first reported by Antler and Laubengayer (88), and this work was subsequently repeated by Fowles (89). The adduct $VCl_3,2NMe_3$ was thought to possess a monomeric D_{3h} structure on the basis of preliminary dipole moment and infrared studies (to 400cm.$^{-1}$) (90), and on the basis of molecular weight and magnetic susceptibility measurements (91). Subsequently, far infrared measurements on this adduct confirmed this view (11). More recently, the adduct $CrCl_3,2NMe_3$ has been isolated (92), and on the basis of its far infrared (to 200 cm.$^{-1}$) and U.V. absorption spectra has been assigned a monomeric D_{3h} structure (93) x-ray studies have subsequently been undertaken for all of these compounds, and they have been shown to adopt what is essentially a D_{3h} trans trigonal bipyramidal geometry, although in the cases of $TiCl_3,2NMe_3$ (94) and $CrCl_3,2NMe_3$ (95), distortions have been observed which effectively lower the symmetry to C_{2V}. Although the origin of these distortions is still somewhat speculative, it has been shown that the magnetic properties of $TiCl_3,2NMe_3$ and $CrCl_3,2NMe_3$ can be accounted for on the basis of a C_{2V} ligand environment (95). The

single crystal x-ray structure of $VCl_3,2NMe_3$ has been reported (96) and confirms it as a D_{3h} trigonal bipyramidal monomer.

No complexes of general formula $MCl_3,2NMe_3$ have been reported for any other metals of the first transition series. However, a number of trialkylphosphine complexes have been prepared. The adducts $VCl_3,2PEt_3$ (97) and $CrCl_3,2PEt_3$ (98) have been prepared and characterised by Isslieb. The adduct $VCl_3,2PEt_3$ has been shown to be monomeric by cryoscopy in benzene, and to have an effective magnetic moment of 2.83 B.M. corresponding to two unpaired spins. By contrast, the adduct $CrCl_3,2PEt_3$ was shown to be dimeric in benzene by cryoscopy and to have an effective magnetic moment of 3.8, corresponding to three unpaired spins. In addition Jensen has prepared a number of complexes of general formulae $CoCl_3,2PR_3$ and $NiCl_3,2PR_3$ (99). Results for the triethylphosphine complexes suggest that $CoCl_3,2PR_3$ is monomeric in solution in benzene, has essentially zero dipole moment in solution in pentane, and has a magnetic moment corresponding to <u>two</u> unpaired spins (i.e. a low spin complex). Similarly the adduct $NiCl_3,2PEt_3$ has a magnetic moment corresponding to <u>one</u> unpaired spin. It seems probable that these complexes too adopt a <u>trans</u> D_{3h} monomeric trigonal bipyramidal structure.

Since, from the foregoing, it appeared likely that complexes of the type $MCl_3 2L$ (where L = NMe_3 or PMe_3) might be quite widespread for the trichlorides of metals of the first transition series, and since there is a considerable body of evidence for the general adoption by them of a monomeric pentacoordinate <u>trans</u> D_{3h} structure, an attempt

was made during the course of this work to prepare and characterise a full range of complexes $MX_3 2L$ for both L = NMe_3 and PMe_3 for as many metals of the first transition series as possible.

Preliminary calculations (see Chapters VI, VII and VIII) suggested that the MCl_3 symmetric and antisymmetric stretching vibrations are likely to be at least 80-90% pure. Therefore values of f_{MCl} and $f_{MCl,MCl}$ could be obtained from the spectral results. Furthermore, since it seemed likely that all of these compounds might be monomeric in benzene solution, and therefore amenable to a study of ligand exchange reactions in solution, it was hoped to be able to obtain information concerning the relative stabilities of the amine and phosphine complexes for any given metal trichloride.

It was thought that a study of these systems would be of interest from the point of view of any systematic changes in the vibrational spectra. Although correlations of the nature of chemical bonding with values of force constants are open to serious question, it was felt that in view of the results of the preliminary calculations, which showed that the MCl_3 unit could be considered approximately as an isolated planar MCl_3 unit, some very broad correlation might be obtained of the vibrational frequency for the a_1' symmetric MCl_3 stretching vibration with the relative stability between the phosphine and amine series, which was not complicated by mass effects.

V. 2. The Preparation of the Adducts.

This work was initiated by the preparation and study of the complexes $TiCl_3,2NMe_3$, $VCl_3,2NMe_3$ and $CrCl_3,2NMe_3$, all of which are known from x-ray measurements to adopt a D_{3h} geometry. The complexes were prepared by the general method developed by Fowles (93). Subsequently, using the same method, the known complexes $VCl_3,2PMe_3$ and $CrCl_3,2PMe_3$ were prepared. Molecular weight studies of $CrCl_3,2PMe_3$ were carried out by cryoscopy in benzene, and the results (see experimental section) indicate that it is monomeric in benzene solution, a result which is at variance with the earlier measurement carried out by Isslieb on $CrCl_3,2PEt_3$ (98). It will be seen that formulation of this adduct as a monomer rather than a dimer is not unreasonable when the results of the studies of the vibrational spectra of these adducts are discussed in Chapters VI and VII.

Finally, the adducts $ScCl_3,2NMe_3$, $ScCl_3,2PMe_3$, $TiCl_3,2PMe_3$, $FeCl_3,2NMe_3$ and $FeCl_3,2PMe_3$ have been prepared by the method of Fowles, and the adducts $CoCl_3,2PMe_3$ and $NiCl_3,2PMe_3$ by the method described by Jensen (99) involving the oxidation of $CoCl_2,2PMe_3$ and $NiCl_2,2PMe_3$ by nitrosyl chloride. Although the complexes of $CoCl_3$ and $NiCl_3$ with trimethylphosphine are less well characterised than those with triethylphosphine (99), it was felt that the former would yield vibrational data which would be less complex in the metal-chlorine stretching region, and therefore easier to interpret. Magnetic susceptibility measurements have been carried out on the 1:2 adducts

of $TiCl_3$, VCl_3, $CrCl_3$, $FeCl_3$ and $NiCl_3$ with trimethylphosphine, and on the $FeCl_3$ 1:2 adduct with trimethylamine. The resulting effective magnetic moments are listed in Table V. 1. It will be seen that the results on the vanadium, chromium and nickel complexes agree with those previously reported, and that the complexes $FeCl_3,2NMe_3$, $FeCl_3,2PMe_3$ and $NiCl_3,2PMe_3$ adopt the low spin configuration of electrons in the 3d orbitals. Unfortunately, no magnetic susceptibility measurements could be obtained for the adduct $CoCl_3,2PMe_3$ since it was not prepared in sufficient quantities. However, magnetic susceptibility measurements by Jensen (99) yield a value of μ_{eff} which corresponds to two unpaired electrons for $CoCl_3,2PEt_3$, indicating that it too adopts the low spin configuration.

TABLE V. 1.

Magnetic measurements at 20°C. on some complexes $MCl_3, 2L$ where L = NMe_3 or PMe_3.

Adduct	μ_{eff} observed (B.M.)	Corresponding No. of unpaired spins
$TiCl_3, 2PMe_3$	1.67	1
$VCl_3, 2PMe_3$	2.63	2
$CrCl_3, 2PMe_3$	3.81	3
$FeCl_3, 2NMe_3$	3.85	3
$FeCl_3, 2PMe_3$	3.68	3
$NiCl_3, 2PMe_3$	1.92	1

V. 3. Experimental.

Preparation of all adducts were carried out in all glass vacuum systems. The anhydrous metal trichlorides were prepared in standard quickfit apparatus and subsequently pumped and heated to remove volatiles before being transferred to breakseal vacuum ampoules in an all glass vacuum system. Chloride analyses were determined by potentiometric titration with silver nitrate after hydrolysis in very dilute nitric acid.

(i) Preparation of the anhydrous trichlorides. Scandium trichloride was prepared as described in the literature (100) by heating "Spec pure" scandium oxide (1 g.) with ammonium chloride (7 g.) at 350°C for four hours. The excess ammonium chloride was sublimed off by heating the mixture in vacuo at 250°C for 12 hours, whereupon the scandium trichloride remaining was transferred to breakseal vacuum ampoules.

Vanadium trichloride was prepared by refluxing vanadium pentoxide with excess sulphur monochloride under white spot nitrogen, as described in the literature (65). The resulting vanadium trichloride was filtered off under nitrogen and washed with a large quantity of carbon disulphide (dried over calcium hydride). It was then heated to 150°C with pumping overnight to remove volatiles and transferred to breakseal vacuum ampoules.

Chromium Trichloride and Ferric Chloride were prepared by the general method described in the literature (101) involving dehydration

of the hydrated trichlorides by refluxing with excess thionyl chloride. The anhydrous trichlorides so prepared were filtered off, washed with fresh thionyl chloride, and heated to 150°C with pumping to remove residual volatiles before being transferred to breakseal ampoules.

The specimen of $TiCl_3$ was the kind gift of the International Synthetic Rubber Company, and was prepared by hydrogen reduction of $TiCl_4$.

The analytical results obtained for these anhydrous trichlorides are listed in Table V. 2.

(ii) Preparation of the Adducts. The complexes $ScCl_3,2NMe_3$, $ScCl_3,2PMe_3$, $TiCl_3,2NMe_3$, $TiCl_3,2PMe_3$, $VCl_3,2NMe_3$ and $FeCl_3,2NMe_3$ were prepared by the general method of Fowles (93) by reaction of the appropriate trichloride with excess of the ligand. Filtration and removal of the excess ligand by pumping yielded crystalline products in all cases. The adducts $CrCl_3,2NMe_3$ and $CrCl_3,2PMe_3$ were prepared in the same way, but with the addition of a trace of zinc dust to the reaction mixture. All the adducts were recrystallised from benzene, except the complexes with $TiCl_3$ which, being insoluble in benzene, were recrystallised from the ligand.

Preparation of the adduct $FeCl_3,2PMe_3$ in this way resulted first in the formation of the required product which then appeared to react with a further quantity of the trimethylphosphine to yield a pale blue-green crystalline product. Presumably the $FeCl_3,2PMe_3$ adduct formed initially was reduced to an Fe(II) species by the excess

trimethylphosphine. It was found that reaction of the $FeCl_3,2PMe_3$ in this way could be prevented by removal of the excess trimethylphosphine as soon as the initial reaction had occurred, and subsequent recrystallisation of the $FeCl_3,2PMe_3$ from benzene.

Similarly, reaction of vanadium trichloride with excess trimethylphosphine resulted in a mixture of the purple red adduct with a yellow crystalline material, which persisted in subsequent attempts to prepare a pure specimen of the adduct even after repeated heating and pumping of the VCl_3 used to ensure complete removal of sulphur. It is presumed that here again reduction by the excess trimethylphosphine occurred. A pure sample of $VCl_3,2PMe_3$ was finally obtained by reaction of VCl_3 with a deficit of trimethylphosphine dissolved in benzene. Under these conditions, no yellow product was detectable, and the product obtained gave a satisfactory chloride analysis (see Table V. 3).

The adducts $CoCl_3,2PMe_3$ and $NiCl_3,2PMe_3$ were prepared by reaction of $CoCl_2,2PMe_3$ and $NiCl_2,2PMe_3$ with nitrosyl chloride as described in the literature (99). The samples of $CoCl_2,2PMe_3$ and $NiCl_2,2PMe_3$ used were similarly prepared as described in the literature (99). Chloride analyses for all of these adducts are listed in Table V. 3.

TABLE V. 2.

Chloride analyses for the anhydrous trichlorides.

Sample	Experimental %Cl.	Theoretical %Cl.
$ScCl_3$	69.87	70.31
$TiCl_3$	68.52	68.95
VCl_3	67.03	67.59
$CrCl_3$	66.64	67.19
$FeCl_3$	64.78	65.55

TABLE V. 3.

Chloride analyses for the trimethylamine and trimethylphosphine adducts.

Adduct	Experimental %Cl.	Theoretical %Cl.
$ScCl_3,2NMe_3$	38.42	39.59
$ScCl_3,2PMe_3$	34.78	35.16
$TiCl_3,2NMe_3$	38.93	39.15
$TiCl_3,2PMe_3$	34.72	34.81
$VCl_3,2NMe_3$	38.28	38.74
$VCl_3,2PMe_3$	34.01	34.46
$CrCl_3,2NMe_3$	38.27	38.68
$CrCl_3,2PMe_3$	33.27	34.36
$FeCl_3.2NMe_3$	37.56	38.04
$FeCl_3,2PMe_3$	32.73	33.92
$CoCl_2,2PMe_3$	24.81	25.21
$CoCl_3,2PMe_3$	32.47	33.59
$NiCl_2,2PMe_3$	24.96	25.21
$NiCl_3,2PMe_3$	32.18	33.59

(iii) The molecular weight determination on $CrCl_3,2PMe_3$ in benzene solution was carried out by the procedure described in Chapter III for the molecular weight of $TiCl_4,PMe_3$. Determinations were carried out at two different concentrations, and were found to be consistent.

$CrCl_3,2PMe_3$ M = 310

Experimental values: M = 287 1.2 mM benzene

294 0.5 mM benzene

(iv) The magnetic susceptibility measurements were carried out using a Gouy balance operating at room temperature. The Gouy tube was constructed from a quickfit B.7 cone and socket, and was loaded in a dry nitrogen box. The tube was calibrated using a sample of mercury tetrathiocyanato cobalt (II). The values obtained for the effective magnetic moment for the adducts studied are listed in Table V. 1.

C H A P T E R VI.

The vibrational spectra of some adducts of general formula $MCl_3.2NMe_3$ for metals of the first transition series.

VI. 1. Introduction.

Although, as outlined in Chapter V, several $MX_3,2NMe_3$ complexes of the first-row transition series have been reported, the work reported on their vibrational spectra is quite scarce. The adducts $TiBr_3,2NMe_3$ (94), $VCl_3,2NMe_3$ (96), $TiCl_3,2NMe_3$ (95) and $CrCl_3,2NMe_3$(95) have been shown by x-ray measurements to be isostructural and to adopt a monomeric D_{3h} trigonal bipyramidal structure. Previously, infrared data (down to 200 $cm.^{-1}$) had been reported for $VCl_3,2NMe_3$ (90), (11) and the spectra had been interpreted in terms of a probable monomeric D_{3h} structure. Infrared data (down to 200 $cm.^{-1}$) have also been reported for $CrCl_3,2NMe_3$ (93).

Vibrational spectra have also been reported for adducts of the type $MX_3,2NMe_3$ where M is a group III(b) metal (46), (102), and have been interpreted in terms of a D_{3h} trigonal bipyramidal structure. Moreover, the adduct $InCl_3,2NMe_3$ has been shown to be isomorphous with $TiCl_3,2NMe_3$, $VCl_3,2NMe_3$ and $CrCl_3,2NMe_3$ (103).

In the present chapter, the vibrational spectra of the adducts of general formula $MCl_3,2NMe_3$ have been measured, (where M = Sc, Ti, V, Cr, Fe). The results for vanadium (III) and chromium (III) are compared with the earlier work, and with the data obtained for scandium (III), titanium (III) and iron (III). A close similarity is seen to exist between the spectra of all of these compounds, and the spectra are all interpretable on the basis of a D_{3h} trigonal bipyramidal model. The results of a G.V.F.F. calculation of the

vibrational frequencies of $TiCl_3,2NMe_3$ are given, for a D_{3h} trigonal bipyramidal model, and these facilitate the assignment of the spectra. This being the case, the data for $TiCl_3,2NMe_3$ are considered first. For a general adduct $MCl_3,2XMe_3$, treating the methyl groups as point masses, and neglecting the two XC_3 torsional modes, we have:

$$\Gamma_{mol} = 4a_1' + 4a_2'' + 6e' + 4e''$$

and of these the a_1' and e" modes are Raman active the a_2'' modes are infrared active and the e' modes are both Raman and infrared active. On a simple basis we should expect one M-Cl stretching mode (a_1') to be Raman active only and one M - Cl stretching mode (e') to be infrared active, and weakly Raman active. However, in addition, we may expect the a_2'' MX_2 stretching mode to occur in this region, and also two pairs of bands due to the XC_3 ligand deformations (see Appendix C). In most cases it is likely that these latter will not be fully resolved, however, and will be detected simply as two broad bands due to ($a_1' + a_2''$) and (e' + e") deformations.

VI. 2. <u>The Adduct $TiCl_3,2NMe_3$</u>.

The Raman and infrared spectra observed for this compound are summarised in Table VI. 2., and the results of the G.V.F.F. calculation in Table VI. 3., the frequencies quoted there being those corresponding to f_{Ti-N} = 0.8 md. $Å^{-1}$., this value being selected as giving the best fit of calculated to observed frequencies. The bands observed above 400 $cm.^{-1}$ are all easily assignable to the trimethylamine deformations,

of which four are expected for a 1:2 adduct of this type (see Appendix C). It should be noted that the agreement between the observed and calculated deformations is not good, but it should be remembered that in these calculations the methyl groups were treated as point masses, and the methyl rocking modes therefore effectively ignored. Similarly, although the band observed at 385 $cm.^{-1}$ (strong and broad) in the infrared can most reasonably be assigned to the e' $TiCl_3$ stretching mode (by analogy with $InCl_3,2NMe_3$ (323 $cm.^{-1}$), (102), $VCl_3,2NMe_3$ (309 $cm.^{-1}$), (11) and $CrCl_3,2NMe_3$ (392 $cm.^{-1}$), (93)) the calculated frequency for this band is approximately 30 $cm.^{-1}$ too high. It is most likely that the approximation made in calculating the values of f_{TiCl} and $f_{TiCl,TiCl'}$ that the ratio $f_{TiCl,TiCl}/f_{TiCl}$ was equal to that found for $TiCl_4$, is not a good one. It is worth noting that a similar result was found in the calculations on D_{3h} $InCl_3,2NMe_3$, where the value of $f_{InCl,InCl}/f_{InCl}$ was taken as equal to the ratio f_{rr}/f_r found for $SnCl_4$, (102). The very strong band at 308 $cm.^{-1}$ in the Raman can be assigned to the a_1' $TiCl_3$ stretching mode, and the values of f_{TiCl} and $f_{TiCl,TiCl}$ were calculated on this assumption (see Appendix C). The band at 264 $cm.^{-1}$ in the infrared (absent in the Raman) can be assigned to the a_2'' TiN_2 stretching mode, in agreement with the assignment made for $CrCl_3,2NMe_3$ (93) for the medium infrared band observed at 274 $cm.^{-1}$. It is also likely that the weak Raman band at 200 $cm.^{-1}$ is to be associated with the a_1' TiN_2 stretching mode,

since the work reported on $InCl_3,2NMe_3$ suggests that this mode occurs at 163 $cm.^{-1}$ for this compound and is only weakly Raman active. If this is so, then the calculated frequency reported here is in error by approximately 60 $cm.^{-1}$. A deuteriation study would help to identify this mode with more certainty. In view of the coincidence of this band with a band at 200 $cm.^{-1}$ in the infrared it is also possible that it is the e' NC_3 rocking mode. The bands observed below 200 $cm.^{-1}$ are in reasonable agreement with the frequencies calculated on the basis of a D_{3h} model. It is unfortunate that no solution data could be obtained for this compound, as polarisation data for the excellent Raman spectra obtained would have been of great help in assigning the bands. Unfortunately the compound is soluble only in trimethylamine, without reaction, and attempts to measure the Raman spectrum in this solvent failed, as the solution boiled in the laser beam. However, the polarisation data obtained for $ScCl_3,2NMe_3$ (Table VI. 1.) helps to confirm the assignment of the 308 $cm.^{-1}$ band observed for $TiCl_3,2NMe_3$ in the Raman as the a_1' totally symmetric $TiCl_3$ stretching mode.

VI. 3. The Adduct $ScCl_3,2NMe_3$.

The Raman and infrared spectra observed for this compound are listed in Table VI. 1. It is quite apparent that there is an overall similarity to the spectral data obtained for $TiCl_3,2NMe_3$. Once again the bands at 502 $cm.^{-1}$, 488 $cm.^{-1}$, 440 $cm.^{-1}$ and 433 $cm.^{-1}$ are

assignable to the trimethylamine deformational modes, whilst the bands at 396 - 401 $cm.^{-1}$ (broad and strong in the infrared, broad and weak in the Raman) and 299 $cm.^{-1}$ (very strong and polarised in the Raman) can be assigned to the e' and a_1' $ScCl_3$ stretching modes respectively. The strong infrared band at 260 $cm.^{-1}$ is likely to be the a_2'' ScN_2 stretching mode. Once again, there is no band which can be unambiguously assigned to the a_1' νScN_2 stretching mode, but it might possibly be assigned to the very weak Raman active band at 197 $cm.^{-1}$. However, from the general similarity to the vibrational spectra obtained for $TiCl_3,2NMe_3$, it seems probable that it too adopts a monomeric D_{3h} trigonal bipyramidal structure both in the solid state and in solution.

VI. 4. The Adducts $VCl_3,2NMe_3$ and $CrCl_3,2NMe_3$.

The vibrational spectra observed for these adducts are collected in Tables VI. 4 and 5. The infrared data reported in this work for these two adducts are in general agreement with the far infrared data reported earlier (11), (93), and in addition data have been obtained in the region below 200 $cm.^{-1}$. Supplementing this, Raman data on the solid adducts have been obtained for the first time. However, the Raman spectra obtained were weak, due to the intense colours of these two adducts. Bands in the Raman were observed at 310 $cm.^{-1}$ and 294 $cm.^{-1}$ for $VCl_3,2NMe_3$ and $CrCl_3,2NMe_3$ respectively, and they are assigned to the a_1' MCl_3 symmetric stretching mode in each case.

This assignment is in accord with the assignment of the bands at 308 cm.$^{-1}$ and 299 cm.$^{-1}$ observed in the Raman spectra of $TiCl_3,2NMe_3$ and $ScCl_3,2NMe_3$ to this mode. Unfortunately, although both of these adducts are soluble in benzene, no solution Raman spectra were detectable, presumably once again because of the intense colours of the solutions.

Inspection of the infrared data given in Tables VI. 4 and 5., reveal bands at 508 cm.$^{-1}$, 448 cm.$^{-1}$ ($VCl_3,2NMe_3$), 525 cm.$^{-1}$, 507 cm.$^{-1}$, 470 cm.$^{-1}$ and 449 cm.$^{-1}$ ($CrCl_3,2NMe_3$) assignable to the Me_3N deformations. Similarly, the strong bands at 415 cm.$^{-1}$ and 399 cm.$^{-1}$ are assignable to the e' MCl_3 antisymmetric stretching modes for $VCl_3,2NMe_3$ and $CrCl_3,2NMe_3$, respectively. Once again similarity with the $TiCl_3,2NMe_3$ infrared spectrum suggests that the bands at 258 cm.$^{-1}$ and 280 cm.$^{-1}$ may be associated with the a_2'' MN_2 antisymmetric stretching mode.

VI. 5. The Adduct $FeCl_3,2NMe_3$.

The infrared and Raman data observed for this adduct are listed in Table VI. 6. Comparison with the corresponding data for the adducts with scandium (III), titanium (III), vanadium (III) and chromium (III) suggests that this adduct also adopts a monomeric D_{3h} trigonal bipyramidal structure both in the solid state and in solution. Despite the orange-brown colour of this adduct, good Raman spectra were easily obtainable, although, in solution, only

the strong bands at 485 cm.$^{-1}$ (polarised) and 305 cm.$^{-1}$ (polarised) were detectable, since the adduct was only of moderate solubility in benzene. However, these bands can confidently be assigned as the a_1' NC_3 deformation and a_1' $FeCl_3$ stretching mode, respectively. The Raman spectrum bears a close resemblance to the Raman spectra observed for $ScCl_3,2NMe_3$ and $TiCl_3,2NMe_3$, and once more it seems likely that the weak band at 196 cm.$^{-1}$ is associated with the a_1' FeN_2 stretching mode. The bands at 496 cm.$^{-1}$ and 466 cm.$^{-1}$ in the infrared may be assigned to symmetric and antisymmetric trimethylamine deformational modes, whilst the strong bands at 360 cm.$^{-1}$ and 310 cm.$^{-1}$ are to be associated with the e' $FeCl_3$ and a_2'' FeN_2 antisymmetric stretching modes respectively. It also seems probable that, whatever their origin, the shoulders observed at 300 cm.$^{-1}$ and 276 cm.$^{-1}$ (separation 24 cm.$^{-1}$) in the infrared spectrum of this adduct are analogous to the shoulders observed at 380 cm.$^{-1}$ and 360 cm.$^{-1}$ (separation 20 cm.$^{-1}$) in the infrared spectrum of $CrCl_3,2NMe_3$.

T A B L E VI. 1.

Observed vibrational frequencies ($cm.^{-1}$) for $ScCl_3, 2NMe_3$.

RAMAN*		INFRARED	
Solid	Benzene Soln.	Mull	Benzene Soln.
92 w.		79 m.	
122 v.s.		120 w.	
137 v.s.			
177 w.		169 s.	170 s.
197 v.w.			250 w.sh.
		260 s.	260 s.
299 v.s.	298 (P)		280 w.sh.
		309 v.w.	305 w.
401 w.br.			
		396 v.s.br.	402 v.s.
433 w.br.		440 s.	436 s.
488 s.		502 s.	498 s.

*Excitation: Argon ion 0.4880 μ laser line.

TABLE VI. 2.

Observed vibrational frequencies ($cm.^{-1}$) for $TiCl_3, NMe_3$.

RAMAN*	INFRARED	CALCULATED
Solid	Mull	
		47
	74 s.	74
101 s.	99 v.w.	94
124 s.	121 m.	137
141 s.	140 w.	146
185 m.	182 s.	224
200 v.w.	200 m.sh.	236
obscured by laser line	264 s.	253
308 v.s.		307
	385 s.br.	410
438 w.	444 s.	410
463 w.	467 w.sh.	427
496 m.		512
	507 s.	517

*Excitation: Argon ion 0.4880 μ laser line.

TABLE VI. 3.

Calculated frequencies ($cm.^{-1}$) for $TiCl_3, 2NMe_3$ in D_{3h} symmetry.

($f_{Ti-N} = 0.8$ md. $Å^{-1}$)

OBSERVED	CALCULATED	SYMMETRY	P.E. CONTRIBUTIONS
	47	e'	δTiN_2
74	74	e"	δTiN_2
99	94	a_2"	$\delta TiCl_3$ O.P.
124	137	a_1'	νTiN_2
140	146	e"	$\delta TiCl_3$ I.P.
185	224	e'	ρ_{rNC_3}
200	236	e"	ρ_{rNC_3}
264	253	a_2"	νTiN_2
308	307	a_1'	$\nu TiCl_3$
385	410	e"	δNC_3
444	410	e'	δNC_3
467	427	e'	$\nu TiCl_3$
496	512	a_1'	δNC_3
507	517	a_2"	δNC_3

TABLE VI. 4.

Observed vibrational frequencies ($cm.^{-1}$) for $VCl_3, 2NMe_3$.

RAMAN*	INFRARED	
Solid	Mull	Benzene Soln.
	90 m.	
	185 s.	184 s.
	258 s.	262 s.
310	304 m.	284 m.
	415 s.	414 s.
	448 s.	447 s.
	508 s.	508 s.

*Excitation: helium/neon laser.

TABLE VI. 5.

Observed vibrational frequencies ($cm.^{-1}$) for $CrCl_3, 2NMe_3$.

RAMAN*	INFRARED	
Solid	Mull	Benzene Soln.
	140 w.	
	208 s.	
	243 w.	254 w.
294	280 s.	286 s.
	350 w.sh.	360 m.sh.
	380 m.sh.	380 w.sh.
	399 v.s.	400 s.
	449 s.	450 m.
	470 w.	470 w.
	507 w.sh.	497 w.
	525 s.	

*Excitation: Argon ion 0.4727 μ and 0.4880 μ laser lines.

TABLE VI. 6.

Observed vibrational frequencies ($cm.^{-1}$) for $FeCl_3, 2NMe_3$.

RAMAN*		INFRARED	
Solid	Benzene Soln.	Mull	Benzene Soln.
106 w.sh.			
		112 s.	
136 m.			
162 s.			
178 w.sh.		173 s.	182 s.
196 w.sh.br.			
		217 w.br.	210 w.br.
234 m.br.			
		276 m.sh.	260 m.
		300 m.sh.	298 m.sh.
305 s.	308 s.P.		
		310 s.	310 s.
350 v.w.br.		360 s.	380 s.
		466 m.	465 w.
489 s.	485 m.P.	496 s.	490 s.

* Excitation: helium/neon laser.

VI. 6. Experimental.

Infrared mull samples were examined between polythene plates and prepared in a dry nitrogen glove box (see Chapter III). Solid Raman samples were contained in vacuum ampoules. Solutions for infrared work were contained in polythene cells and were prepared on a vacuum line. Solution Raman samples, contained in pyrex capillary cells, were prepared in an all glass vacuum system.

Infrared spectra were run on a Beckman I.R. 11 spectrometer and Raman spectra were run on both a Cary Raman spectrometer and a Spex monochromator with both helium/neon and argon ion laser excitation.

C H A P T E R VII.

The vibrational spectra of some adducts of general formula $MCl_3,2PMe_3$ for metals of the first transition series.

VII. 1. Introduction.

Although, as discussed in Chapter V, the preparation of a few phosphine complexes of the trichlorides of metals in the first transition series have been described, no data on their far infrared or Raman spectra have so far been reported. Recently, however, the vibrational spectra of some group III(b) trihalide complexes with trimethylphosphine have been reported (56). The adducts $AlCl_3,2PMe_3$ and $InCl_3,2PMe_3$ were considered to adopt a monomeric trans D_{3h} structure, since their vibrational spectra were shown to be closely comparable with those of the adducts $AlCl_3,2NMe_3$ and $InCl_3,2NMe_3$.

During the course of this work, vibrational spectra were measured for the adducts $MCl_3,2PMe_3$, (where M = Sc, Ti, V, Cr, Fe, Co, Ni), whose preparation and characterisation were described in Chapter V. It will be shown that the spectra obtained all bear a close similarity to each other, and to the spectra of the analogous $MCl_3,2NMe_3$ adducts, described in Chapter VI. In each case, the spectra are interpretable in terms of a monomeric D_{3h} geometry, and support for these assignments is provided by the observation that the adduct $CrCl_3,2PMe_3$ is monomeric in benzene solution (see Chapter V). A G.V.F.F. calculation has been carried out for $TiCl_3,2PMe_3$ and the results obtained confirm the interpretation in terms of D_{3h} geometry. For this reason the $TiCl_3$ adduct will be considered first.

VII. 2. The Adduct $TiCl_3,2PMe_3$.

The vibrational spectra observed for this molecule are listed in Table VII. 2. Comparison with the results for $TiCl_3,2NMe_3$ immediately shows that the Me_3P deformations, as expected, are at much lower frequencies than those for Me_3N. The highest frequency strong band at 353 $cm.^{-1}$ in the infrared is therefore assignable to the e' antisymmetric $TiCl_3$ stretching mode. The trimethylphosphine deformations, by comparison with the assignment for $TiCl_4,2PMe_3$ (Chapter IV) and the analogous group III(b) trihalide complexes, are expected to occur in the regions 360 - 310 $cm.^{-1}$ and 270 - 250 $cm.^{-1}$ (19). It is therefore likely that the a_1' and a_2'' deformations which are expected to occur at similar frequencies are concealed beneath the strong 353 $cm.^{-1}$ band. By analogy with the results of Chapter VI, assignment of the strong 305 $cm.^{-1}$ band in the infrared as being principally due to the a_2'' TiP_2 stretching mode is the most likely possibility, since the a_1' and a_2'' Me_3P deformations are expected to be much weaker, as is found to be the case in the results for $InCl_3,2PMe_3$ (56). The strong band at 288 $cm.^{-1}$ can be assigned to the antisymmetric e' and e" Me_3P deformations (likely to be very close in frequency - see Table VII. 3.) and the strong band in the Raman at 282 $cm.^{-1}$ to the a_1' symmetric $TiCl_3$ stretching mode. Reference to the results of the G.V.F.F. calculation for this molecule reported in Table VII. 3., lends support to this assignment of the bands observed in the Ti - Cl stretching region. However, it is apparent that, as was

found to be the case for the $TiCl_3,2NMe_3$ calculations reported in Chapter VI, the agreement between observed and calculated frequencies for the e' $TiCl_3$ and the a_2'' TiP_2 stretching modes is rather poor. However, as stated there, the approximation used in the calculation that $f_{TiCl,TiCl}/f_{TiCl}$ = the free $TiCl_4$ value may be a poor one to adopt for this molecule. Moreover, the calculations suggest that the a_1' and a_2'' TiP_2 stretching modes couple strongly with the PC_3 deformations. For the infrared spectrum below 280 $cm.^{-1}$ there is good agreement between the calculated and observed frequencies.

From these results, it is evident that the spectra obtained for this molecule closely resemble those obtained for $TiCl_3,2NMe_3$ and that they can be interpreted satisfactorily on the basis of D_{3h} symmetry for the molecule. However, the calculation suggests that although the Ti - Cl_3 stretching modes may be quite pure, the a_1' and a_2'' TiP_2 stretching modes couple seriously with the PC_3 deformations. It is therefore less meaningful to assign bands in these and the following spectra specifically to TiP_2 stretching vibrations. It seems evident that several bands will possess considerable (approximately 30 - 70%) TiP bond stretching character.

Deuteriation studies will undoubtedly help to assign these bands with more certainty. It is unfortunate that the Raman spectrum obtained was weak, but this is most probably due to the intense dark blue colour of the adduct. Similarly no polarisation data are available, since the adduct is insoluble in benzene and it was not

found possible to obtain spectra from a solution in trimethylphosphine.

VII. 2. The Adduct $ScCl_3$,$2PMe_3$.

The vibrational spectra obtained for this adduct are reported in Table VII. 1. It is immediately apparent that a close similarity exists between these and the data obtained for $TiCl_3$,$2PMe_3$. Accordingly, the strong band at 359 $cm.^{-1}$ in the infrared can be assigned to the e' $ScCl_3$ stretching mode. It is also likely that the strong band observed at 350 $cm.^{-1}$ in the Raman is due to the a_1' PMe_3 deformation, as the e' $ScCl_3$ stretching mode, although Raman active, might reasonably be expected to be weak. This would represent a coincidence of these two modes, and a consequent masking of the a_1' deformation by the e' $ScCl_3$ stretching mode in the infrared, as suggested in the discussion of the results for $TiCl_3$,$2PMe_3$ above. By analogy with the results for the latter adduct, the strong shoulder at 337 $cm.^{-1}$ may be tentatively assigned as being due, partially at least, to the a_2'' ScP_2 stretching mode. The band at 288 $cm.^{-1}$ (strong in the infrared) and 284 $cm.^{-1}$ (medium in the Raman) together with the band at 276 $cm.^{-1}$ (strong in the infrared) may be assigned partially to the e' and e" PC_3 deformations, whilst the very strong band at 268 $cm.^{-1}$ in the Raman spectrum can be confidently assigned to the a_1' totally symmetric $ScCl_3$ stretching mode. The calculated results on $TiCl_3$,$2PMe_3$ suggest that either of the weak bands observed in the Raman at 192 $cm.^{-1}$ and 154 $cm.^{-1}$ may

be due to the a_1' ScP_2 stretching mode, and that the medium shoulder observed in the Raman at 250 cm.$^{-1}$ might be a mixed mode due to the a_2'' PC_3 deformation, ScP_2 stretch and $ScCl_3$ out of plane deformation, and correspond to the strong infrared band at 240 cm.$^{-1}$. Although vibrations of a_2'' symmetry are not expected to be Raman active, the observation of this band in the Raman spectrum of the solid may be due to a solid state effect. (The treatment of the single crystal Raman data for $InCl_3,2NMe_3$ has been carried out on the basis of D_{2h} symmetry for a molecule in the crystal (102). On this basis modes of a_2'' symmetry type for a free molecule under D_{3h} symmetry can give rise to Raman active components in the crystal). Unfortunately, due to its limited solubility in benzene, no solution Raman data could be obtained for this adduct.

It is apparent from the above results that the spectra obtained for this molecule may be assigned satisfactorily in terms of a <u>trans</u> D_{3h} geometry, both for the solid state and in solution in benzene, as was shown to be the case for the corresponding adduct with trimethylamine (Chapter VI).

VII. 3. <u>The Adducts $VCl_3,2PMe_3$ and $CrCl_3,2PMe_3$</u>.

The vibrational spectra obtained for these two adducts are collected in Tables VII. 4 and 5. Once more a close similarity exists between them and the data for the other phosphine adducts studied. Unfortunately, due to the intense colours of these

adducts, the Raman spectra obtained for the solid state were weak, and only the strongest band was detected. Consequently, no solution Raman spectra were detectable, but despite this the bands at 292 $cm.^{-1}$ and 300 $cm.^{-1}$ have been assigned to the a_1' VCl_3 and $CrCl_3$ stretching modes respectively. The band observed in the Raman spectrum of $VCl_3,2PMe_3$ decreased with time, the adduct being decomposed by the laser beam. In the infrared spectra, the strong asymmetric bands at 357 $cm.^{-1}$ and 360 $cm.^{-1}$ may be assigned to the e' VCl_3 and $CrCl_3$ stretching modes respectively. The asymmetry of these bands may be due to partial concealment of the a_1' and a_2'' PC_3 deformations (expected to be weak). The bands at 291 $cm.^{-1}$ and 308 $cm.^{-1}$ again may be partially due to the a_2'' VP_2 and CrP_2 stretching modes, and the band at 280 $cm.^{-1}$ for $VCl_3,2PMe_3$ to the e' and e" PC_3 deformations. As for the cases of $ScCl_3,2PMe_3$ and $TiCl_3,2PMe_3$ bands are observed in the infrared around 250 $cm.^{-1}$ for these adducts, and from the calculated results for $TiCl_3,2PMe_3$, are likely to be due to contributions from the a_2'' νMP_2, δPC_3 and δMCl_3 O.P. modes. The observation that the complex $CrCl_3,2PMe_3$ is monomeric in benzene lends support to the assignment of the spectral results in terms of a monomeric D_{3h} structure.

VII. 4. The Adducts $FeCl_3,2PMe_3$, $CoCl_3,2PMe_3$ and $NiCl_3,2PMe_3$.

The vibrational spectra observed for these adducts are collected in Tables VII. 6, 7 and 8. Once again the spectra are very similar

to each other and to the results for the foregoing adducts. Because of the dark red colours of all of these adducts the Raman spectra obtained for the solid state were weak, and no solution data were obtainable. However, bands were observed at 330 $cm.^{-1}$, 340 $cm.^{-1}$ and 364 $cm.^{-1}$ and these have been assigned to the a_1' $FeCl_3$, $CoCl_3$ and $NiCl_3$ totally symmetric stretching modes, respectively. These bands were found, in each case, to decrease with time, indicating that decomposition of the adducts was occurring in the laser beam. By analogy with the results of the foregoing sections, the bands in the infrared have been assigned on the basis of D_{3h} symmetry for both solid and solution states, as follows. The strong bands at 356 $cm.^{-1}$, 358 $cm.^{-1}$ and 350 $cm.^{-1}$ have been assigned to the e' $FeCl_3$, $CoCl_3$ and $NiCl_3$ stretching modes respectively, and the strong bands at 303 $cm.^{-1}$, 320 $cm.^{-1}$ and 332 $cm.^{-1}$ to the a_2'' FeP_2, CoP_2 and NiP_2 stretching modes. The medium bands observed at 342 $cm.^{-1}$ for $FeCl_3,2PMe_3$ and 340 $cm.^{-1}$ for $NiCl_3,2PMe_3$ can be assigned to the a_1' or a_2'' PC_3 deformations, and would correspond to a resolution of the asymmetries observed for the e' VCl_3 and $CrCl_3$ stretching bands (Tables VI. 4 and 5). The bands at 266 $cm.^{-1}$, 271 $cm.^{-1}$ and 280 $cm.^{-1}$ can be assigned to the e' and e'' PC_3 deformations. The infrared spectra obtained for these adducts were of good quality, except that the mull spectrum for $CoCl_3,2PMe_3$ was rather poor. This is attributable to the rather sticky nature of this adduct as it was prepared during the course of this work. Because of this, it was

rather difficult to produce a good quality mull. The solution data also are rather poor, since the solution in benzene decomposed slowly during the course of the measurement (decolourised after one hour). There is no doubt, however, as to the general similarity of the spectra for this adduct to the spectra obtained for $FeCl_3,2PMe_3$, and $NiCl_3,2PMe_3$. It should be noted that solutions of $NiCl_3,2PMe_3$ in benzene also rapidly decomposed (decolourised after approximately 10 minutes), so that no solution data were obtainable for this adduct.

The assignment described above for the vibrational spectra of $NiCl_3,2PMe_3$ leads to a rather unusual conclusion, namely, that the e' $NiCl_3$ stretching mode occurs <u>below</u> the a_1' $NiCl_3$ stretching mode. Although this state of affairs is unusual, it is by no means unknown and the assignment of the antisymmetric stretching mode <u>below</u> the symmetric stretching mode has been made for such species as $TiCl_6^{2-}$ (59), Me_3N (8) and Me_3P (104). This assignment would suggest an unusually high value of $f_{NiCl,NiCl}/f_{NiCl}$ for $NiCl_3,2PMe_3$. Further discussion of this problem is postponed until Chapter VIII.

VII. 5. <u>Conclusion</u>.

From the results of Chapters VI and VII, it is evident that the two series of complexes, $MCl_3,2NMe_3$ and $MCl_3,2PMe_3$, exhibit closely similar spectra which are interpretable in terms of a monomeric D_{3h} geometry both for the solid state, and in solution. This conclusion is supported by the results of calculations on D_{3h} $TiCl_3,2NMe_3$

and $TiCl_3,2PMe_3$. However, the approximation employed in these calculations that $f_{TiCl,TiCl}/f_{TiCl}$ is equal to the value of this ratio for free $TiCl_4$ is of only limited usefulness, and in the light of the results for $NiCl_3,2PMe_3$ is likely to become even more inappropriate for the analogous adducts of the later members of the first transition series. For both series of complexes, the calculations suggest that the MCl_3 stretching vibrations are likely to be essentially pure modes, but that the MP_2 stretching modes are likely to couple seriously with the Me_3P deformations. In the light of these general conclusions, the two series of spectral results will be compared more closely in Chapter VIII, and the results of this comparison discussed in terms of the probable nature of the bonding involved in these complexes.

TABLE VII. 1.

Observed vibrational frequencies ($cm.^{-1}$) for $ScCl_3, 2PMe_3$.

RAMAN*	INFRARED	
Solid	Mull	Benzene Soln.
	74 m.	
116 s.	120 w.	
136 s.	143 m.	152 w.
154 w.		
192 w.	193 w.	
	239 s.	238 s.
251 m.sh.		
268 v.s.	276 m.sh.	268 s.sh.
284 m.sh.	288 s.	294 s.
326 w.		
	337 s.sh.	334 s.sh.
350 s.	359 s.	372 s.

*Excitation: Argon ion 0.4880 μ laser line.

TABLE VII. 2.

Observed vibrational frequencies ($cm.^{-1}$) for $TiCl_3, 2PMe_3$.

RAMAN*	INFRARED	CALCULATED
Solid	Mull	
	75 w.	52
	87 w.	96
		122
		128
		131
	140 m.	145
	150 m.	175
	249 m.	248
282 s.		279
	288 s.sh.	291
	305 s.	291
	353 s.	336
380 w.		372
		387

*Excitation: Argon ion 0.4880 μ laser line.

TABLE VII. 3.

Calculated vibrational frequencies for $TiCl_3, 2PMe_3$ in D_{3h} symmetry (f_{Ti-P} = 1.0 md. $Å^{-1}$).

OBSERVED	CALCULATED	SYMMETRY	P.E. CONTRIBUTIONS
75	52	e'	δTiP_2
87	96	e"	δTiP_2
	122	a_2"	$\delta TiCl_3$ O.P.
	128	a_1'	δPC_3 + νTiP_2
	131	e'	$\delta TiCl_3$ I.P. + ρrPC_3
140	145	e"	ρrPC_3
150	175	e'	$\delta TiCl_3$ I.P. + ρrPC_3
249	248	a_2"	δPC_3 + νTiP_2 + $\delta TiCl_3$ O.P.
282	279	a_1'	$\nu TiCl_3$
288	291	e'	δPC_3
305	291	e"	δPC_3

T A B L E VII. 3 (cont.)

OBSERVED	CALCULATED	SYMMETRY	P.E. CONTRIBUTIONS
353	336	a_1'	δPC_3, νTiP_2
380	372	a_2''	δPC_3, νTiP_2
	387	e'	$\nu TiCl_3$

TABLE VII. 4.

Observed vibrational frequencies ($cm.^{-1}$) for $VCl_3, 2PMe_3$

RAMAN*	INFRARED	
Solid	Mull	Benzene Soln.
	76 m.	
	135 m.	
	157 w.	
	181 w.	180 w.br.
	246 m.	
	265 m.	252 w.br.
	281 m.	270 m.br.
292	291 m.	288 m.
	357 s. (asymmetric)	362 s.

*Excitation: Helium/neon laser.

TABLE VII. 5.

Observed vibrational frequencies ($cm.^{-1}$) for $CrCl_3, 2PMe_3$.

RAMAN*	INFRARED	
Solid	Mull	Benzene Soln.
	154 w.	164 m.
	205 w.	212 m.
	250 m.	257 m.sh.
300		
	308 s.	314 s.br.
	360 v.s. (asymmetric)	369 s. (asymmetric)

*Excitation: Argon ion 0.4880 μ laser line.

TABLE VII. 6.

Observed vibrational frequencies ($cm.^{-1}$) for $FeCl_3$, $2PMe_3$.

RAMAN*	INFRARED	
Solid	Mull	Benzene Soln.
	144 w.	146 w.
	194 m.	204 m.
	250 s.	250 m.
	266 m.	284 m.
	303 s.	304 s.
330		
	342 m.sh.	346 m.sh.
	356 s.	370 s.

*Excitation: Helium/neon laser.

TABLE VII. 7.

Observed vibrational frequencies ($cm.^{-1}$) for $CoCl_3, 2PMe_3$.

RAMAN*	INFRARED	
Solid	Mull	Benzene Soln.
	186 w.br.	
	251 m.sh.	250 m.
	280 s.	282 s.
	320 s.	305 s.
340		
	358 s.	374 s.

*Excitation: Helium/neon laser.

TABLE VII. 8.

Observed vibrational frequencies ($cm.^{-1}$) for $NiCl_3, 2PMe_3$.

RAMAN*	INFRARED
Solid	Mull
	70 w.
	96 w.
	212 m.
	251 s.
	271 s.
	332 s.
	340 m.
	350 s.
364	

*Excitation: Helium/neon laser.

VII. 6. Experimental.

Infrared mull samples were examined between polythene plates and prepared in a dry nitrogen glove box (see Chapter III). Solid Raman samples were contained in vacuum ampoules. Solutions for infrared work were contained in polythene cells and were prepared on a vacuum line. Solution Raman samples, contained in pyrex capillary cells, were prepared in an all glass vacuum system.

Infrared spectra were run on a Beckman I.R. 11 spectrometer, and Raman spectra were run on both a Cary Raman spectrometer and a Spex monochromator with both helium/neon and argon ion laser excitation.

C H A P T E R VIII.

A comparison of the vibrational spectra obtained for the 2:1 complexes of trimethylamine and trimethylphosphine with the trichlorides of metals in the first transition series.

VIII. 1. Bonding in Pentacoordinate Transition Metal Complexes with D_{3h} Symmetry.

(a) The crystal field approach. According to simple crystal field theory, where the interaction between a metal ion and its surrounding ligands in a complex is considered to be a purely electrostatic one, the d-orbitals of a free gas ion are split under D_{3h} symmetry according to the following scheme:

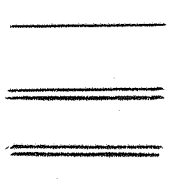

The separations of these levels relative to the energy of the levels in the free ion are expressible in general in terms of two crystal field parameters (105) one representing the contribution to the crystal field of axial ligands and one of equatorial ligands. In simple crystal field theory, electrons occupying the d-orbitals are assumed to play a non-bonding role in the metal ligand bonding. The basic assumption of the crystal field theory that purely electrostatic interactions occur between the metal ion and the surrounding ligands is an obvious over-simplification of the state of affairs pertaining in real complexes. At the other extreme, one can treat this problem in terms of purely covalent bonding between the metal ion and its surrounding ligands, by the methods of molecular orbital theory.

(b) The molecular orbital approach. The molecular orbital description of the bonding in pentacoordinate molecules with D_{3h}

symmetry has been described in detail elsewhere (8). The resulting molecular orbital diagram giving the molecular orbitals which from symmetry considerations one can form from the appropriate combinations of ligand orbitals and acceptor orbitals of the same symmetry is shown in Figure VIII. 1. The energy separations shown there are purely diagrammatic, but represent qualitatively the order of the molecular orbitals in increasing energy. It can be seen that the orbitals enclosed within the broken lines are analogous to the d-orbital splitting predicted on the crystal field model, and on filling up the molecular orbitals with electrons, it is just these orbitals which will take the "d-electrons" of the metal ions of the first transition series. However, although the e"and e' degenerate pairs are formally non-bonding, as in the case of the crystal field treatment, it can be shown (8) that it is possible to form linear combinations of the ligand orbitals with which, on symmetry considerations, the e" and e' degenerate pairs of orbitals may form π-type molecular orbitals. Furthermore, whilst the e' pair can form π-type molecular orbitals with orbitals from the equatorial ligands only, the e" pair can form π-type molecular orbitals in <u>both</u> the axial and equatorial directions. This treatment therefore suggests that, <u>from symmetry arguments</u>, there is the possibility of electrons in the e" and e' orbitals being involved in π-bonding with the ligands. Of course whether π-bonding is <u>energetically</u> likely for any given case is much more difficult to decide, and the <u>extent</u> of π-bonding in

coordination compounds generally is very much an unknown factor.

Finally, it is perhaps worth noting that the highest "d-shell" molecular orbital (a_1') is predicted to be antibonding in character. For the series of compounds considered in this thesis in their ground states, no electrons are likely to occupy this orbital until the Fe(III) case (d^5). The results of the magnetic measurements recorded during this work indicate (Chapter V) that the complexes $FeCl_3,2NMe_3$, $FeCl_3,2PMe_3$ and $NiCl_3,2PMe_3$ all adopt the low spin arrangement, and work on $CoCl_3,2PEt_3$ (99) shows that this too adopts a low spin configuration of its d-electrons. These results are therefore in agreement with the bonding scheme outlined above, and the assignment of antibonding character to the a_1' orbital (originating from the metal d_{z2} orbital).

VIII. 2. The Classification of Donor-Acceptor Interactions.

The first comprehensive classification scheme was proposed by Ahrland, Chatt and Davies (106) in 1958. These authors divided both acceptor ions and molecules into two general classes. Class (a): Those which form their most stable complexes with the first ligand atom in each Periodic Group, i.e. N, O, F. Class (b): Those which form their most stable complexes with the second or a subsequent ligand atom of each Periodic Group. Stability was measured in terms of the free energy of a reaction, usually quoted as a stability constant, without regard to solvent. It was noted that Class (b) cationic acceptors in water in their normal valence states were found together

in one part of the Periodic Table in a more or less triangular area. The apex of the triangle was at copper, and the base stretched from tungsten to polonium (approximately). Acceptor ions well removed from this area of the Periodic Table were found to be well defined Class (a) acceptors. Acceptor ions on the borders of this triangle e.g. Fe(II), Fe(III), Co(II), Co(III), Ni(II), Mn(II), etc. were considered to be borderline cases.

The second general classification scheme which has gained currency was due to Pearson (107). By comparing ΔH values for the gaseous replacement reaction $MX(g) + Y^-(g) = MY(g) + X^-(g)$ where X^- and Y^- are halides, one can measure the amount of stability which Y^- the fluoride has over X^-, the iodide, and this Pearson considered (107) to be a measure of Class (b) character. Having listed a wide range of metal ions and Lewis acids as Class (a), Class (b) and borderline, Pearson related these divisions from considerations of polarisability to the terms "hard" and "soft" for Class (a) and Class (b) respectively. Pearsons "hard" and "soft" classification corresponds roughly with the Class (a) and Class (b) classification of Ahrland et al. (106).

However, rather than being closely related to classical polarisability, the (a) and (b) classification has been shown to be closely linked with the balance between ionic and covalent bonding (108), (109), (110). It has also been shown that Class (a) or (b) character is often dependent on changes in solvent, and in the charge

type of the reaction under consideration. Specifically, since the classification schemes outlined above were drawn up on the basis of thermodynamic measurements on reactions of metal ions and halide ions either in aqueous solution or in the gas phase, it must not be expected that these classifications will hold in detail when one considers the donor-acceptor interactions of neutral molecules in "non coordinating" solvents such as benzene. In this case, the ionic contribution to the coordinate bond has been reduced to a dipole - dipole interaction, and covalent bonding will become more important. It must not therefore be thought too surprising if the halide of a particular metal ion (normally thought to be of Class (a) character as judged by its relative affinity for halide ions) displays pronounced (b) character. In addition, energy terms due to London attraction and classical polarisability must be considered in the expression for the energy of the bond concerned (108). Since calculations of these last two terms and also the covalent term are extremely unreliable, it is not possible to predict donor-acceptor properties in cases of this type. Moreover, in a comprehensive review of the acceptor properties of molecules of the group III(b) elements, towards neutral molecules, Stone (111) has demonstrated the complexities of the problem of attempting to predict from an accumulated mass of experimental data on similar systems, the precise stability sequence to be observed from any series of neutral donors and acceptors. From a brief consideration of the formation of a

neutral adduct from neutral acceptor and donor molecules in terms of a thermodynamic cycle of formation, Stone shows that it is impossible to assign definite strengths to electron-pair donors and acceptors valid for every donor acceptor reaction. Thus the acceptor properties of a given acceptor molecule will depend on the base in question, and the same will hold true for donor molecules. No completely rigid classification scheme can be drawn up to cover all conceivable cases.

Finally, it should be mentioned that for the donor-acceptor interactions of molecules, steric factors are likely to become important in determining relative stabilities, especially for bulky donor molecules such as trimethylamine and trimethylphosphine.

VIII. 3. Studies of the Relative Affinities of $ScCl_3$ and $FeCl_3$ towards NMe_3 and PMe_3.

In order to compare the spectral results of Chapters VI and VII in terms of the nature of the bonding involved in the complexes studied, it is necessary to have some knowledge of the relative affinities of the trichlorides of the metals of the first transition series for the neutral donor molecules NMe_3 and PMe_3. Ideally, one requires values of the heats of formation for the series of adducts in the gas phase:

$$MCl_3(g) + 2\ Me_3P(N)\ (g) \longrightarrow MCl_3, 2Me_3P(N)\ (g)$$

However, this is not experimentally possible. Moreover, due to the

insoluble nature of the parent trichlorides in non coordinating solvents such as benzene, no heats of formation can be obtained in solution. In order to obtain some idea of relative stabilities, it is therefore necessary to carry out relative stability studies in solution, e.g:

$$MCl_3,2NMe_3 + \text{excess } Me_3P \longrightarrow \text{products}$$

and $$M'Cl_3,2NMe_3 + M''Cl_3,2PMe_3 \longrightarrow \text{products}$$

etc. However, a complete study of the relative stabilities of the adducts in question is clearly outside the scope of this work. Instead, a series of competition reactions was undertaken to provide a qualitative idea of the relative affinities of $ScCl_3$ and $FeCl_3$ towards NMe_3 and PMe_3. In these, solutions of $ScCl_3,2NMe_3$, $ScCl_3,2PMe_3$, $FeCl_3,2NMe_3$ and $FeCl_3,2PMe_3$ were made up in benzene, and to each of these was added a benzene solution of the alternative donor, so that a 10:1 mole excess of alternative donor to complex studied was present in the mixtures:

(a) $ScCl_3,2NMe_3 + PMe_3$ (c) $FeCl_3,2NMe_3 + PMe_3$

(b) $ScCl_3,2PMe_3 + NMe_3$ and (d) $FeCl_3,2PMe_3 + NMe_3$

On evaporation to dryness, the infrared spectra of the solid products were measured and the results are listed in Tables VIII. 1 and 2. It was assumed here that the volatilities of Me_3N and Me_3P, and the solubilities of the adducts $MCl_3,2NMe_3$ and $MCl_3,2PMe_3$ were comparable, so that evaporation of the equilibrium mixture to dryness did not disturb the equilibrium to any large extent. Quite clearly, the

addition of PMe_3 to $ScCl_3,2NMe_3$ and NMe_3 to $ScCl_3,2PMe_3$ results essentially in a mixture of the two adducts (or in a mixed adduct $ScCl_3,(NMe_3)(PMe_3)$). However, addition of PMe_3 to $FeCl_3,2NMe_3$ and NMe_3 to $FeCl_3,2PMe_3$ results only in the formation of $FeCl_3,2PMe_3$. No bands due to coordinated trimethylamine between 400 - 500 $cm.^{-1}$ could be detected in the infrared spectra (unlike the case for the scandium complexes) and so it is reasonable to assume that the result of these two experiments is largely the formation of $FeCl_3,2PMe_3$. Similarly, addition of excess trimethylamine produced no spectroscopically detectable effect on the adduct $CoCl_3,2PMe_3$ (Table VIII. 3.).

It seems from the results of these experiments that the complexes $ScCl_3,2NMe_3$ and $ScCl_3,2PMe_3$ are of comparable stability, whilst the complex $FeCl_3,2PMe_3$ is considerably more stable than $FeCl_3,2NMe_3$. It also seems likely that the high stability of the trimethylphosphine complexes is at least carried over (if not enhanced) in the complexes of $CoCl_3$ and $NiCl_3$. It is presumed that a gradual transition of relative stabilities from P > N to P ≒ N is observed on moving from Ni, Co and Fe to Sc through Mn, Cr, V and Ti. It should be noted that these results approximate roughly to the stability order predictable on the basis of the classification due to S. Ahrland et al. (106).

VIII. 4. Comparison of the Spectral Results for the L_2MX_3 Complexes Studied.

Part of the purpose of this work was to compare the vibrational spectral results obtained for the series of L_2MX_3 complexes obtained with L = trimethylamine and trimethylphosphine, to see if changes in the frequencies of the metal-chlorine and metal-ligand vibrations could be correlated either with the d-electron configuration of the central metal or with the (a) and (b) donor-acceptor classification. With regard to the effects of d-electrons on metal-halogen vibrations it should be noted that a study of the infrared spectra of the high-spin MCl_6^{3-} species where M = Cr, Mn, Fe, In and Ir has been undertaken with this purpose in mind (112a), and that, significantly, from a comparison of the frequency of ν_3 in the infrared spectra of these species ν_3 for $FeCl_6^{3-}$ was found to be very low as compared with ν_3 for the other species. This was rationalised in terms of the anti-bonding character of the e_g orbitals and the d-electronic configuration $t_{2g}^3 \; e_g^2$ for this ion. In studies of this type it should, of course, always be borne in mind that bond stretching force constants and bond strengths are <u>not</u> equivalent (112b), but for a series of closely related species, a comparison of stretching frequencies or force constants with relative bond strength can be of interest.

Comparison of the frequencies found for the a_1' MCl_3 totally symmetric stretching mode, the a_2'' "ML_2 antisymmetric stretching mode", and the e' MCl_3 antisymmetric stretching mode for the two series of

L_2MX_3 complexes studied in this work are presented in Figure VIII 2, 3 and 4 respectively.

In the case of the a_1' MCl_3 symmetric stretch it is apparent that, whilst there seems to be no obvious correlation with the d-electron configuration as such (in terms of crystal field stabilisation energies) there is a marked difference in behaviour between the two series of complexes. Whilst the frequencies for the $MX_3,2NMe_3$ complexes remain, with slight variations, around the 300 $cm.^{-1}$ position, there is a steady increase in the frequency of this mode for the trimethylphosphine complexes. The results of Beattie and Ozin for the adducts $InCl_3,2NMe_3$ (46) and $InCl_3,2PMe_3$ (56) have been included in Figures VIII. 2, 3 and 4 to provide a d^{10} case. (The adducts $GaCl_3,2NMe_3$ and $GaCl_3,2PMe_3$ have not been prepared so far, only the 1:1 adducts) and have been linked to the results obtained in this work by broken lines. Assuming the frequency separation between a_1' ν MCl_3 for the hypothetical 1:2 $GaCl_3$ adducts with NMe_3 and PMe_3 to be of the same order (and in the same sense, i.e. ν a_1' $GaCl_3(N) > \nu$ a_1' $GaCl_3(P)$), a sharp decrease in the frequency of this mode for the phosphine adduct series is predicted for $d^7 \rightarrow d^{10}$, whilst the corresponding frequency for the amine adduct series is expected to remain roughly constant for $d^7 \rightarrow d^{10}$.

The most obvious inference to be made from these results is that the metal-chlorine bond strengths increase on passing from scandium to nickel, and then drop again at d^{10}, for the phosphine adducts, but

remain fairly constant for the amine series. The results of the competition experiments described in section VIII. 3 suggest moreover, that this increase in metal-chlorine bond strength is not at the expense of the metal-phosphorus bond strength, as these results suggest that there is a corresponding increase in this relative to the metal nitrogen bond strength.

A comparison of the frequencies of the a_2'' ML_2 antisymmetric stretching mode suggests such an increase in the metal-phosphorus bond strengths, the frequencies reaching a maximum around Fe, Co and Ni, with a final drop from Ni to In (corresponding to the behaviour of the a_1' ν MCl_3 mode). The high value of the a_2'' FeN_2 frequency is somewhat disturbing in this context. However, it should be remembered that (a) this mode is likely to be considerably coupled with other ligand modes, especially for the phosphines, and (b) since this mode involves movement of the central metal atom it is not so reliable as a guide to the relative strengths of metal-ligand bonds as the a_1' totally symmetric MCl_3 stretching mode is, where no movement of the central metal atom occurs.

A similar consideration applies to the e' antisymmetric MCl_3 stretching mode, but the calculations on $TiCl_3,2NMe_3$ and $TiCl_3,2PMe_3$ (Chapters VI and VII), suggest that it is likely at least to be relatively unmixed with other modes. Examination of Figure VIII. 4 reveals that whilst the frequency of this mode decreases for the amine series, it stays roughly constant for the phosphine series, with

a final drop in frequency from Ni to In (corresponding to the behaviour of the a_1' ν MCl_3 mode). This could be due to a balancing of increase in mass and increase in bond strength, although it is seen that for the cases of $FeCl_3,2PMe_3$, $CoCl_3,2PMe_3$ and $NiCl_3,2PMe_3$ we have the rather unusual situation of the symmetric and antisymmetric stretching frequencies being almost coincident. As stated in Chapter VII, it is likely that these results could also be explained by an increase in the value of the ratio $f_{MCl,MCl}/f_{MCl}$ along the series of the phosphine complexes.

It is apparent from the foregoing results that, for the series of phosphine complexes, a steady increase in M - Cl and M - P bond strengths is likely and that those complexes with the greatest a_1' ν MCl_3 frequencies are those which the competition experiments suggest are the more stable as compared to the corresponding amine complexes. Furthermore, the metals for which these observations occur are just those which are expected to show the greatest Class (b) acceptor behaviour. It would be tempting to ascribe this behaviour to the formation of $d\pi$ - $d\pi$ bonds between the metal and the phosphorus donor atom, rather in the way in which the bonding in the carbonyls of these metals is explained. However, there is no justification for doing this on the basis of the results described in this work. It seems more probable that these results can be explained in terms of the steric interaction of Me_3N and Me_3P with the planar MCl_3 grouping. It can readily be shown that this factor is much more serious for

Me_3N than it is for Me_3P. For the phosphine complexes, a steady contraction may occur along the series from Sc to Ni in the M - Cl and M - P bond lengths with an accompanying increase in the strengths of the M - Cl and M - P bonds (whatever the origin of the increase in bond strength) and a consequent increase in ν a_1' MCl_3. The more serious steric interaction in the amine complexes may prevent this occurring, resulting in an erratic movement of the frequency of ν a_1' MCl_3 around 300 $cm.^{-1}$, along the series.

If this is correct, contraction of the M - Cl and M - P bond lengths is likely to lead to increasingly large values of the stretch-stretch interaction force constants as suggested above, which would lead to the near coincidence of the a_1' and e' MCl_3 stretching modes observed in the later complexes.

VIII. 5. Conclusion.

In view of these results, quantitative relative stability data would be desirable for the series of adducts studied here, to provide a more detailed assessment of the (a) or (b) character of the acceptors involved, and x-ray studies of all of them, yielding values of M - Cl and M - L bond lengths, would be of great interest.

These studies might also usefully be extended to an examination of analogous $MCl_3,2NMe_3$ and $MCl_3,2PMe_3$ adducts of metals whose (b) class character is much more pronounced than those studied here. Although the trivalent state is not a very stable one for palladium

and platinum, the analogous adducts of ruthenium (III), osmium (III), rhodium (III) and iridium (III) chlorides might be expected to be accessible.

Further, studies of the frequencies of the a_{1g} totally symmetric stretching mode of a series of MX_6^{3-} ions might also yield some interesting results which might possibly be related to the (b) class character of M.

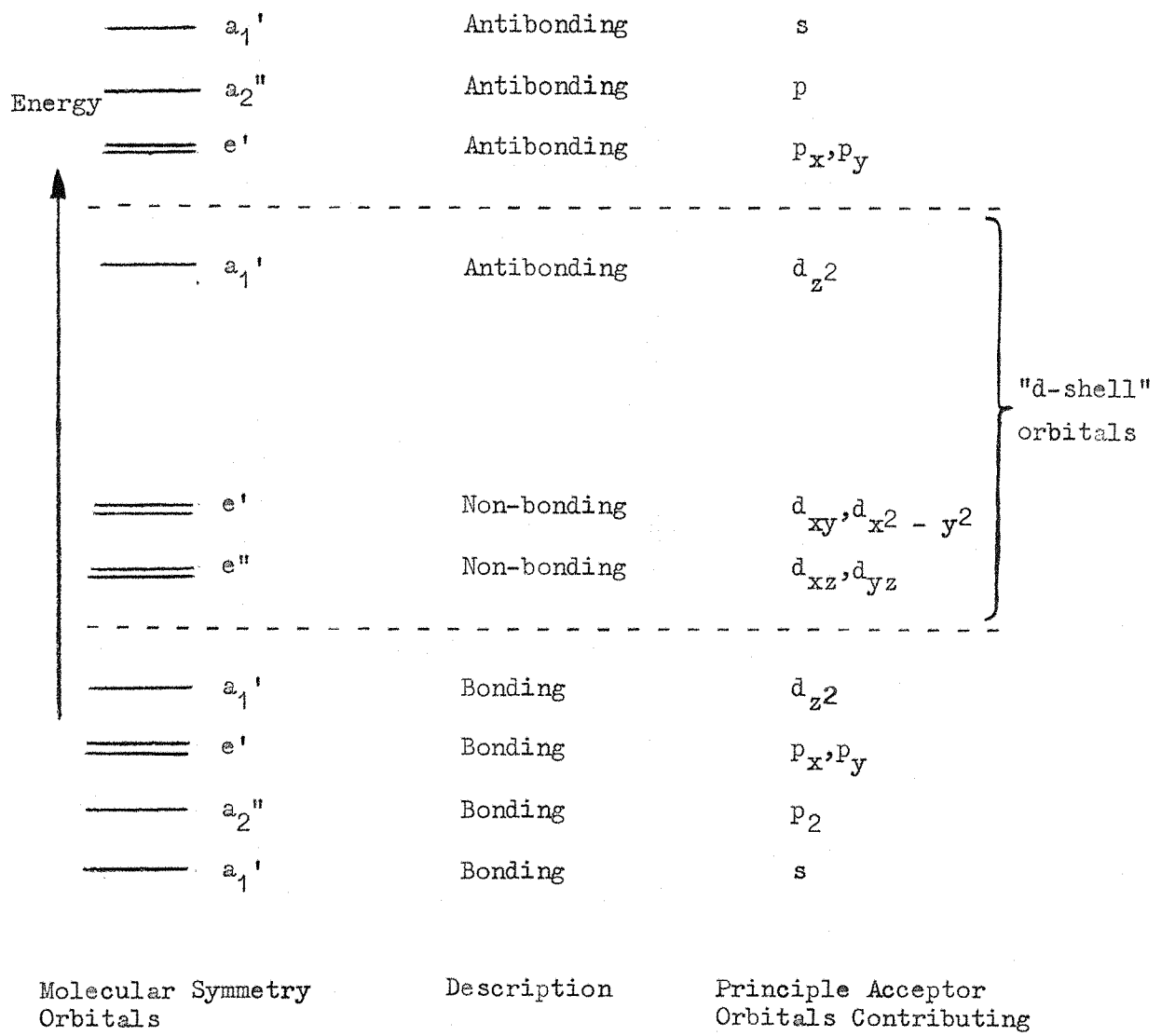

FIGURE VIII. 1. M.O. Diagram for a D_{3h} Pentacoordinate Molecule ML_5

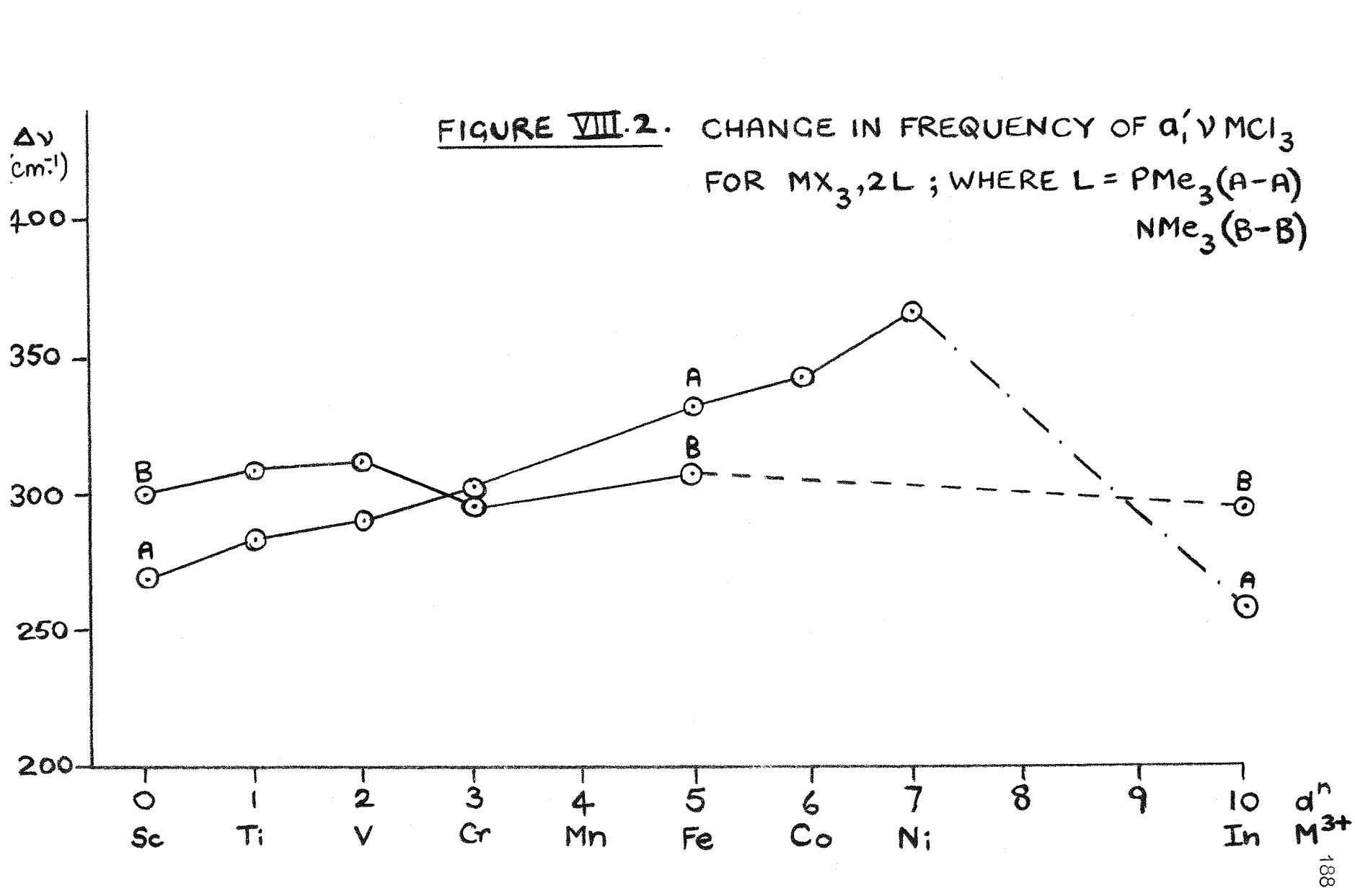
FIGURE VIII.2. CHANGE IN FREQUENCY OF a'1 ν MCl3
FOR MX3,2L ; WHERE L = PMe3(A-A)
NMe3(B-B)
Δν (cm-1)
400
350
300
250
200
A
B
A
B
B
A
0 Sc
1 Ti
2 V
3 Cr
4 Mn
5 Fe
6 Co
7 Ni
8
9
10 In
dn M3+

FIGURE VIII.3. CHANGE IN FREQUENCY OF a_2'' νML_2 FOR $MX_3,2L$; WHERE L= PMe_3 (A-A) NMe_3 (B-B)

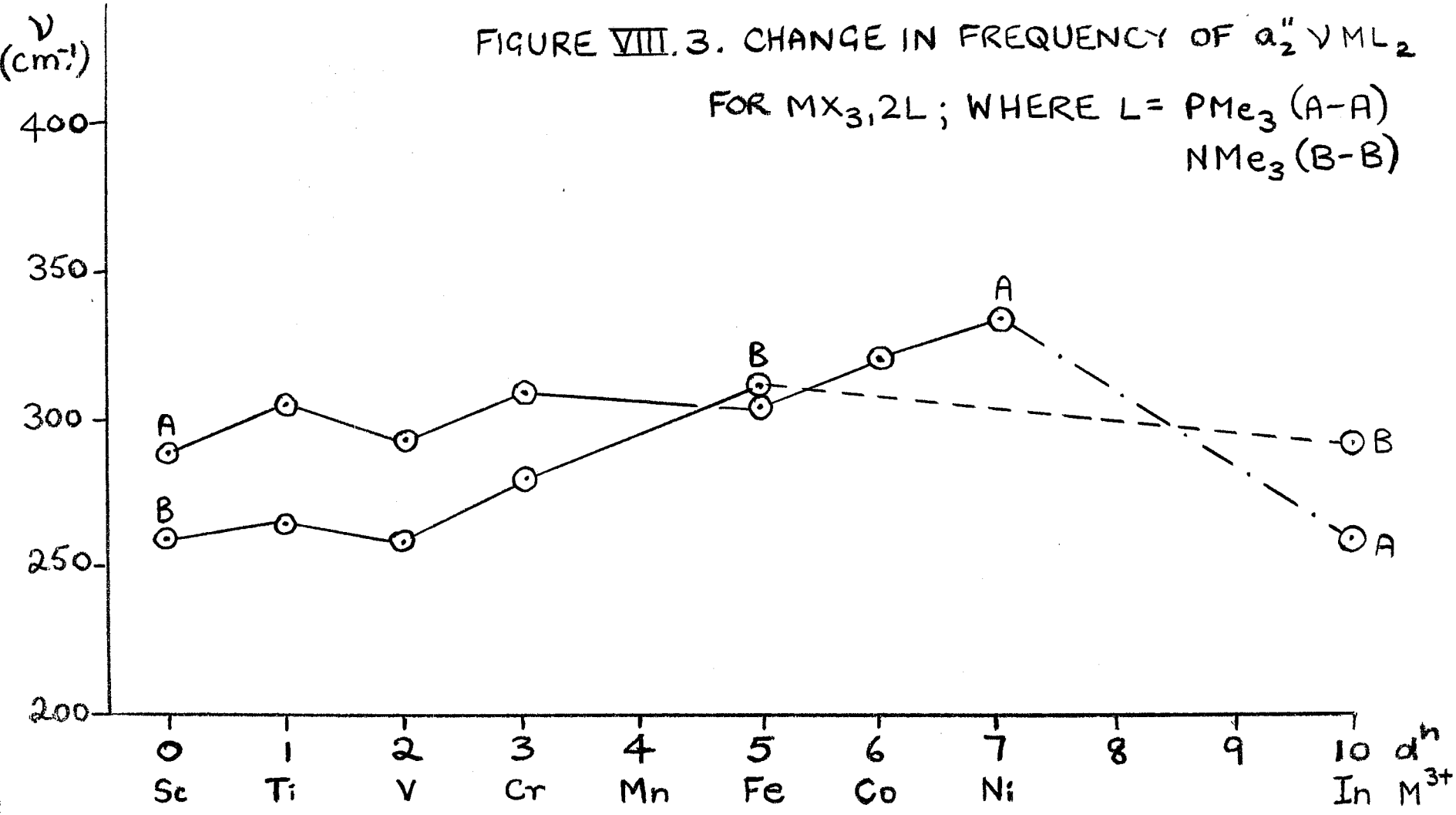

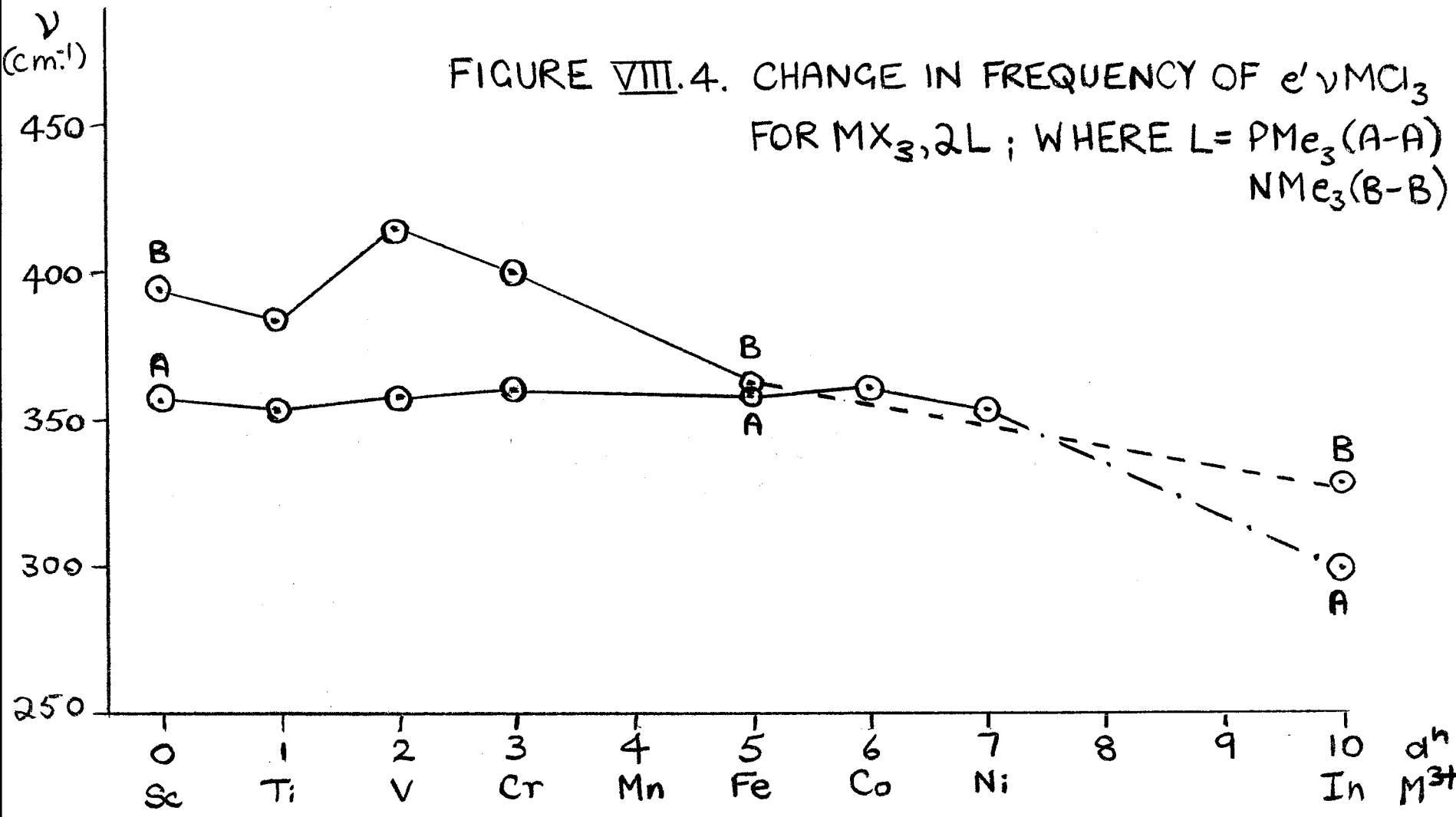

FIGURE VIII.4. CHANGE IN FREQUENCY OF $e'\nu MCl_3$ FOR $MX_3,2L$; WHERE L= PMe_3(A-A) NMe_3(B-B)

T A B L E VIII. 1.

Infrared mull spectra observed for the starting adducts and final products of the competition reactions on $ScCl_3,2NMe_3$ and $ScCl_3,2PMe_3$. (Frequencies in $cm.^{-1}$).

$ScCl_3,2NMe_3$ (Pure)	$ScCl_3,2NMe_3$ $+PMe_3$	$ScCl_3,2PMe_3$ $+NMe_3$	$ScCl_3,2PMe_3$ (Pure)
79 m.			74 m.
120 w.			120 w.
	140 m.		143 m.
169 s.	172 m.	170 m.	
			193 w.
	246 s.		239 s.
260 s.	266 w.sh.		
	278 m.sh.	270 m.br.	276 w.sh.
309 v.w.	290 s.		288 s.
	336 s.		337 s.sh.
	360 s.br.	358 s.br.	359 s.
396 v.s.br.			
440 s.	434 w.	438 w.	
502 s.	506 m.	506 s.	

TABLE VIII. 2.

Infrared mull spectra observed for the starting adducts and final products of the competition reactions on $FeCl_3$, $2NMe_3$ and $FeCl_3$, $2PMe_3$. (Frequencies in $cm.^{-1}$).

$FeCl_3$, $2NMe_3$ (Pure)	$FeCl_3$, $2NMe_3$ $+PMe_3$	$FeCl_3$, $2PMe_3$ $+NMe_3$	$FeCl_3$, $2PMe_3$ (Pure)
112 s.			
			144 w.
173 s.	187 v.w.br.		194 m.
217 w.br.			
	250 m.		250 s.
	270 m.sh.	270 m.sh.	266 m.
276 m.sh.			
300 m.sh.	303 s.	300 s.br.	303 s.
310 s.			
	340 m.sh.	346 m.sh.	342 sh.
360 s.	360 s.	358 s.	356 s.
466 m.			
496 s.			

TABLE VIII. 3.

Infrared mull spectra of $CoCl_3,2PMe_3$ and the product of its reaction with excess trimethylamine. (Frequencies in $cm.^{-1}$).

$CoCl_3,2PMe_3$	$CoCl_3,2PMe_3 + NMe_3$
186 w.br.	167 v.w.br.
251 m.sh.	250 m.
280 s.	282 s.
320 s.	304 s.
358 s.	374 s.

A P P E N D I C E S

APPENDIX A

Vibrational analyses of $TiCl_4$,PR_3 in C_{2V} and C_{3V} symmetries.

The force constants for titanium tetrachloride were first evaluated, using the F-matrix elements listed below (41):

$$F_{11}\ (A_1) = f_r + 3f_{rr}$$

$$F_{22}\ (E) = f_\alpha - 2f_{\alpha\alpha}$$

$$F_{33}\ (F_2) = f_r - f_{rr}$$

$$F_{34}\ (F_2) = 2(f_{r\alpha})$$

$$F_{44}\ (F_2) = f_\alpha$$

Numerical values for the above F-matrix elements have been calculated by Morino and Vehara (113). The set of force constants thus obtained for free titanium tetrachloride were then modified for use in the $TiCl_4$,PR_3 problem. Values of f_α,$f_{\alpha\alpha}$ and $f_{r\alpha}$ were used without modification, whilst values for f_r and f_{rr} were taken as 0.8 of the free tetrahalide values. The final set of force constants employed, together with the values of the ligand force constants used are listed in Table 1, with the appropriate units. It may be noted that f_{rr} trans was taken as 0.75 of the value of f_{rr} cis. The value of f_{Ti-P} was taken as 1.8 md. $Å^{-1}$, this value giving the best fit of computed and experimental results. Where certain Ti - Cl bonds are not required by symmetry to be equivalent, they were, in general, taken to be so, so far as force constant and interatomic

distance were concerned. The values of interatomic distances used are listed in Table 2 together with references to their sources, the value for the titanium phosphorus bond length was taken as the sum of the covalent radii. The value for the titanium chlorine bond length is that reported for the $TiCl_6^{2-}$ anion (117). Ideal trigonal bipyramidal angles were used throughout.

(i) Vibrational analysis of $TiCl_4$,PR_3 in C_{2V} symmetry. Gilson and Beattie have calculated the G and F matrix elements for C_{2V} LMX_2Y_2 using general angles (8), (11). The extension of the problem to consideration of L as Z_3W in "C_{2V}" $Z_3WMX_2Y_2$ has been considered by Livingston (20). Assuming free rotation of the WZ_3 group, the molecule as a whole has C_{2V} symmetry. The $W\text{-}MX_2Y_2$ gives $3a_1 + 3b_1 + 3b_2 + a_2$ vibrational modes. The MWZ_3 symmetric top has $3a_1 + 3e$ vibrational modes under local C_{3V} symmetry, but in the whole molecule, with C_{2V} symmetry, each e mode is split into two equivalent modes b_1 and b_2. One of the a_1 modes (symmetry coordinate = ΔMW) is common to both the symmetric top and the framework. Thus for the whole molecule we have:

$$\text{symmetric top} = 2a_1 + 3b_1 + 3b_2$$

$$\text{framework} = 4a_1 + 3b_1 + 3b_2 + a_2$$

In addition, there is an extra a_1 mode common to both. No new redundancies arise other than those for the separate top and framework.

Assuming tetrahedral, 90° and 120° angles, we can now write down

the symmetry coordinates. These are just the symmetry coordinates for the separate top and framework, each b_1 and b_2 pair for the top taking the place of the pair of symmetry coordinates for each degenerate e mode in the free top. Moreover, we may note that in C_{2V} symmetry, b_1 and b_2 are interchangeable, the convention used here is that of Gilson (8), that b_1 modes are symmetric to the WMX_1X_2 mirror plane and antisymmetric to the WMY_1Y_2 mirror plane, and b_2 is the reverse of this.

Figure 1 gives the internal coordinates used, and it is obvious by comparison with the general case that:

$$Z = R, \quad W = P, \quad M = Ti, \quad X = Cl, \quad Y = Cl'.$$

Only some angular coordinates are shown in Figure 1, to avoid confusion. The complete list is:

a_1'	=	R_3PR_2	a_2'	=	R_1PR_3	a_3'	=	R_1PR_2
b_1'	=	R_1PTi	b_2'	=	R_2PTi	b_3'	=	R_3PTi
a_1	=	$PTiCl_1$	a_2	=	$PTiCl_2$	c_3	=	$Cl_2'TiCl_1$
b_1	=	$PTiCl_1'$	b_2	=	$PTiCl_2'$	c_4	=	$Cl_2'TiCl_2$
c_1	=	$Cl_1'TiCl_1$	c_2	=	$Cl_1'TiCl_2$			
d	=	Cl_1TiCl_2	e	=	$Cl_1'TiCl_2'$			

The symmetry coordinates are as follows:

a_1 type

$$S_1 = \frac{1}{\sqrt{3}} (\Delta PR_1 + \Delta PR_2 + \Delta PR_3)$$

$$S_2 = \frac{1}{\sqrt{3(1 + n_1^2)}} [(\Delta b_1' + \Delta b_2' + \Delta b_3' - n_1(\Delta a_1' + \Delta a_2' + \Delta a_3')]$$

$S_3 = \Delta TiP$

$S_4 = \frac{1}{\sqrt{2}} (\Delta TiCl_1' + \Delta TiCl_2')$

$S_5 = \frac{1}{\sqrt{2}} (\Delta TiCl_1 + \Delta TiCl_2)$

$S_6 = \frac{1}{\sqrt{(3/2 + 4n_3^2)}} [\Delta e - 1/2\Delta b_1 - 1/2 \Delta b_2 + n_3(\Delta c_1'' + \Delta c_2'' + \Delta c_3'' + \Delta c_4'')]$

$S_7 = \frac{1}{\sqrt{(3/2 + 4n_2^2)}} [\Delta d - 1/2 \Delta a_1 - 1/2 \Delta a_2 + n_2(\Delta c_1' + \Delta c_2' + \Delta c_3' + \Delta c_4')]$

where: $n_1 = \sqrt{3} \cos b/\cos a'/2$ ($b = 180 - b'$) $= 2\sqrt{3} \cos b/\sqrt{1 + 3\cos^2\beta}$ ($\sqrt{}$ + ve)

$n_2 = \cos b/2 \sin a/2/2 \sin c$

$n_3 = \cos a/2 \sin b/2/2 \sin c$

c' and c" = 1/2c (involving $Cl_{1,2}$ and $Cl'_{1,2}$ respectively)

a_2 type

$S_1 = 1/2(\Delta c_1 - \Delta c_2 - \Delta c_3 + \Delta c_4)$

b_1 type

$S_1 = \frac{1}{\sqrt{6}} (2\Delta PR_1 - \Delta PR_2 - \Delta PR_3)$

$S_2 = \frac{1}{\sqrt{6}} (2\Delta a_1' - \Delta a_2' - \Delta a_3')$

$S_3 = \frac{-1}{\sqrt{6}} (2\Delta b_1' - \Delta b_2' - \Delta b_3')$

$S_4 = \frac{1}{\sqrt{2}} (\Delta TiCl_1 - \Delta TiCl_2)$

$S_5 = \frac{1}{\sqrt{2}} (\Delta a_1 - \Delta a_2)$

$S_6 = 1/2 (\Delta c_1 - \Delta c_2 + \Delta c_3 - \Delta c_4)$

b_2 type

$$S_1 = \frac{1}{\sqrt{6}} (2\,\Delta PR_1 - \Delta PR_2 - \Delta PR_3)$$

$$S_2 = \frac{1}{\sqrt{6}} (2\,\Delta a_1' - \Delta a_2' - \Delta a_3')$$

$$S_3 = \frac{-1}{\sqrt{6}} (2\,\Delta b_1' - \Delta b_2' - \Delta b_3')$$

$$S_4 = \frac{1}{\sqrt{2}} (\Delta TiCl_1' - \Delta TiCl_2')$$

$$S_5 = \frac{1}{\sqrt{2}} (\Delta b_1 - \Delta b_2)$$

$$S_6 = 1/2(\Delta c_1 + \Delta c_2 + \Delta c_3 + \Delta c_4)$$

The G-matrix elements except those involving cross terms between the top and the framework are the same as those obtained in the case of the free top and framework (8), (118). The G-matrix elements involving cross terms have been calculated by Livingston (20).

The computer programme used required only the values of the force constants, and calculated the values of the symmetrised F-matrix, so that general F-matrix elements were never actually obtained. The force constants used in the calculation, including interaction force constants not set equal to zero, together with their relationship to the force constants taken for the free ligands and the (modified) force constants derived for titanium tetrachloride, are given in Table 3.

(ii) Vibrational analysis of $TiCl_4.PR_3$ in C_{3V} symmetry. Under C_{3V} symmetry we have for the whole molecule $6a_1 + a_2 + 7e$, the a_2 mode is inactive in both the Raman and the infrared.

The internal coordinates are shown in Figure 2, and the symmetry coordinates are listed below:

a_1 type

$$S_1 = \frac{1}{\sqrt{3}} (\Delta PR_1 + \Delta PR_2 + \Delta PR_3)$$

$$S_2 = \frac{-1}{\sqrt{3(1 + n^2_1)}} [(\Delta b_1' + \Delta b_2' + \Delta b_3' - n_1(\Delta a_1' + \Delta a_2' + \Delta a_3')]$$

$$S_3 = \Delta PTi$$

$$S_4 = \frac{1}{\sqrt{3}} (\Delta TiCl_1 + \Delta TiCl_2 + \Delta TiCl_3)$$

$$S_5 = \frac{1}{\sqrt{3(2 + n^2_2)}} [(\Delta b_1 + \Delta b_2 + \Delta b_3 - \Delta b_1'' - \Delta b_2'' - \Delta b_3'' + n_2 (\Delta a_1 + \Delta a_2 + \Delta a_3)]$$

$$S_6 = \Delta TiCl'$$

where $n_1 = \sqrt{3} \cos b/\cos a'/2$ $(b = 180 - b') = 2\sqrt{3} \cos b/\sqrt{1 + 3 \cos^2 b}$ $(\sqrt{}$ + ve)

$$n_2 = \sqrt{3} \cos b/\cos a/2 = 2\sqrt{3} \cos b/\sqrt{1 + 3 \cos^2 b}\ (\sqrt{}\text{ + ve})$$

e type

$$S_1 = \frac{1}{\sqrt{6}} (2\Delta PR_1 - \Delta PR_2 - \Delta PR_3)$$

$$S_2 = \frac{1}{\sqrt{6}} (2\Delta a_1' - \Delta a_2' - \Delta a_3')$$

$$S_3 = \frac{-1}{\sqrt{6}} (2\Delta b_1' - \Delta b_2' - \Delta b_3')$$

$$S_4 = \frac{1}{\sqrt{6}} (2\Delta TiCl_1 - \Delta TiCl_2 - \Delta TiCl_3)$$

$$S_5 = \frac{1}{\sqrt{6}} (2\Delta a_1 - \Delta a_2 - \Delta a_3)$$

$$S_6 = \frac{-1}{\sqrt{6}} (2\Delta b_1'' - \Delta b_2'' - \Delta b_3'')$$

$$S_7 = \frac{-1}{\sqrt{6}} (2\Delta b_1 - \Delta b_2 - \Delta b_3)$$

The G and F matrix elements for $C_{3V}X_3YWZ_4$ with general angles have been calculated by Beattie and Gilson (8), (11). The matrix elements are only quoted for S.V.F.F., and although in the present analysis a number of interaction force constants were used, the general symmetrised F-matrix elements were never actually calculated, since as stated above, the computer programme used required only the valence force constants and calculated the numerical values of the symmetrised F-matrix.

The force constants used in the calculation, including the interaction force constants not set equal to zero, together with their relationship to the force constants in Table 1 are listed in Table 4.

Frequencies were calculated for $TiCl_4$, PR_3 assuming both C_{2V} and C_{3V} symmetries, tetrahedral and trigonal bipyramidal angles and the force constants and G-matrix elements as listed above. Calculations were carried out for R = H, D, CH_3 and CD_3 for both the C_{2V} and C_{3V} cases. The computer programme used was devised by Dr. T. R. Gilson and this calculated both the frequencies and percentage potential energy contributions of each symmetry coordinate for the normal modes. The L vector matrices were calculated and these gave the normal coordinate vectors in terms of the symmetry coordinates (e.g. $\overline{Q}_i = \sum_j L_{ij} \overline{S}_j$). The functions $F_{kk} (L_{ik})^2$ were then evaluated. These functions give the approximate contribution of the potential field of the symmetry coordinate to the potential energy function of the given mode. They are normalised to be

fractions of an arbitrary total potential energy of unity, and give a direct measure of the nature of the mode (8), (119).

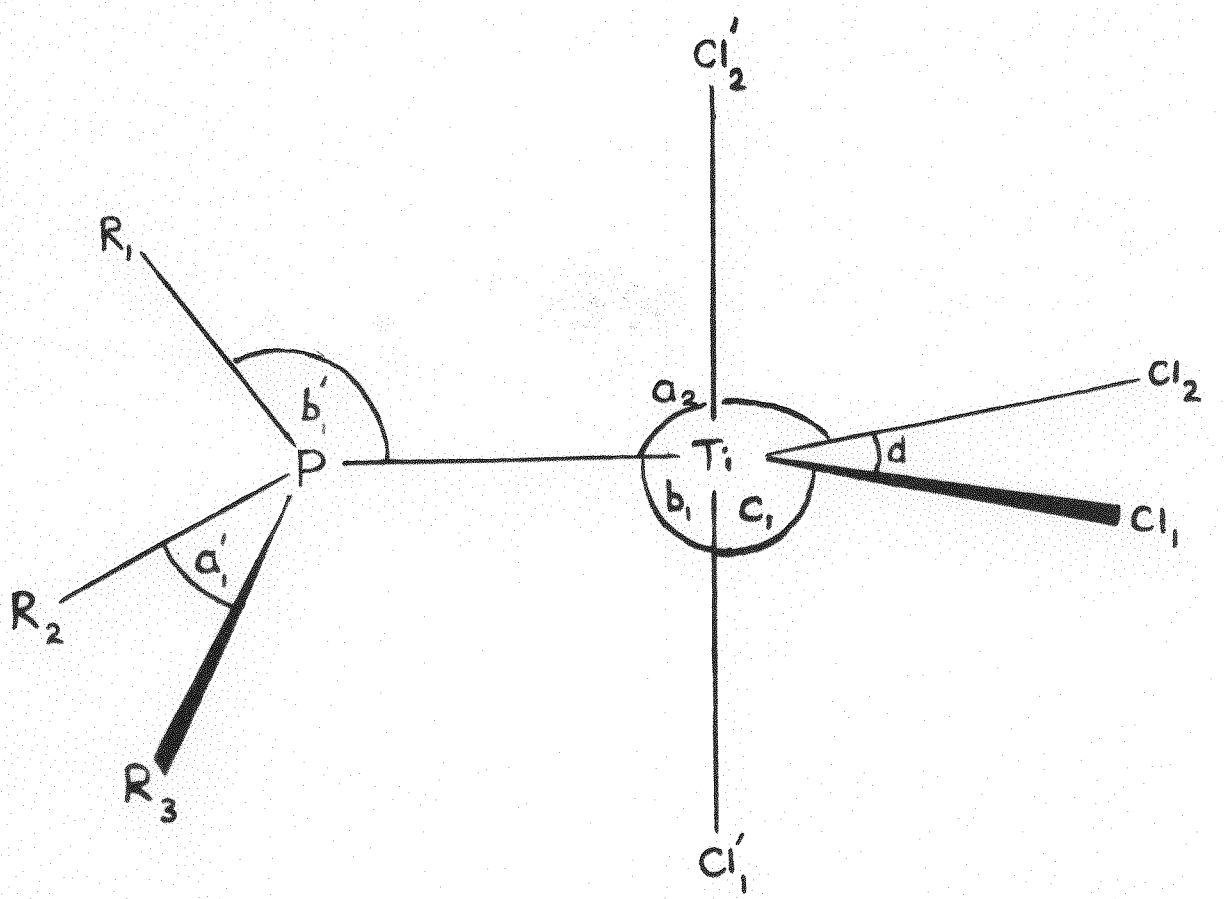

FIGURE 1.

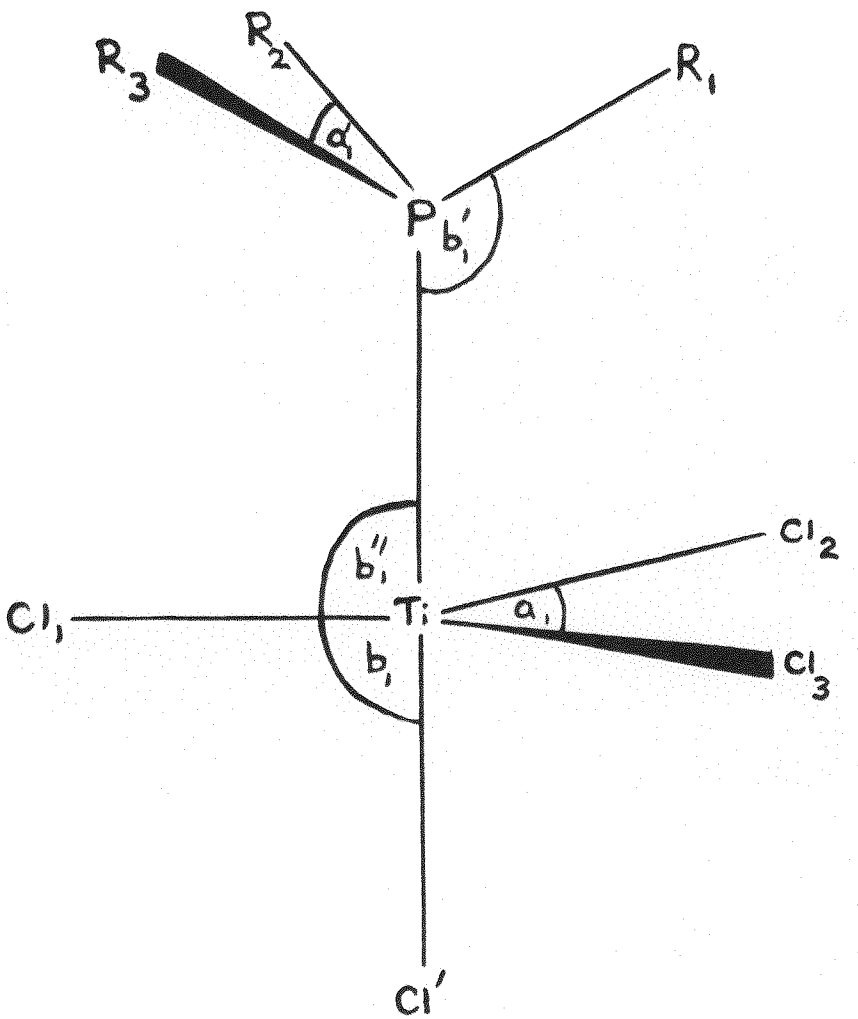

FIGURE 2.

TABLE 1.

Force Constant	PH_3 (114)	PMe_3 (115)	$TiCl_4$
f_r (md.Å^{-1})	3.3326	2.870	2.168†
f_α (md.Å rad^{-2})	0.7326	0.833	0.5408
f_{rr}(md.Å^{-1})	0.0544	- 0.010	0.12*†
$f_{\alpha\alpha}$(md.Å rad^{-2})	- 0.0286	0.036	0.0484
$f_{r\alpha}$(md.rad^{-1})	- 0.0344	-	0.088

† f_r and f_{rr} values = $TiCl_4$ values x 0.8.

* f_{rr}cis = f_{rr} = 0.12 and f_{rr} trans = 3/4 f_{rr} cis = 0.09.

TABLE 2.

Bond lengths used in C_{2V} and C_{3V} $TiCl_4$,PR_3

(where R = H, Me)

r_{PH}	1.419Å	(116)
r_{TiP}	2.55 Å	
r_{PMe}	1.85 Å	(115)
r_{TiCl}	2.3 Å	(117)

TABLE 3.

Force constant relationships for C_{2V} $TiCl_4,PR_3$.

(where R = H or Me).

Force constant in $TiCl_4,PR_3$	Relationship to value quoted in Table 1	Force constant in $TiCl_4,PR_3$	Relationship to value quoted in Table 1
$f_{TiCl'}$	f_r	$f_{TiCl'c}$	$f_{r\alpha}$
f_{TiCl}	f_r	$f_{TiClTiCl}$	f_{rr}cis
f_b	f_α	f_{TiCla}	$f_{r\alpha}$
f_e	$\frac{1}{4} f_\alpha$	f_{TiCld}	$f_{r\alpha}$
f_a	f_α	f_{TiClc}	$f_{r\alpha}$
f_d	f_α	f_{bb}	$f_{\alpha\alpha}$
f_c	f_α	f_{be}	$\frac{5}{8} f_{\alpha\alpha}$
$f_{TiPTiCl'}$	f_{rr}trans	f_{ba}	$f_{\alpha\alpha}$
$f_{TiPTiCl}$	f_{rr}cis	f_{bc}	$f_{\alpha\alpha}$
$f_{TiP\ b}$	$f_{r\alpha}$	f_{ed}	$\frac{5}{8} f_{\alpha\alpha}$
$f_{TiP\ a}$	$f_{r\alpha}$	f_{ec}	$\frac{5}{8} f_{\alpha\alpha}$
$f_{TiCl'TiCl'}$	f_{rr}trans	f_{aa}	$f_{\alpha\alpha}$
$f_{TiCl'TiCl}$	f_{rr}cis	f_{ad}	$f_{\alpha\alpha}$
$f_{TiCl'\ b}$	$f_{r\alpha}$	f_{ac}	$f_{\alpha\alpha}$
$f_{TiCl'\ e}$	$\frac{5}{8} f_{r\alpha}$	f_{dc}	$f_{\alpha\alpha}$
		f_{cc}	$f_{\alpha\alpha}$

TABLE 4.

Force constant relationships for C_{3V} $TiCl_4$,PR_3.

(where R = H or Me)

Force constant in $TiCl_4$,PR_3	Relationship to value quoted in Table 1	Force constant in $TiCl_4$,PR_3	Relationship to value quoted in Table 1
f_{TiCl}	f_r	$f_{TiCl\ b''}$	$f_{r\alpha}$
f_a	ff_α	$f_{TiCl\ TiCl'}$	f_{rr}^{cis}
$f_{b''}$	f_α	$f_{TiCl\ b}$	$f_{r\alpha}$
$f_{TiCl'}$	f_r	f_{aa}	$f_{\alpha\alpha}$
f_b	f_α	$f_{ab''}$	$f_{\alpha\alpha}$
$f_{TiPTiCl}$	f_{rr}^{cis}	$f_{TiCl'a}$	$f_{r\alpha}$
$f_{TiP\ a}$	$f_{r\alpha}$	f_{ab}	$f_{\alpha\alpha}$
$f_{TiP\ b''}$	$f_{r\alpha}$	$f_{b''b''}$	$f_{\alpha\alpha}$
$f_{TiP\ TiCl'}$	f_{rr}^{trans}	$f_{TiCl'b}$	$f_{r\alpha}$
$f_{TiP\ b}$	$f_{r\alpha}$	$f_{bb''}$	$f_{\alpha\alpha}$
$f_{TiCl\ TiCl}$	f_{rr}^{cis}	$f_{TiCl'b}$	$f_{r\alpha}$
$f_{TiCl\ a}$	$f_{r\alpha}$	f_{bb}	$f_{\alpha\alpha}$

APPENDIX B.

Vibrational analysis of $TiCl_4, 2CH_3CN$ in C_{2V} symmetry.

The vibrational analysis of this molecule, and its deuteriated analogue, was carried out using the programme devised by Dr. T. R. Gilson (8), described in Appendix (A).

For $TiCl_4, 2CH_3CN$, with the methyl groups treated in full, we have for the whole molecule (neglecting the two methyl torsional modes):

$$\Gamma_{mol} = 15a_1 + 7a_2 + 8b_1 + 13b_2$$

The internal coordinates used are shown in Figure 1. In addition to those given there, we have also for the linear C - C - N - Ti residue -

$$\left.\begin{matrix} a_1' \text{ and } a_1'' \\ b_1' \text{ and } b_1'' \end{matrix}\right\} \text{ perpendicular to } \left\{\begin{matrix} a' \text{ and } a'' \\ b' \text{ and } b'' \end{matrix}\right.$$

In order to write down the symmetry coordinates we note the following correlation scheme for the symmetry types for the WXY_3, WXYZ and $Z_2WX_2Y_2$ portions of the completed molecule:

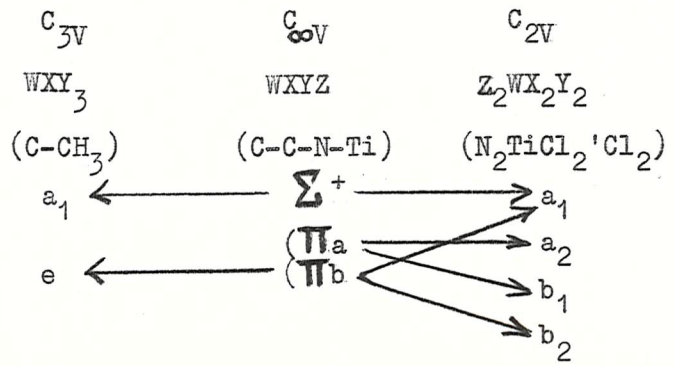

The symmetry coordinates are:

a_1 type

$S_1 = \Delta C_2'N'$

$S_2 = \Delta a_1'$

$S_3 = \Delta b_1'$

$S_4 = \Delta C_1'C_2'$

$S_5 = \frac{1}{\sqrt{3}} (\Delta C_1'H_1' + \Delta C_1'H_2' + \Delta C_1'H_3')$

$S_6 = \frac{-1}{\sqrt{3(1 + n^2)}} [\Delta\beta_1' + \Delta\beta_2' + \Delta\beta_3' - n(\Delta a_1' + \Delta a_2' + \Delta a_3')]$

$S_7 = \frac{1}{\sqrt{6}} (2\Delta C_1'H_1' - \Delta C_1'H_2' - \Delta C_1'H_3')$

$S_8 = \frac{1}{\sqrt{6}} (2\Delta a_1' - \Delta a_2' - \Delta a_3')$

$S_9 = \frac{1}{\sqrt{6}} (2\Delta\beta_1' - \Delta\beta_2' - \Delta\beta_3')$

$S_{10} = \frac{1}{\sqrt{2}} (\Delta TiCl_1 + \Delta TiCl_2)$

$S_{11} = \frac{1}{\sqrt{2}} (\Delta TiCl_1' + \Delta TiCl_2')$

$S_{12} = \frac{1}{\sqrt{2}} (\Delta a - \Delta d)$

$S_{13} = \frac{1}{2} (\Delta a + \Delta d - \Delta c_1 - \Delta c_2)$

$S_{14} = \frac{1}{2\sqrt{2}} (\Delta b_{11} + \Delta b_{12} + \Delta b_{21} + \Delta b_{22} - \Delta P_{11} - \Delta P_{12} - \Delta P_{21} - \Delta P_{22})$

$S_{15} = \frac{1}{\sqrt{2}} (\Delta TiN' + \Delta TiN'')$

where:

$n = \sqrt{3} \cos\beta / \cos\frac{\alpha'}{2}$ $(\beta = 180^\circ - \beta') = 2\sqrt{3} \cos\beta / \sqrt{1 + 3\cos^2\beta}$ ($\sqrt{}$ +ve)

a_2 type

$S_1 = \Delta a'$

$S_2 = \Delta b'$

$S_3 = \frac{1}{\sqrt{6}} (2\Delta C_1'H_1' - \Delta C_1'H_2' - \Delta C_1'H_3')$

$S_4 = \frac{1}{\sqrt{6}} (2\Delta \alpha_1' - \Delta \alpha_2 - \Delta \alpha_3)$

$S_5 = \frac{-1}{\sqrt{6}} (2\Delta \beta_1' - \Delta \beta_2' - \Delta \beta_3')$

$S_6 = \frac{1}{2} (\Delta b_{11} - \Delta b_{12} - \Delta b_{21} + \Delta b_{22})$

$S_7 = \frac{1}{2} (\Delta P_{11} - \Delta P_{12} - \Delta P_{21} + \Delta P_{22})$

b_1 type

$S_1 = \Delta a'$

$S_2 = \Delta b'$

$S_3 = \frac{1}{\sqrt{6}} (2\Delta C_1'H_1' - \Delta C_1'H_2' - \Delta C_1'H_3')$

$S_4 = \frac{1}{\sqrt{6}} (2\Delta \alpha_1' - \Delta \alpha_2' - \Delta \alpha_3')$

$S_5 = \frac{-1}{\sqrt{6}} (2\Delta \beta_1' - \Delta \beta_2' - \Delta \beta_3')$

$S_6 = \frac{1}{\sqrt{2}} (\Delta TiCl_1' - \Delta TiCl_2')$

$S_7 = \frac{1}{2} (\Delta b_{11} + \Delta b_{12} - \Delta b_{21} - \Delta b_{22})$

$S_8 = \frac{1}{2} (\Delta P_{11} + \Delta P_{12} - \Delta P_{21} - \Delta P_{22})$

b_2 type

$S_1 = \Delta C_2'N'$

$S_2 = \Delta a_1'$

$$S_3 = \Delta b_1'$$

$$S_4 = \Delta C_1'C_2'$$

$$S_5 = \frac{1}{\sqrt{3}} (\Delta C_1'H_1' + \Delta C_1'H_2' + \Delta C_1'H_3')$$

$$S_6 = \frac{-1}{\sqrt{3(1+n^2)}} [\Delta\beta_1' + \Delta\beta_2' + \Delta\beta_3' - n(\Delta\alpha_1' + \Delta\alpha_2' + \Delta\alpha_3')]$$

$$S_7 = \frac{1}{\sqrt{6}} (2\Delta C_1'H_1' - \Delta C_1'H_2' - \Delta C_1'H_3')$$

$$S_8 = \frac{1}{\sqrt{6}} (2\Delta\alpha_1' - \Delta\alpha_2' - \Delta\alpha_3')$$

$$S_9 = \frac{1}{\sqrt{6}} (2\Delta\beta_1' - \Delta\beta_2' - \Delta\beta_3')$$

$$S_{10} = \frac{1}{\sqrt{2}} (\Delta TiCl_1 - \Delta TiCl_2)$$

$$S_{11} = \frac{1}{2\sqrt{2}} (\Delta b_{11} - \Delta b_{12} + \Delta b_{21} - \Delta b_{22} + \Delta P_{11} - \Delta P_{12} + \Delta P_{21} - \Delta P_{22})$$

$$S_{12} = \frac{1}{\sqrt{2}} (\Delta c_1 - \Delta c_2)$$

$$S_{13} = \frac{1}{\sqrt{2}} (\Delta TiN' - \Delta TiN'')$$

where:

$$n = \sqrt{3} \cos\beta / \cos\frac{\alpha'}{2} = 2\sqrt{3} \cos\beta / \sqrt{1 + 3\cos^2\beta} \quad (\beta = 180^\circ - \beta';\sqrt{\ } + ve)$$

The G-matrix elements used have been calculated by Gilson (8), and the programme using values of the force constants, calculated the values of the symmetrised F-matrix elements direct. The force constants and bond lengths used in the calculation are given in Tables 1, 2 and 3. The force constants used for the coordinated methylcyanide were obtained from the values of the symmetrised F_{ij} matrix elements reported by Duncan (120). Force constants for the $L_2TiCl_2'Cl_2$ skeleton were transferred directly from those for the

$SnCl_6^{2-}$ ion (121). The method of transference is given in Table 4. The value of the Ti - N bond stretching force constant was taken as 1.0 md. $Å^{-1}$, and tetrahedral and trigonal bipyramidal angles were used.

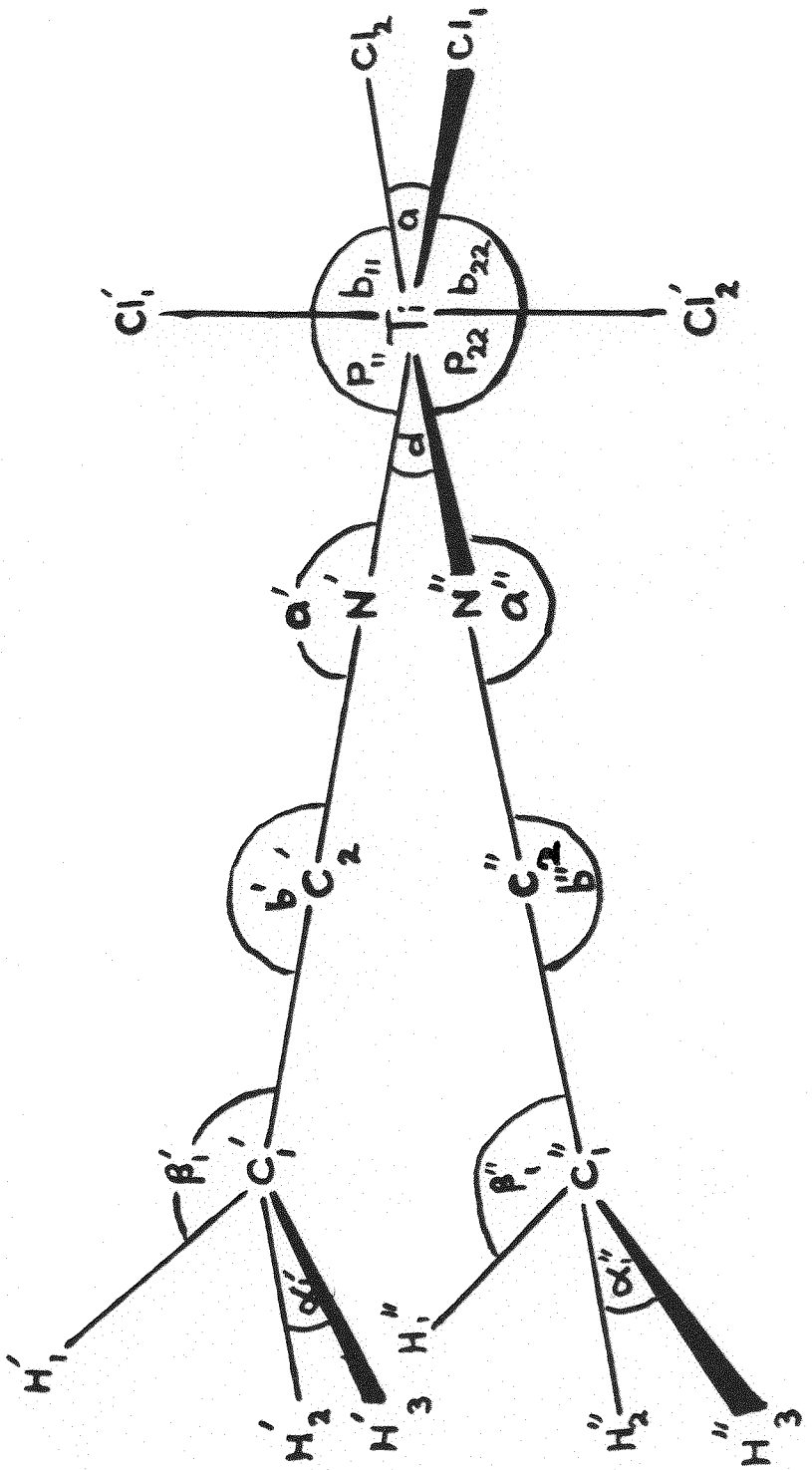
$C_1 = N'Ti Cl_2$
$C_2 = N''Ti Cl_1$
$b_{21} = Cl_2' Ti Cl_2$
$P_{12} = N'' Ti Cl_1'$
Cl_2
Cl_1
Cl_1'
Cl_2'
b_{11}
b_{22}
P_{11}
P_{22}
Ti
a
d
N'
N''
a'
a''
b'
b''
C_2'
C_2''
β_1'
β_1''
C_1'
C_1''
α_1'
α_1''
H_1'
H_2'
H_3'
H_1''
H_2''
H_3''

FIGURE 1.

TABLE 1.

Methylcyanide momental force constants

(from symmetrised F_{ij} (120)).

f_{CH}	=	4.938 md. Å^{-1}	$f_{CC\beta}$	=	0.475 md. rad^{-1}
f_{CC}	=	5.159 md. Å^{-1}	$f_{CC\alpha}$	=	0.475 md. rad^{-1}
f_{CN}	=	18.110 md. Å^{-1}	f_{α}	=	0.655 md. Å rad^{-2}
$f_{CC,CN}$	=	0.299 md. Å^{-1}	f_{β}	=	0.861 md. Å rad^{-2}
$f^{opp}_{CH\alpha}$	=	- 0.55 md.rad^{-1}	$f_{b'}$	=	0.592 md. Å rad^{-2}
$f^{adj}_{CH\alpha}$	=	0.038 md.rad^{-1}	$f^{adj}_{\alpha\beta}$	=	- 0.058 md. Å rad^{-2}
$f^{opp}_{CH,\beta}$	=	0.55 md. rad^{-1}	$f_{\alpha\alpha}$	=	- 0.091 md. Å rad^{-2}
$f^{adj}_{CH,\beta}$	=	0.038 md.rad^{-1}	$f_{\beta\beta}$	=	- 0.120 md. Å rad^{-2}
			$f_{\beta b'}$	=	- 0.205 md. Å rad^{-2}

TABLE 2.

Momental force constants for $SnCl_6^{2-}$ (121)

f_r	=	1.793 md. Å $^{-1}$
f_α	=	0.983 md. Å rad^{-2}
f_{rr}^{trans}	=	0.052 md. Å $^{-1}$
f_{rr}^{cis}	=	0.104 md. Å $^{-1}$
$f_{r\alpha}$	=	0.228 md. rad^{-1}
$f_{\alpha\alpha}$	=	0.067 md. Å rad^{-2}

TABLE 3.

Bond lengths (Å) used in C_{2V} $TiCl_4$,2MeCN (117).

H-C	1.11
C-C	1.458
C-N	1.157
N-Ti	2.19
Ti-Cl	2.3

TABLE 4.

Force constant transference scheme for L_2TiCl_4 skeleton.

Force constant in L_2TiCl_4	Relationship to value in Table 2	Force constant in L_2TiCl_4	Relationship to value in Table 2
f_{TiCl}	f_r	$f_{TiCl,TiCl}$	f_{rr}^{cis}
$f_{TiCl'}$	f_r	$f_{TiCl,TiCl'}$	f_{rr}^{cis}
f_{TiN}	1.0	$f_{TiCl_1',TiCl_2'}$	f_{rr}^{trans}
f_a	f_a	$f_{TiCl,TiN'}$	$3/4\ f_{rr}^{cis}$
f_d	$1/2\ f_a$	$f_{TiCl,TiN''}$	$3/4\ f_{rr}^{cis}$
f_c	$3/4\ f_a$	$f_{TiCl',TiN'}$	$3/4\ f_{rr}^{cis}$
f_b	f_a	$f_{TiN',TiN''}$	$1/2\ f_{rr}^{cis}$
f_p	$3/4\ f_a$	$f_{TiCl,a}$	f_{ra}
		$f_{TiCl'd}$	$1/2\ f_{ra}$
		f_{TiCl,c_1}	f_{ra}

T A B L E 4. (cont.)

Force constant in L_2TiCl_4	Relationship to value in Table 2	Force constant in L_2TiCl_4	Relationship to value in Table 2
$f_{TiN',Cl}$	$3/4\ f_{ra}$	$f_{b_{11},b_{21}}$	f_{aa}
$f_{a,c}$	f_{aa}	$f_{TiCl',p_{11}}$	$3/4\ f_{ra}$
$f_{d,c}$	$3/4\ f_{aa}$	$f_{TiN',p_{11}}$	$1/2\ f_{ra}$
$f_{TiCl,b_{11}}$	f_{ra}	$f_{d,p_{11}}$	$1/2\ f_{aa}$
$f_{TiN',b_{11}}$	$3/4\ f_{ra}$	$f_{c_{11},p_{11}}$	$1/2\ f_{aa}$
$f_{a,b_{12}}$	f_{aa}	$f_{b_{12},p_{12}}$	$3/4\ f_{aa}$
$f_{c_1,b_{11}}$	$3/4\ f_{aa}$	$f_{b_{21},p_{22}}$	$3/4\ f_{aa}$
$f_{b_{11},b_{12}}$	f_{aa}	$f_{p_{11},p_{12}}$	$1/2\ f_{aa}$
		$f_{p_{12},p_{22}}$	$1/2\ f_{aa}$

APPENDIX C.

Vibrational analysis of $TiCl_3, 2XMe_3$ in D_{3h} symmetry.

The vibrational analysis of this molecule was carried out using the programme described in Appendix (A), for X = N and P.

Assuming free rotation of the methyl groups, and consequent D_{3h} symmetry, we have for the whole molecule, treating the methyl groups as point masses, and neglecting the two XC_3 torsional modes $(a_1'' + a_2')$:

$$\Gamma_{mol} = 4a_1' + 4a_2'' + 6e' + 4e''$$

The two XC_3 torsional modes have also been neglected in the following analysis, since they are both inactive.

The internal coordinates used are shown in Figure 1 for the case of $TiCl_3, 2PMe_3$. In order to write down symmetry coordinates, we note the following correlation scheme between the symmetry types for the individual portions of the molecule, Me_3X-Ti and X_2TiCl_3 (both of C_{3V} symmetry) and the completed molecule with D_{3h} symmetry:

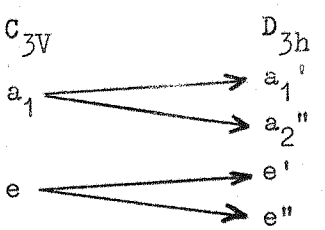

It should be noted that the a_1 and e type vibrations of the two $C_{3V}Me_3X$-Ti residues couple in the following way:

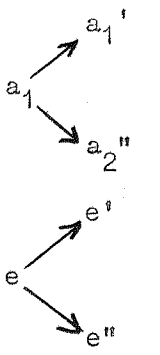

sym. + sym.

sym. - sym.

antisym. + antisym.

antisym. - antisym.

This therefore gives rise to four XC_3 stretching modes and deformational modes (a_1', a_2'', e' and e"), two XC_3 rocking modes (e' + e") and two Ti-X stretching modes (a_1' and a_2''). From the point of view of the programme, it was convenient to treat the problem in an analogous way to $TiCl_4$,R_3P with C_{3V} symmetry (see Appendix (A)). The symmetry coordinates used have therefore been listed under the symmetry types appropriate to C_{3V} symmetry:

a_1 type

$$S_1 = \frac{1}{\sqrt{3}} (\Delta P'Me_1' + \Delta P'Me_2' + \Delta P'Me_3')$$

$$S_2 = \frac{-1}{\sqrt{3(1+n^2)}} [\Delta b_1' + \Delta b_2' + \Delta b_3' - n(\Delta a_1' + \Delta a_2' + \Delta a_3')]$$

$$S_3 = \frac{1}{\sqrt{3}} (\Delta P''Me_1'' + \Delta P''Me_2'' + \Delta P''Me_3'')$$

$$S_4 = \frac{-1}{\sqrt{3(1+n^2)}} [\Delta b_1'' + \Delta b_2'' + \Delta b_3'' - n(\Delta a_1'' + \Delta a_2'' + \Delta a_3'')]$$

$$S_5 = \Delta TiP'$$

$$S_6 = \frac{1}{3} (\Delta TiCl_1 + \Delta TiCl_2 + \Delta TiCl_3)$$

$$S_7 = \frac{1}{\sqrt{3(2 + n_1^2)}} \left[(\Delta b_1 + \Delta b_2 + \Delta b_3 - \Delta b_1''' - \Delta b_2''' - \Delta b_3''' + n(\Delta a_1 + \Delta a_2 + \Delta a_3) \right]$$

$$S_8 = \Delta TiP''$$

where $n = \sqrt{3} \cos b/\cos a'/2$ $(b = 180 - b')$

$$= 2\sqrt{3} \cos b/\sqrt{1 + 3\cos^2 b} \quad (\sqrt{} + ve)$$

$$n_1 = \sqrt{3} \cos b/\cos \frac{a}{2}$$

$$= 2\sqrt{3} \cos b/\sqrt{1 + 3\cos^2 \beta} \quad (\sqrt{} + ve)$$

e type

$$S_1 = \frac{1}{\sqrt{6}} (2\Delta P'Me_1' - \Delta P'Me_2' - \Delta P'Me_3')$$

$$S_2 = \frac{1}{\sqrt{6}} (2\Delta a_1' - \Delta a_2' - \Delta a_3')$$

$$S_3 = \frac{-1}{\sqrt{6}} (2\Delta b_1' - \Delta b_2' - \Delta b_3')$$

$$S_4 = \frac{1}{\sqrt{6}} (2\Delta P''Me_1'' - \Delta P''Me_2'' - \Delta P''Me_3'')$$

$$S_5 = \frac{1}{\sqrt{6}} (2\Delta a_1'' - \Delta a_2'' - \Delta a_3'')$$

$$S_6 = \frac{-1}{\sqrt{6}} (2\Delta b_1'' - \Delta b_2'' - \Delta b_3'')$$

$$S_7 = \frac{1}{\sqrt{6}} (2\Delta TiCl_1 - \Delta TiCl_2 - \Delta TiCl_3)$$

$$S_8 = \frac{1}{\sqrt{6}} (2\Delta a_1 - \Delta a_2 - \Delta a_3)$$

$$S_9 = \frac{-1}{\sqrt{6}} (2\Delta b_1''' - \Delta b_2''' - \Delta b_3''')$$

$$S_{10} = \frac{-1}{\sqrt{6}} (2\Delta b_1 - \Delta b_2 - \Delta b_3)$$

The G-matrix elements have been calculated by Gilson (8), and the programme, using values of the force constants, calculated the values of the symmetrised F-matrix elements direct. The force constants and bond lengths used in the calculations are given in Tables 1, 2 and 3. The values of f_r and f_{rr} for the X_2TiCl_3 skeleton in Table 2 were calculated using the position of the a_1' symmetric $TiCl_3$ stretching mode:

$$\mu_{Cl}\,(f_r + 2f_{rr}) = \lambda_{\nu a_1'TiCl_3}$$

(ν = 282 cm.$^{-1}$ for $TiCl_3,2PMe_3$; 308 cm.$^{-1}$ for $TiCl_3,2NMe_3$)

where $\lambda_{292} = 0.58851\ \left(\frac{\nu a_1'TiCl_3}{1000}\right)^2$

and μ_{Cl} = the reduced mass of chlorine,

and assuming $\frac{f_{rr}}{f_r} = \frac{0.15}{2.71}$ (the ratio of the free $TiCl_4$ values, as calculated in Appendix A).

The values of f_α, $f_{\alpha\alpha}$ and $f_{r\alpha}$ were transferred directly from free $TiCl_4$ (see Appendix A)). The method of transference of force constants is given in Table 4 for $TiCl_3,2NMe_3$ and Table 5 for $TiCl_3,2PMe_3$. Values of f_{TiN} = 0.8 md. Å^{-1} and f_{TiP} = 1.0 md. Å^{-1} were taken, and tetrahedral and trigonal bipyramidal angles were used. The calculated frequencies, classified as a_1 and e types under C_{3V} symmetry were identified as a_1' or a_2'' and e' or e'' by inspection of the signs of the L-matrix elements calculated, corresponding to those symmetry coordinates making contributions > 30% to the whole vibration. Contributions > 75% were regarded as pure modes.

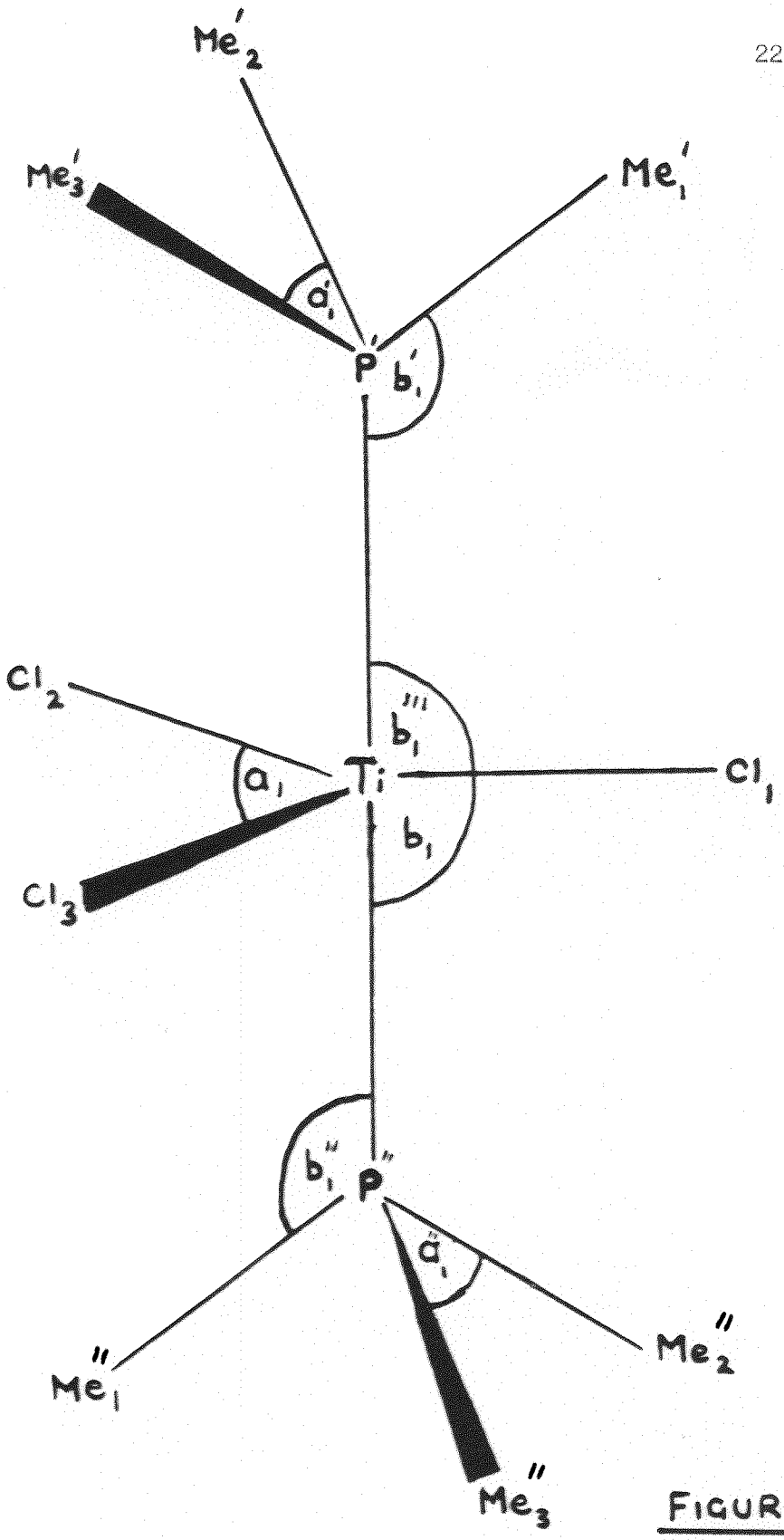

FIGURE 1.

TABLE 1.

Momental force constants taken for the complex ligands in the calculation on D_{3h} $TiCl_3$,$2XMe_3$.

	Me_3N (11)	Me_3P (115)	
f_r	4.68	2.87	md. $Å^{-1}$
f_{rr}	0.065	-0.010	"
f_α	1.01	0.833	md. Å rad^{-2}
$f_{\alpha\alpha}$	-	0.036	"
f_β	0.638	0.417	"
$f_{\beta\beta}$	-	0.018	"
$f_{r\alpha}$	0.065	-	md. rad^{-1}

T A B L E 2.

Momental force constants taken for the X_2TiCl_3 skeleton for D_{3h} $TiCl_3$, $2XMe_3$.

f_{TiX}	0.8 md. $Å^{-1}$	(X = N)
	1.0 "	(X = P)
f_r	1.8 "	(X = N)
	1.5 "	(X = P)
f_{rr}	0.1 "	(X = N)
	0.08"	(X = P)
f_α, $f_{\alpha\alpha}$, $f_{r\alpha}$	free $TiCl_4$ values used (see Table 1, Appendix A)	

T A B L E 3.

Dimensions (Å) used in the calculations on D_{3h} $TiCl_3$, $2XMe_3$.

ν_{N-Me}	1.54	(11)
ν_{Ti-N}	2.183	(95)
ν_{P-Me}	1.85	(115)
ν_{Ti-P}	2.55	(117)
ν_{Ti-Cl}	2.216	(95)

TABLE 4.

Transference scheme for skeletal force constants in D_{3h} $TiCl_3, 2NMe_3$.

Force constant for $TiCl_3, 2NMe_3$	Relationship to value quoted in Table 2	Force constant for $TiCl_3, 2NMe_3$	Relationship to value quoted in Table 2
$f_{TiN'}$	0.8	$f_{TiCl\ a}$	f_{ra}
f_{TiCl}	f_r	$f_{TiCl\ b'''}$	$3/4f_{ra}$
f_a	f_a	$f_{TiCl,TiN''}$	$3/4f_{rr}$
$f_{b'''}$	$1/2f_a$	$f_{TiCl\ b}$	$3/4f_{ra}$
$f_{TiN''}$	0.8	f_{aa}	f_{aa}
		$f_{ab'''}$	$3/4f_{aa}$
f_b	$1/2f_a$	$f_{TiN''\ a}$	$3/4f_{ra}$
$f_{TiN'TiCl}$	$3/4f_{rr}$	f_{ab}	$3/4f_{aa}$
$f_{TiN'a}$	$3/4f_{ra}$	$f_{b'''b'''}$	$1/2f_{aa}$
$f_{TiN'b'''}$	$1/2f_{ra}$	$f_{bb'''}$	$1/2f_{aa}$
$f_{TiN'TiN''}$	$1/4f_{rr}$	$f_{TiN''b}$	$1/2f_{ra}$
$f_{TiCl,TiCl}$	f_{rr}	f_{bb}	$1/2f_{aa}$

TABLE 5.

Transference scheme for skeletal force constants in D_{3h} $TiCl_3,2PMe_3$

Force constant for $TiCl_3,2PMe_3$	Relationship to value quoted in Table 2	Force constant for $TiCl_3,2PMe_3$	Relationship to value quoted in Table 2
$f_{TiP'}$	1.5	$f_{TiCl\ a}$	$f_{r\alpha}$
f_{TiCl}	f_r	$f_{TiCl\ b"'}$	$f_{r\alpha}$
f_a	f_α	$f_{TiClTiP"}$	f_{rr}
$f_{b"'}$	f_α	$f_{TiCl\ b}$	$f_{r\alpha}$
$f_{TiP"}$	1.5	f_{aa}	$f_{\alpha\alpha}$
f_b	f_α	$f_{ab"'}$	$f_{\alpha\alpha}$
$f_{TiP'TiCl}$	f_{rr}	$f_{TiP"a}$	$f_{r\alpha}$
$f_{TiP'a}$	$f_{r\alpha}$	f_{ab}	$f_{\alpha\alpha}$
$f_{TiP'b"'}$	$f_{r\alpha}$	$f_{b"'b"'}$	$f_{\alpha\alpha}$
$f_{TiP'TiP"}$	$1/4f_{rr}$	$f_{bb"'}$	$f_{\alpha\alpha}$
$f_{TiClTiCl}$	f_{rr}	$f_{TiP"b}$	$f_{r\alpha}$
		f_{bb}	$f_{\alpha\alpha}$

REFERENCES

(1) R. Freeman, R. P. H. Gasser and R. E. Richards, Mol. Phys., (1959), 2, 301

(2) E. R. Andrew, A. Bradbury, R. G. Eades and G. F. Jenks, Nature, (1960), 188, 1097.

(3) H. M. McConnell and D. M. Chestnut, J. Chem. Phys., (1958), 28, 107.

(4) J. H. Emsley, J. Feeney and L. H. Sutcliffe, "High Resolution Nuclear Magnetic Resonance Spectroscopy", Pergamon Press, (1965), 1, 240.

(5) F. A. Cotton, J. W. George and J. S. Waugh, J. Chem. Phys., (1958), 28, 994.

(6) C. A. Hoffman, B. E. Holder and W. L. Jolly, J. Phys. Chem. (1958), 62, 364.

(7a) P. A. W. Dean and D. F. Evans, J. Chem. Soc., (A), (1968), 1154.

(7b) E. L. Muetterties, J. Amer. Chem. Soc., (1960), 82, 1082.

(8) T. Gilson, Ph.D. Thesis, London (1964).

(9) R. G. Snyder and J. H. Schachtschneider, Spectrochim. Acta, (1963), 19, 85.

(10) I. R. Beattie and T. Gilson, J. Chem. Soc., (1964), 3528.

(11) I. R. Beattie and T. Gilson, J. Chem. Soc., (1965), 6595.

(12) I. R. Beattie, K. M. S. Livingston and T. Gilson, J. Chem. Soc., (1968), 1.

(13) I. R. Beattie and T. R. Gilson, Proc. Roy. Soc., (1968), A., 307, 407.

(14) I. R. Beattie, K. M. S. Livingston, G. A. Ozin and D. J. Reynolds, J. Chem. Soc., (A), (1969), 958.

(15) I. R. Beattie, T. R. Gilson and G. A. Ozin, J. Chem. Soc., (A), (1968), 2765.

(16) S. P. S. Porto, P. A. Fleury and T. C. Daman, Phys. Rev., (1967), 154, 522.

(17) J. Behringer, Observed Resonance Raman Spectra, in "Raman Spectroscopy", Plenum, (1967), 168.

(18) P. A. Fleury, S. P. S. Porto, L. E. Cheesman and H. J. Guggenheim, Phys. Rev. Lett., (1967), 18, 658.

(19) G. A. Ozin, D. Phil. Thesis, Oxford, (1967).

(20) K. M. S. Livingston, Ph.D. Thesis, London, (1967).

(21) M. W. Duckworth, G. W. A. Fowles and P. T. Green, J. Chem. Soc., (A), (1967), 1592.

(22a) K. S. Pitzer, J. Amer. Chem. Soc., (1948), 70, 2140.

(22b) I. R. Beattie and T. Gilson, Nature (1962), 193, 1041.

(23) A. Pidcock, R. E. Richards and L. M. Venanzi, J. Chem. Soc., (A), (1966), 1707.

(24) L. Pauling, J. Amer. Chem. Soc., (1931), 53, 1367.

(25) D. P. Craig, A. MacColl, R. S. Nyholm, L. E. Orgel and L. E. Sutton, J. Chem. Soc., (1954), 332.

(26) D. P. Craig and C. Zauli, J. Chem. Phys., (1962), 37, 601.

(27) P. Palmieri and C. Zauli, J. Chem. Soc., (A), (1967), 813.

(28) F. Gianturco, J. Chem. Soc., (A), (1969), 1293.

(29) C. G. Barraclough, J. Lewis and R. S. Nyholm, J. Chem. Soc., (1959), 3552.

(30) Y. Y. Kharitonov and Y. A. Buslaev, Izv. Akad. Nauk SSR, Otd. Khim, Nauk, (1962) 393.

(31) K. Dehnike, Z. Anorg. Allgem. Chem. (1961), 309, 266.

(32) G. W. A. Fowles, D. F. Lewis and R. A. Walton, J. Chem. Soc., (A), (1968), 1468.

(33) A. A. Feltz, Z. Chem. (1967), 7, 158.

(34) I. R. Beattie and V. Fawcett, J. Chem. Soc., (1967), 1583.

(35) W. Haase and H. Hoppe, Acta Cryst. (1968), B, 24, 288.

(36) R. P. Dodge, D. H. Templeton and A. Zalkin, J. Chem. Phys., (1961), 35, 55.

(37) M. Cox, J. Lewis and R. S. Nyholm, J. Chem. Soc., (1965), 2840.

(38) A. Yamamoto and S. Kambara, J. Amer. Chem. Soc., (1957), 79, 4344; J. Chem. Soc., Japan, (1959), 80, 1239.

(39) V. Fawcett, Ph.D. Thesis, London, (1967).

(40) M. Cox, Ph.D. Thesis, London, (1961).

(41) K. Nakamoto, Infrared Spectra of Inorganic and Coordination Compounds, Wiley, New York, (1963).

(42) K. Watenpaugh and C. N. Caughlan, Inorg. Chem., (1966), 5, 1782.

(43) K. Nakamoto, Y. Morimoto and A. E. Martell, J. Amer. Chem. Soc., (1961), 83, 4533.

(44) A. Pflugmacher, H. J. Carduck and M. Zucketto, Naturwiss, (1958), 45, 490.

(45) W. H. Nelson and D. F. Martin, J. Inorg. Nuclear Chem., (1965), 27, 89.

(46) I. R. Beattie, T. Gilson and G. A. Ozin, J. Chem. Soc., (A), (1968), 1092.

(47) I. R. Beattie and G. A. Ozin, J. Chem. Soc., in press.

(48) E. L. Muetterties, W. Mahler, K. J. Packer and R. Schmutzler, Inorg. Chem., (1964), 3, 1298.

(49) P. L. Goggin, H. L. Roberts and L. A. Woodward, Trans. Faraday Soc., (1961), 57, 1877.

(50) M. Radhakrishnan, J. Mol. Spect., (1963), 10, 111.

(51) R. R. Holmes, R. P. Carter, jun., and G. E. Peterson, Inorg. Chem., (1964), 3, 1748.

(52) G. W. A. Fowles and R. A. Hoodless, J. Chem. Soc., (1963), 33.

(53) G. W. A. Fowles, Progr. Inorg. Chem., (1964), 6, 1.

(54) R. Holtje, Z. Anorg. Allgem. Chem., (1930), 190, 241.

(55) A. Balls, N. N. Greenwood and B. P. Straughan, J. Chem. Soc., (A), (1968), 753.

(56) I. R. Beattie and G. A. Ozin, J. Chem. Soc., (A), (1968), 2373.

(57) J. Chatt and R. G. Hayter, J. Chem. Soc., (1963), 1343.

(58) A. D. Westland and L. Westland, Canad. J. Chem., (1965), 43, 426.

(59) R. J. H. Clark, L. Maresca and R. J. Puddenhart, Inorg. Chem. (1968), 7, 1605.

(60) J. E. Griffiths, R. P. Carter and R. R. Holmes, J. Chem. Phys., (1964), 41, 863.

(61) M. Webster, Ph.D. Thesis, London (1962).

(62) I. R. Beattie and G. J. Leigh, J. Inorg. Nuclear Chem., (1961), 23, 55.

(63) E. Wiberg and K. Modritzer, Z. Naturforsch., (1956), 116, 747.

(64) E. Lee and C. K. Wu, Trans. Faraday Soc., (1939), 35, 1366.

(65) G. Brauer, Handbook of Preparative Inorganic Chemistry, Academic Press, (1963).

(66) L. Maier, Angew. Chem., (1959), 71, 574.

(67) H. R. Linton and E. R. Nixon, Spectrochim. Acta. (1959), 146.

(68) G. W. Parshall, Organic Syntheses, (1965), 45, 102.

(69) R. K. Harris and R. G. Hayter, Canad. J. Chem. (1964), 42, 2282.

(70) K. Isslieb and A. Tzschach, Chem. Ber., (1960), 93, 1852.

(71) H. C. Beachell and B. Katlafsky, J. Chem. Phys., (1957), 27, 182.

(72) F. G. Mann and A. F. Wells, J. Chem. Soc., (1938), 702.

(73) H. Siebert, Z. Anorg. Chem., (1965), 273, 162.

(74) I. R. Beattie, Quart. Revs., (1963), 17, 382.

(75) I. R. Beattie, T. Gilson, M. Webster and G. P. McQuillan, J. Chem. Soc., (1964), 238.

(76) I. R. Beattie, T. R. Gilson and G. A. Ozin, J. Chem. Soc., (A), (1968), 2772.

(77) M. Webster, Private Communication.

(78) R. Hulme, G. J. Leigh and I. R. Beattie, J. Chem. Soc., (1960), 366.

(79) I. R. Beattie, M. Milne, M. Webster, H. E. Blayden, P. J. Jones, R. C. G. Killean and J. L. Lawrence, J. Chem. Soc., (A), (1969), 482.

(80) I. R. Beattie, G. P. McQuillan and M. Webster, J. Chem. Soc., (1963), 1514.

(81) I. R. Beattie, G. P. McQuillan, L. Rule and M. Webster, J. Chem. Soc., (1963), 1514.

(82) R. J. Goodfellow, J. G. Evans, P. L. Goggin and D. A. Duddell, J. Chem. Soc., (A), (1968), 1604.

(83) M. Milne, D. Phil. Thesis, Oxford, (1968).

(84) H. J. Emeleus and G. S. Rao, J. Chem. Soc., (1958), 4245.

(85) I. R. Beattie and M. Webster, J. Chem. Soc., (1964), 3507.

(86) T. L. Brown and M. Kubota, J. Amer. Chem. Soc., (1961), 83, 331.

(87) I. R. Beattie, P. J. Jones and M. Webster, J. Chem. Soc., (A), (1969), 218.

(88) M. Antler and A. W. Laubengayer, J. Amer. Chem. Soc., (1955), 77, 5250.

(89) G. W. A. Fowles and R. A. Hoodless, J. Chem. Soc., (1963), 33.

(90) M. W. Duckworth, G. W. A. Fowles and R. G. Williams, Chem. and Ind., (1962), 1285.

(91a) G. W. A. Fowles and C. M. Pleass, Chem. and Ind. (1955), 1743.

(91b) G. W. A. Fowles and C. M. Pleass, J. Chem. Soc., (1957), 1674.

(92) G. W. A. Fowles and P. T. Greene, Chem. Comm. (1966), 784.

(93) M. W. Duckworth, G. W. A. Fowles and P. T. Greene, J. Chem. Soc., (A), (1967), 1592.

(94) B. J. Russ and J. S. Wood, Chem. Comm. (1966), 20, 745.

(95) G. W. A. Fowles, P. T. Greene and J. S. Wood, Chem. Comm. (1967), 971.

(96) P. T. Greene and P. L. Orioli, J. Chem. Soc., (A), (1969),1621.

(97) K. Isslieb and G. Bohn, Z. Anorg. Chem., (1959), 301, 188.

(98) K. Isslieb and H. O. Frohlich, Z. Anorg. Chem., (1959), 298, 84.

(99) K. A. Jensen, B. Nygaard and C. T. Pedersen, Acta. Chem. Scand., (1963), 17, 1126.

(100) R. C. Young and J. L. Hastings, J. Amer. Chem. Soc., (1937), 59, 765.

(101) J. H. Freeman and M. L. Smith, J. Inorg. Nuclear Chem., (1958), 7, 224.

(102) I. R. Beattie and G. A. Ozin, J. Chem. Soc., (A), (1969), 542.

(103) J. S. Wood, Private Communication.

(104) G. Bouquet and M. Bigorgne, Spectrochim. Act., (1967), 23A, 1231.

(105) M. J. Norgett, J. H. M. Thornley and L. M. Venanzi, J. Chem. Soc., (A), (1967), 540.

(106) S. Ahrland, J. Chatt and N. R. Davies, Quart. Revs., (1958), 12, 265.

(107) R. G. Pearson, J. Amer. Chem. Soc., (1963), 85, 3533.

(108) R. J. P. Williams and J. D. Hale, Structure and Bonding, (1966), 1, 249.

(109) S. Ahrland, Structure and Bonding, (1968), 5, 118.

(110) C. K. Jørgensen, Structure and Bonding, (1967), 3, 106.

(111) F. G. A. Stone, Chem. Revs., (1958), 58, 101.

(112a) D. M. Adams and D. M. Morris, J. Chem. Soc., (A), (1968), 694.

(112b) T. L. Cottrell, "The Strengths of Chemical Bonds", Butterworth's, London, (1954).

(113) Y. Morino and H. Vehara, J. Chem. Phys., (1966), 45, 4543.

(114) G. de Alti, G. Costa and V. Galasso, Spectrochim. Acta., (1964), 20, 965.

(115) H. G. M. Edwards, B.A. Thesis, Oxford, (1966).

(116) V. M. McConaghie and H. H. Nielsen, J. Chem. Phys., (1953), 21, 1838.

(117) Tables of Interatomic Distances, Chemical Society Special Publication, No. 11, (1958).

(118) A. Meister and F. Cleveland, Am. J. Phys., (1946), 14, 13.

(119) Y. Morino and K. Kuchitsu, J. Chem. Phys., (1952), 20, 1809.

(120) J. L. Duncan, Spectrochim. Acta., (1964), 20, 1197.

(121) I. R. Beattie, T. Gilson, K. Livingston, V. Fawcett and G. A. Ozin, J. Chem. Soc., (A), (1967), 712.